Benchmark Calculations of Projection and Variational Coupled Cluster Methods

Bridgette Cooper

Thesis submitted for the Degree of PhD

Department of Chemistry
Cardiff University

November 23, 2010

ProQuest LLC
789 East Eisenhower Parkway
P.O. Box 1346
Ann Arbor, MI 48106-1346

Acknowledgements

I would like to thank my supervisor, Professor Peter Knowles for giving me the opportunity to work on such an interesting topic, and for his help, guidance and patience throughout. I would like to thank Doctors Ian Merrick and Andy May for all of their help. I extend my thanks to Róbert Izsák and others with whom I have shared an office for providing many lively discussions. Finally, I would also like to thank friends and family who have been a great support throughout, especially Ceri-Anne Fiddler and Christian Jowett.

Contents

List of Tables

List of Figures

Chapter 1

Introduction

1.1 The Time Independent Schrödinger equation

The non-relativistic time-independent Schrödinger equation:

$$\mathscr{H}|\Psi\rangle = \mathscr{E}|\Psi\rangle \tag{1.1}$$

is an eigenvalue problem. The eigenvector Ψ is the wavefunction, a vector that completely describes the state of the system. $\mathscr{E}$ is the energy of the system and the eigenvalue that is to be determined. $\mathscr{H}$ is the Hamiltonian operator that is given in atomic units by the following expression:

$$\mathscr{H} = -\sum_{i=1}^{N} \frac{1}{2}\nabla_i^2 - \sum_{A=1}^{N} \frac{1}{2M_A}\nabla_A^2 - \sum_{i=1}^{N}\sum_{A=1}^{M} \frac{Z_A}{r_{iA}} + \sum_{i=1}^{N}\sum_{j<i}^{N} \frac{1}{r_{ij}} + \sum_{A=1}^{M}\sum_{B<A}^{M} \frac{Z_A Z_B}{R_{AB}} \tag{1.2}$$

where N is the number of electrons in the system and M is the number of nuclei, M_A is the mass of the nucleus A relative to the mass of an electron, Z_A its atomic number, and ∇^2 are Laplacian operators involving differentiation with respect to the coordinates of the particles in the system. $\mathscr{H}$ is constructed from the potential and kinetic energies of the particles in the system and thus depends on the momentum and position of the particles. The first term is the operator for the kinetic energy of the electrons in the system, the second the kinetic energy operator for the nuclei, the third term is the coulomb potential between the electrons and the nuclei, the fourth term the potential between electrons and the final term the potential between nuclei.

1.1.1 Born-Oppenheimer approximation

Since the mass of an electron is approximately 1/1836 that of a proton, the nuclei move much more slowly in comparison with electrons. Hence, when electrons in molecules are considered, the Born-Oppenheimer approximation that the electrons are moving in a fixed field of nuclei can be adopted. This assumes that when nuclei are moved the electrons instantaneously adjust themselves to the new positions of the nuclei. This simplifies the above expression for Hamiltonian operator as the motions of the electrons are separated from the motion of the nuclei. When the Hamiltonian operator for the electrons is considered, the term for the kinetic energy of the nuclei is neglected, and

the term for the nuclear repulsion can be consider as constant. Therefore, the electronic Hamiltonian becomes:

$$\mathscr{H}_{\text{elec}} = -\sum_{i=1}^{N}\frac{1}{2}\nabla_i^2 - \sum_{i=1}^{N}\sum_{A=1}^{M}\frac{Z_A}{r_{iA}} + \sum_{i=1}^{N}\sum_{j<i}^{N}\frac{1}{r_{ij}} \tag{1.3}$$

This allows the evaluation of the electronic Schrödinger equation:

$$\mathscr{H}_{\text{elec}}|\Psi_{\text{elec}}\rangle = \mathscr{E}_{\text{elec}}|\Psi_{\text{elec}}\rangle \tag{1.4}$$

The electronic wavefunction Ψ_{elec} depends explicitly on the coordinates of the electrons, and parametrically on the nuclear coordinates, as when the nuclei are moved Ψ_{elec} becomes a different function describing the motion of the electrons. The total energy of the system has to take into account the nuclei repulsion term:

$$\mathscr{E}_{\text{tot}} = \mathscr{E}_{\text{elec}} + \sum_{A=1}^{M}\sum_{B<A}^{M}\frac{Z_A Z_B}{R_{AB}} \tag{1.5}$$

1.1.2 Variational Principle

The Schrödinger equation cannot be solved exactly except for very simple problems. Therefore approximate solutions must be found. An infinite number of exact solutions to the Schrödinger equation exist:

$$\mathscr{H}|\Psi_\alpha\rangle = \mathscr{E}_\alpha|\Psi_\alpha\rangle; \alpha = 0, 1, 2, 3... \tag{1.6}$$

where $\mathscr{E}_0$ is the lowest eigenvalue, and each subsequent eigenvalue is either greater than or equal to the previous eigenvalue and the eigenvectors Ψ_α form a complete set.

The Hamiltonian operator $\mathscr{H}$ is Hermitian, and therefore has the properties that the eigenvalues are real and the eigenvectors are orthogonal. The eigenvectors are also chosen to be normalised.

$$\langle\Psi_\alpha|\Psi_\alpha\rangle = 1 \tag{1.7}$$

$$\langle\Psi_\alpha|\Psi_\beta\rangle = 0 \tag{1.8}$$

Here, *bra-ket* notation has been introduced, where the *bra* $\langle\Psi_\alpha|$ denotes a specific complex conjugate wavefunction, and the *ket* $|\Psi_\beta\rangle$ denotes a different wavefunction, and the whole *bracket* denotes that the expression should be integrated over all coordinates.

A consequence of Ψ_α forming a complete set, is that any normalised wavefunction Φ can be expressed as a linear combination of Ψ_α:

$$\begin{aligned} |\Phi\rangle &= \sum_\alpha c_\alpha |\Psi_\alpha\rangle \\ &= \sum_\alpha |\Psi_\alpha\rangle\langle\Psi_\alpha|\Phi\rangle \end{aligned} \tag{1.9}$$

Therefore, the expectation value of the Hamiltonian with the wavefunction Φ becomes:

$$\langle\Phi|\mathscr{H}|\Phi\rangle = \sum_{\alpha\beta}\langle\Phi|\Psi_\alpha\rangle\langle\Psi_\alpha|\mathscr{H}|\Psi_\beta\rangle\langle\Psi_\beta|\Phi\rangle \tag{1.10}$$

As Ψ_α form an orthonormal set, $\langle\Psi_\alpha|\mathscr{H}|\Psi_\beta\rangle = \mathscr{E}_\alpha\delta_{\alpha\beta}$ and hence the above expectation value can be expressed as:

$$\begin{aligned} \langle\Phi|\mathscr{H}|\Phi\rangle &= \sum_\alpha \mathscr{E}_\alpha |\langle\Psi_\alpha|\Phi\rangle|^2 \\ &= \sum_\alpha \mathscr{E}_\alpha |c_\alpha|^2 \end{aligned} \tag{1.11}$$

Given that all $\mathscr{E}_\alpha \geq \mathscr{E}_0$ this leads to the variational principle that for any normalised wavefunction Φ that satisfies the same boundary conditions as the set Ψ_α, the expectation value of the Hamiltonian operator will give an upper bound to the exact ground state energy, that is:

$$\langle\Phi|\mathscr{H}|\Phi\rangle \geq \mathscr{E}_0 \tag{1.12}$$

This is a very useful principle, as a trial wavefunction can be guessed as a linear combination of eigenstates of the Hamiltonian and the energy minimised with respect to the parameters c_α and an upper bound to the exact ground state energy will be obtained. As the expectation value has the term $|c_\alpha|^2$ the error in energy will be of the order of the error in the wavefunction squared, therefore it is possible to obtain a very good estimate of the energy with a fair guess of the initial wavefunction.

If only linear combinations of eigenstates are considered, the eigenvalue problem can be expressed in matrix form:

$$\underline{\underline{H}}\underline{c} = E\underline{c} \tag{1.13}$$

where $\underline{c}$ is a vector of coefficients of the finite set of N basis functions. The Hamiltonian matrix $\underline{\underline{H}}$ is symmetric as the Hamiltonian operator is Hermitian and the basis functions are real and orthonormal, and of dimension $N \times N$. This is then solved by diagonalising the matrix, with the lowest eigenvalue obtained an upper bound to the exact ground state energy.

1.2 Wavefunctions for Many Electron Systems

1.2.1 Orbitals

An orbital ψ is defined as a wavefunction for a single electron. In the Born interpretation of quantum mechanics, $\psi^*\psi$ is a real function interpreted as a probability distribution. A spatial orbital, $\psi(\mathbf{r})$ is a function of the position of the electron. The position of the electron is continuous, it cannot be pinned down to a single location, therefore $\psi(\mathbf{r})^*\psi(\mathbf{r})d\mathbf{r}$ is interpreted as the probability of finding an electron in the volume element $d\mathbf{r}$. The spatial orbitals form an orthonormal set, that is:

$$\int d\mathbf{r}\psi_i(\mathbf{r})^*\psi_j(\mathbf{r}) = \delta_{ij} \tag{1.14}$$

To completely define the wavefunction for a single electron, the spin function must also be included. In the presence of an external magnetic field the spin quantum number, 1/2, of the electron can be in one of two states. Firstly it can be aligned with the field denoted by α spin, or be aligned opposing the direction of the external magnetic field, denoted β spin. These spin functions also have orthonormal conditions:

$$\int d\omega\, \alpha^*(\omega)\alpha(\omega) = \int d\omega\, \beta^*(\omega)\beta(\omega) = 1 \tag{1.15}$$

$$\int d\omega\, \beta^*(\omega)\alpha(\omega) = \int d\omega\, \alpha^*(\omega)\beta(\omega) = 0 \tag{1.16}$$

A wavefunction that describes both the spatial distribution and the spin is described as a spin orbital, $\phi(\mathbf{r},\omega) = \phi(\mathbf{x})$.

1.2.2 Slater Determinants

The total electronic wavefunction must be antisymmetric with respect to changing any two electron coordinates. This is a consequence of the Pauli Principle that no two electrons can have all quantum numbers equal. An antisymmetric wavefunction can be

achieved by building it from Slater Determinants:

$$\Phi_{\mathrm{SD}} = \frac{1}{\sqrt{N!}} \begin{vmatrix} \phi_1(1) & \phi_2(1) & \dots & \phi_N(1) \\ \phi_1(2) & \phi_2(2) & \dots & \phi_N(2) \\ \dots & \dots & \dots & \dots \\ \phi_1(N) & \phi_2(N) & \dots & \phi_N(N) \end{vmatrix} \tag{1.17}$$

In this equation, $\frac{1}{\sqrt{N!}}$ is the normalisation factor, the rows are labelled by electrons, and the columns are labelled by spin-orbitals. If any two rows or columns in the Slater Determinant are swapped, the sign of the determinant will change, and if any two rows or columns are the same the Determinant will take the value zero. Thus, a Slater Determinant obeys the antisymmetry principle and the Pauli exclusion principle. By using Slater Determinants the probability distribution for two electrons with the same spin is correlated, but if the electrons have opposing spins there is no correlation.

Configuration State functions

As the electronic Hamiltonian is spin-independent, the wavefunction should be an eigenfunction of the S_z and S^2 spin operators. A single Slater Determinant is only a spin eigenfunction for high spin and closed-shell, that is all paired electrons, systems. By taking linear combinations of Slater Determinants, a wavefunction that is a spin eigenfunction can be constructed. These are termed configuration state functions.

1.3 Hartree-Fock

The Hartree-Fock (HF) approximation uses a single Slater Determinant to describe the ground state, or lowest energy state, wavefunction of an N-electron system of interest. This simple approximation is fundamental in quantum chemistry, as it leads to the approximation that electrons occupy molecular orbitals, as well as being a starting point for more advanced quantum chemical methods that include the effects of electron correlation more accurately. By utilising the variational principle and minimising the energy with respect to the choice of spin-orbitals, the Hartree-Fock eigenvalue equation can be

derived:

$$f(i)\phi(\mathbf{x_i}) = \varepsilon\phi(\mathbf{x_i}) \tag{1.18}$$

Where $f(i)$ is the Fock operator that reduces a many electron operator to a one electron operator by averaging the electron-electron repulsion:

$$f(i) = -\frac{1}{2}\nabla_i^2 - \sum_{A=1}^{M}\frac{Z_A}{r_{iA}} + \sum_j J_j(i) - K_j(i) \tag{1.19}$$

The first two terms are recognisable from the Hamiltonian operator for electrons, Eq.(1.3) as being the kinetic energy of the electrons and the Coulombic term from the electrons interacting with the nuclei. The final two terms in the above equation arise from electron-electron interactions.

$J_j(i)$ is the coulomb operator, that arises from the coulomb repulsion experienced by the electron in the ith spin orbital ϕ_i with an electron in the jth spin orbital:

$$J_i(1)\phi_j(1) = \left[\int d\mathbf{x}_2\phi_i^*(2)r_{12}^{-1}\phi_i(2)\right]\phi_j(1) \tag{1.20}$$

$K_j(i)$ is the exchange operator, that arises for each unique pair of electrons that has parallel spins;

$$K_i(1)\phi_j(1) = \left[\int d\mathbf{x}_2\phi_i^*(2)r_{12}^{-1}\phi_j(2)\right]\phi_i(1) \tag{1.21}$$

The probability of finding two electrons of parallel spin in the same place is zero by the Pauli exclusion principle. The motion of parallel spins are said to be correlated. However, the same is not true in this approximation for pairs of electrons that have opposing spins, which remain uncorrelated.

The effect of the sum in Eq.(1.19) is to average the potential that the ith electron feels from the $N-1$ remaining electrons. The coulomb and exchange integrals for the ith electron depend on the spin orbitals of the remaining electron spin orbitals, therefore the Hartree-Fock equations are non-linear and must be solved iteratively. This involves taking an initial guess of the spin-orbitals and then solving the eigenvalue equation to obtain a new set of orbitals. This process is repeated until a consistent result is obtained. The optimisation of the orbitals must be constrained so that the orbitals remain orthonormal.

1.3.1 Roothaan-Hall Equations

For closed-shell molecules, the spin-orbitals can be restricted so that they have the same spatial functions for both α and β spins, leading to $N/2$ spatial orbitals, each doubly occupied where N is the number of electrons. This allows the Hartree-Fock equation to be written in terms of spatial orbitals by integrating out spin, and with the Fock operator given by:

$$f(\mathbf{r_1})\psi_i(\mathbf{r_1}) = \varepsilon_i\psi_i(\mathbf{r_1}) \tag{1.22}$$

$$f(1) = h(1) + \sum_{j}^{N/2} 2J_j(1) - K_j(1) \tag{1.23}$$

where $h(1)$ is the first two terms in Eq.(1.19) for the kinetic energy of the electrons and the coulomb interaction of the electrons with the nuclei, and the J and K terms are the coulomb and exchange integrals for the electron-electron interactions.

Roothaan [1] showed that by introducing a basis of known spatial functions, $\chi_a(\mathbf{r})$ to describe the unknown spatial molecular orbitals, $\psi_i(\mathbf{r})$, the differential equations could be converted into alegbraic equations and solved using matrix techniques:

$$\psi_i(\mathbf{r}) = \sum_{a}^{K} c_{ia}\chi_a(\mathbf{r}) \quad a = 1, 2, \ldots, K \tag{1.24}$$

The set of expansion coefficients c_{ia} must be found instead of solving the Hartree-Fock equations for the molecular orbitals. In practice the basis expansion is limited to a set K of known spatial functions. If the set K were complete the spatial functions would coincide with the exact molecular spatial orbitals ψ_i.

By substituting the linear basis expansion Eq.(1.24) for the spatial molecular orbitals into the Hartree-Fock equation, Eq.(1.22) , multiplying on the left by $\chi_b(\mathbf{r})$ and integrating, the Roothaan equations are obtained:

$$\mathbf{FC} = \mathbf{SC}\varepsilon \tag{1.25}$$

$\mathbf{C}$ is a $K \times K$ matrix containing the coefficients of the basis spatial functions, and ε is a diagonal matrix containing the orbital energies. The elements of the overlap matrix $\mathbf{S}$ are evaluated from:

$$S_{ab} = \int d\mathbf{r}\chi_a^*(1)\chi_b(1) \tag{1.26}$$

The basis functions are usually normalised but not necessarily orthogonal so the diagonal elements of **S** are 1 and the off diagonal elements have a magnitude less than one. The **S** matrix is Hermitian, and usually real and symmetric.

The elements of the Fock matrix, F are given by:

$$F_{ab} = \int d\mathbf{r_1} \chi_a^*(1) f(1) \chi_b(1) \tag{1.27}$$

The Fock matrix is also Hermitian, which is the matrix representation of the Fock operator $f(1)$ with the basis expansion of the molecular spatial orbitals. The Fock operator depends on the charge density matrix of the set of basis functions.

1.3.2 Basis Sets

There are many choices of basis functions that can be used to describe the molecular orbitals for performing calculations on molecules. In principle, any function can be used, such as a polynomial, exponential, plane wave or gaussian function. There are two principle considerations. Firstly, the functions should be able to describe the physics of the problem accurately and as such should tend to zero as the distance between the nucleus and electron becomes large. This will ensure that as the number of functions used to describe the molecular orbitals is increased convergence to the exact answer will be rapid. Secondly, the functions chosen should make the integrals relatively straightforward to calculate.

In this thesis several classes of basis set are used. Firstly, the STO-3G basis set [2] is used for calculations involving accurate methods for accounting for electron correlation such as full configuration interaction (FCI) for reasons of computational cost. In this basis set a Slater type orbitals is approximated with three primitive gaussian type orbitals. Slater type orbitals (STOs) have the following form in spherical coordinates:

$$\chi_{\zeta,n.l.m}(r,\theta,\rho) = N Y_{l,m}(\theta,\rho) r^{n-1} \exp(-\zeta r) \tag{1.28}$$

where N is a normalisation constant and $Y_{l,m}(\theta,\rho)$ are the spherical functions. The exponential dependence on the distance r between the nuclei and electrons ensures that the

STOs replicated the exact orbitals for a hydrogen atom, and by taking linear combinations of STOs radial nodes are introduced. The drawback to these type of functions is that the two-electron integrals for three or more centres cannot be performed analytically.

Gaussian type orbitals (GTOs) have the following form in spherical coordinates:

$$\chi_{\zeta,n.l.m}(r,\theta,\rho) = NY_{l,m}(\theta,\rho)r^{n-1}\exp(-\zeta r^2) \tag{1.29}$$

The exponential term now has r^2 dependence leading to a greater number of GTO needed to be able to describe the molecular orbitals to a given degree of accuracy in comparison to STOs. However, the electron-integrals are more easily calculated, making these orbitals computationally more efficient.

The larger basis sets, 6-31G [3] and 6-31G* are split basis sets, where the core orbitals are a contraction of 6 primitive GTOs, the inner part of the valence orbitals are a contraction of 3 primitive GTOs and the outer orbitals are represented by a single primitive GTO. This basis set has more primitive GTOs to describe the valence orbitals in comparison to the STO-3G basis set. The presence of a * indicates that a polarisation function has been added to the basis set, in this case a single set of d-functions to heavy atoms. These types of functions can help to describe the nonuniform field arising from the non-spherical environment in a molecule.

The final type of basis sets used here are the correlation consistent basis sets of Dunning [4] termed cc-pVXZ where X can be D, T, Q corresponding to double, triple, quadruple etc. These basis sets are designed to recover consistently the correlation in the valence electrons, by adding polarisation functions that have similar contributions to the correlation energy at the same stage. For example the addition of a single d-function lowers the energy significantly, but the addition of a second d-function lowers the energy by a similar amount to adding an f-orbital, so these two functions will be added at the same stage.

1.4 Electron Correlation

The motion of electrons is correlated, in that the instantaneous position of an electron is dependent on the other electrons in the system. In the Hartree Fock (HF) method the

electrons feel the average force of the other electrons, but in reality electrons avoid each other more than the HF description suggests. The correlation energy is defined as the difference between the HF energy and the exact energy:

$$E_{\text{corr}} = E_{0\text{exact}} - E_{0\text{HF}} \tag{1.30}$$

1.4.1 Static Correlation

Correlation is important as without properly accounting for the electron correlation, a method can give qualitatively incorrect results. This is the case with the Restricted HF method when molecules dissociate to open-shell products. Considering the H_2 molecule, the wavefunction is given by:

$$\Psi = \hat{\mathscr{A}}^2 \sigma_g^\alpha(1)\sigma_g^\beta(2) \tag{1.31}$$

where $\mathscr{A}$ is the antisymmetry operator, and the bonding orbital, σ_g is given by;

$$\sigma_g = c_g(\chi_A + \chi_B) \tag{1.32}$$

where c is a normalisation factor, and χ_X is a basis function centred on the atom X. When the bond in the Hydrogen molecule is stretched to infinity, χ_A becomes like an s-shaped orbital centred on atom A, and similarly for χ_B and the normalisation factor goes to $1/\sqrt{2}$. Therefore the RHF wavefunction becomes:

$$\Psi = 2\hat{\mathscr{A}}^2(1s_A^\alpha 1s_B^\beta + 1s_B^\alpha 1s_A^\beta + 1s_A^\alpha 1s_A^\beta + 1s_B^\alpha 1s_B^\beta) \tag{1.33}$$

The first two of these terms contain an electron on each atom centre, which is expected when H_2 dissociates. However, the final two terms are ionic, both the electrons are either on atom A or atom B. This leads to an overestimation of the energy, and a qualitatively incorrect potential energy curve.

The problem can be overcome by using Unrestricted orbitals in the Hartree Fock equations. With unrestricted orbitals there is a set of spatial orbitals for electrons with α spin and a second set with β spin, rather than the restricted case of one set of orbitals doubly occupied with a pair of electrons with opposing spins. The unrestricted orbitals, ψ_α and ψ_β are written as a linear combination of both the bonding σ_g and the anti-bonding σ_u

restricted molecular orbital:

$$\sigma_g = c_g(\chi_A + \chi_B) \qquad \sigma_u = c_u(\chi_A - \chi_B) \tag{1.34}$$

$$\psi_\alpha = cos\theta\,\sigma_g + \sin\theta\,\sigma_u \quad \psi_\beta = -\sin\theta\,\sigma_u + \cos\theta\,\sigma_g \tag{1.35}$$

These orbitals will give the correct solutions at infinite separation of an electron located onto each atom centre and no ionic terms. The drawback of using an unrestricted set of orbitals for the Hartree-Fock equations is that the wavefunction is no longer a spin eigenfunction, and are thus the UHF wavefunction is said to be spin contaminated with higher spin-states. A more detailed analysis of how this arises and how it can effect the results of calculations is in Chapter 3.

This type of correlation is often referred to as static correlation or long range correlation. It occurs when molecules dissociate to open shell products, and other cases where a single reference wavefunction is a poor description of the wavefunction when multiple states become near degenerate. The methods used to correct for this type of correlation are based on having a multi-reference wavefunction.

1.4.2 Dynamic Correlation

Electron correlation is important even when HF appears to give reasonable results, for example at equilibrium bond lengths. The terms involving the electron-electron interaction involve r_{12}^{-1} terms. As such when the interelectronic distance, r_{12} tends to zero, these terms have a large effect on the energy as they become singular. However, $E\Psi$ in Schrödinger's equation is well behaved, therefore Coulombic singularities must cancel out. There are terms in the kinetic energy that provide additional singularities in $\mathscr{H}\Psi$ to cancel out the Coulombic singularities, leading to the nuclear and interelectronic cusp conditions for electrons with opposing spins:

$$\left.\frac{\partial\Psi}{\partial r_i}\right|_{r_i=0} = -Z\Psi(r_i = 0); \qquad \left.\frac{\partial\Psi}{\partial r_{12}}\right|_{r_{ij}=0} = \frac{1}{2}\Psi(r_{12} = 0) \tag{1.36}$$

The interelectronic cusp condition for same spin electrons is given by:

$$\left.\frac{\partial\Psi}{\partial r_{12}}\right|_{r_{ij}=0} = \frac{1}{4}\Psi(r_{12} = 0) \tag{1.37}$$

The Hartree-Fock wavefunction does not depend on r_{12}^{-1} near $r_{12} = 0$ and therefore overestimates the probability of finding two electrons very close together, leading to an underestimation of the electron-electron repulsion energy. This leads to overestimation of bond lengths and underestimations of the binding energy.

The dynamic correlation is important for electrons with opposing spins, incorporation of the Pauli Principle by a Slater Determinant representation of the wavefunction leads to the correct behaviour for electrons with parallel spins, termed Fermi correlation. Dynamic correlation is a short range effect. Post Hartree-Fock methods such as perturbation methods, configuration interaction and coupled cluster methods can account for this correlation.

1.5 Single- and Multi-Reference Methods

There are shortcomings to using the Hartree-Fock method for quantum chemical calculations because the HF method does not account for electron correlation. The following methods go beyond the HF method. A single reference method is defined to be a method that uses a single configuration to define the molecular orbitals used to make the wavefunction, and only the basis functions are varied to optimise the molecular orbitals. In a multi-reference method the wavefunction is built from a linear combination of electron configurations to approximate the exact electronic wavefunction. Both the set of coefficients for the configuration functions and the basis functions in the molecular orbitals are varied to obtain an optimised wavefunction that gives the lowest possible energy.

1.5.1 Configuration Interaction

In the HF approximation, the a single Slater Determinant is used to describe the wavefunction built from N occupied molecular spin-orbitals. By replacing one or more of the occupied molecular spin orbitals in the HF determinant by a virtual orbital a whole series of different Slater determinants can be obtained. These are denoted by singly (S), doubly (D), triple(T) etc excited Slater determinants.

In the Configuration Interaction method the trial wavefunction is built using a linear combination of Slater Determinants:

$$\Psi_{\mathrm{CI}} = c_0\Phi_0 + \sum_S c_S\Phi_S + \sum_D c_D\Phi_D \ldots \tag{1.38}$$

Φ_S is a Slater determinant with one virtual MO in comparison with the HF Slater Determinant Φ_0. The coefficients c_0, c_S, c_D etc are found by minimising the energy with respect to these parameters.

The CI wavefunction can also be written in operator form:

$$\Psi_{\mathrm{CI}} = (1+\hat{C})|\Phi_0\rangle \tag{1.39}$$

$$\hat{C} = \sum_{ia} c_a^i a^\dagger i + \sum_{ijab} c_{ab}^{ij} a^\dagger b^\dagger j i + \ldots \tag{1.40}$$

where Φ_0 is a reference wavefunction usually HF, and the excitation operator that generates the Slater determinants for different excited states $\hat{C}$ is given in terms of annihilation and creation operators, where i destroys an electron from an occupied molecule orbital i in the reference function and $a^\dagger$ creates an electron in a virtual orbital a in its place in the reference wavefunction. The first term in $\hat{C}$ creates all the singly excited Slater Determinants from the reference wavefunction, and the second term the doubly excited states. The operator $\hat{C}$ potentially holds up to N-fold excitations, where N is the number of electrons.

This leads to the following variational energy functional:

$$E = \frac{\langle\Phi_0|(1+\hat{C}^\dagger)\hat{H}(1+\hat{C})|\Phi_0\rangle}{1+\langle\Phi_0|\hat{C}^\dagger\hat{C}|\Phi_0\rangle} \tag{1.41}$$

The optimisation that is performed is constrained so that the CI wavefunction Ψ_{CI} is normalised. The variational procedure works by setting the derivative of the energy with respect to the expansion coefficients to zero. This generates a set of equations of the same number as there are unknown parameters, allowing the problem to be cast as a set of secular equations and solved using matrix algebra:

$$(\mathbf{H} - E\mathbf{I})\mathbf{c} = 0 \tag{1.42}$$

where $\mathbf{c}$ is a vector containing all the expansion coefficients. These can be solved by diagonalising the CI matrix with the lowest eigenfunction corresponding to the ground state energy, and the eigenvector will contain the expansion coefficients.

The Slater Determinants corresponding to excited states are not necessarily eigenfunctions of the $\hat{S}^2$ operator. Therefore Configuration State Functions (CSFs) are used instead, composed of combinations of Slater Determinants that are proper eigenfunctions. CSFs can also be symmetry adapted so that each of the functions has the same symmetry requirement as the overall wavefunction. Thus, if one is interested in the ground state wavefunction, only determinants with the same symmetry will contribute. These considerations will reduce the size of the CI matrix.

If Ψ_{CI} contains all the possible excitations for a given system, then the CI wavefunction is capable of representing the exact wavefunction of the basis set used. Such a calculation is term Full Configuration Interaction (FCI). Unfortunately these calculations are impractical except for small systems and employing small basis sets. This is because the number of CSFs grows factorially with the number of basis functions. Therefore CI expansions are usually truncated to a given level of excitations that are included. Most commonly, the CISD method is used which includes single and double excitations relative to the reference wavefunction. This method scales as N^6 where N is a measure of the system size.

Size Extensivity and Size Consistency

When the CI wavefunction is truncated it is no longer size extensive or size consistent. Size extensivity refers to whether the method scales properly with system size. A lack of size extensivity means that as systems get larger less electron correlation is recovered. A method is size consistent if the energy obtained for a system of two identical fragments at infinite separation is twice that of one fragment. It can be shown that for CID method considering two infinitely separated hydrogen molecules in a minimal basis this is not the case.

Labelling the two hydrogen molecules A and B, the bonding orbitals σ_g and the antibonding orbitals σ_u, the CID wavefunction for the two hydrogen molecules at infinite separation is:

$$\Psi_{\mathrm{CID}} = |\sigma_{gA}^{\alpha}\sigma_{gA}^{\beta}\sigma_{gB}^{\alpha}\sigma_{gB}^{\beta}\rangle + c_1|\sigma_{uA}^{\alpha}\sigma_{uA}^{\beta}\sigma_{gB}^{\alpha}\sigma_{gB}^{\beta}\rangle + c_2|\sigma_{gA}^{\alpha}\sigma_{gA}^{\beta}\sigma_{uB}^{\alpha}\sigma_{uB}^{\beta}\rangle \qquad (1.43)$$

The CID wavefunction for a hydrogen molecule is:

$$\Psi_{\mathrm{CI}} = |\sigma_{gA}^{\alpha}\sigma_{gA}^{\beta}\rangle + c_1|\sigma_{uA}^{\alpha}\sigma_{uA}^{\beta}\rangle \tag{1.44}$$

The product of two infinitely seperated hydrogen molecules is given by:

$$\begin{aligned}\Psi_{A\mathrm{CI}}\Psi_{B\mathrm{CI}} &= (|\sigma_{gA}^{\alpha}\sigma_{gA}^{\beta}\rangle + c_{1A}|\sigma_{uA}^{\alpha}\sigma_{uA}^{\beta}\rangle)(|\sigma_{gB}^{\alpha}\sigma_{gB}^{\beta}\rangle + c_{1B}|\sigma_{uB}^{\alpha}\sigma_{uB}^{\beta}\rangle) \\ &= |\sigma_{gA}^{\alpha}\sigma_{gA}^{\beta}\sigma_{gB}^{\alpha}\sigma_{gB}^{\beta}\rangle + c_{1B}|\sigma_{gA}^{\alpha}\sigma_{gA}^{\beta}|\sigma_{uB}^{\alpha}\sigma_{uB}^{\beta}\rangle + c_{1A}|\sigma_{uA}^{\alpha}\sigma_{uA}^{\beta}\sigma_{gB}^{\alpha}\sigma_{gB}^{\beta}\rangle \\ &+ c_{1A}c_{1B}|\sigma_{uA}^{\alpha}\sigma_{uA}^{\beta}\sigma_{uB}^{\alpha}\sigma_{uB}^{\beta}\rangle\end{aligned} \tag{1.45}$$

The CID wavefunction for the two hydrogen molecules at infinite separation Eq. (1.43) is missing the contribution from the quadruple excitation that is present in the exact answer given in Eq. (1.45), leading to the truncated method to be size inconsistent. As the number of electrons in the system increases size consistency becomes increasingly more important.

Multi-Configurational Self-Consistent Field

The CI method discussed so far is a single reference method that is based on excitations from a single reference Slater determinant, usually a Hartree-Fock wavefunction. There are cases for which the RHF wavefunction is not a good starting point for a CI calculation. For open shell molecules an unrestricted Hartree-Fock wavefunction has the potential to be used instead, except this wavefunction is usually spin-contaminated with states of a higher spin multiplicity. The Hartree-Fock wavefunction is also not a good starting point where more than one configuration of the electrons in the molecular orbitals with differing energies is need to accurately describe the ground state. In these cases using a multi-reference wavefunction is more appropriate as multiple configurations are included.

The idea behind Multi-Configurational Self-Consistent Field [5–8] is to optimise the energy by using a truncated CI expansion and optimising both the coefficients and the molecular orbitals contained in $|\Psi_I\rangle$:

$$|\Psi_{\mathrm{MCSCF}}\rangle = \sum_I |\Psi_I\rangle \tag{1.46}$$

If only one configuration is included in the MCSCF wavefunction, then it is simply the HF wavefunction. The equations needed to solve the MCSCF wavefunctions are more

complicated than the HF case and similarly they are solved iteratively. Initial implementations involved a two step process of first performing a limited CI calculation to obtain the expansion coefficients, and then optimising the orbitals, whilst keeping the expansion coefficients fixed. Subsequently formalisms were developed where the molecular orbitals and expansion coefficients were determined simultaneously by using unitary transformations of the molecular orbitals and coefficients [9].

Increasing the number of configurations included in the MCSCF wavefunction increases the number of iterations needed to get a consistent answer. Care must also be taken that the MCSCF wavefunction has converged to a minimum rather than just a stationary point. The optimisation procedure therefore involves expanding the energy to second order in the orbital and configurational coefficients [10, 11]. MCSCF wavefunctions are used to recover the static correlation associated with having a qualitatively correct wavefunction if not necessarily quantitative. The CSFs used in the MCSCF wavefunction are pure spin states, and therefore it is not spin contaminated unlike UHF wavefunction. One of the main difficulties with MCSCF is deciding which configurations to use in the expansion.

Complete Active Space Self-Consistent Field

One method for choosing the configurations to be included is to divide the space into active and inactive spaces which is the idea in the Complete Active Space Self-Consistent Field (CASSCF) approach [12–14]. The active orbitals will consist of some of the highest occupied molecular orbitals and some of the lowest unoccupied molecular orbitals. In this space an FCI calculation is carried out. The remaining orbitals will be doubly occupied or unoccupied from an RHF calculation. The choice of molecular orbitals included in the active space depends on the system that is of interest, and the computational cost. These CASSCF calculations can become very large very quickly. There are other methods that divide the space up into more sections, so that for some of the space all possible configurations are considered and for others only single or double excitations from the reference are considered.

Multi-Reference Configuration Interaction

As well as using a Hartree-Fock wavefunction as the reference wavefunction from which a CI calculation can be performed to generate excited configurations, an MCSCF wavefunction can also be used. A CI calculation is performed on all the determinants that enter the MCSCF reference wavefunction. For example a MRCISD calculation will generate all the single and double excitations on all the determinants in the MCSCF reference wavefunction. By using a combination of MCSCF and CISD a quantitatively good description of potential energy surfaces can be obtained. The size of the configuration expansion and the computational cost increases rapidly with the number of configurations in the reference. Schemes for truncating the configurations included are therefore required. There has been much development of MRCISD methods so that larger numbers of configurations can be included in the reference more efficiently via direct CI procedures [15, 16], contraction of the configuration expansion [17] and efficient methods of calculating the coupling coefficients each time that they are needed [18, 19].

Brillouin's Theorem

Brillouin's Theorem states that single excitations will not interact directly with a Hartree-Fock reference determinant, that is:

$$\langle \Phi_0 | H | \Phi_S \rangle = 0 \tag{1.47}$$

If a wavefunction composed of the Hartree-Fock reference determinant and single excitations is considered, the coefficients c_S are found by digonalising the Hamiltonian matrix:

$$\begin{pmatrix} \langle \Phi_0 | H | \Phi_0 \rangle & \langle \Phi_0 | H | \Phi_S \rangle \\ \langle \Phi_S | H | \Phi_0 \rangle & \langle \Phi_S | H | \Phi_S \rangle \end{pmatrix} \begin{pmatrix} c_0 \\ c_S \end{pmatrix} = E_0 \begin{pmatrix} c_0 \\ c_S \end{pmatrix} \tag{1.48}$$

The mixing of the singlet states with the ground states depends on the off diagonal elements, $\langle \Phi_0 | H | \Phi_S \rangle$. If the rules for evaluating matrix elements are used, these elements are simple the matrix elements of the Fock operator:

$$\langle \Phi_0 | H | \Phi_S \rangle = \langle \chi_i | f | \chi_a \rangle \tag{1.49}$$

Solving the Hartree-Fock eigenvalue problem requires that these elements $\langle\chi_i|f|\chi_j\rangle$ are zero. Therefore the lowest solution Eq. (1.48) is:

$$\begin{pmatrix} \langle\Phi_0|H|\Phi_0\rangle & 0 \\ 0 & \langle\Phi_S|H|\Phi_S\rangle \end{pmatrix} \begin{pmatrix} c_0 \\ 0 \end{pmatrix} = E_0 \begin{pmatrix} c_0 \\ 0 \end{pmatrix} \tag{1.50}$$

Therefore there is no mixing of the ground state with the single excited states, and the double excitations are expected to be the leading term in corrections to the Hartree-Fock wavefunction. However, single excitations will appear in the exact wavefunction, as the single excitations can indirectly mix with the ground state determinant via doubly excited determinants.

1.5.2 Electron Pair and Coupled Electron Pair Methods

A pair theory can be defined as any method that has as many two-electron functions as there are electron pairs. These types of theories are expected to approximate an N-electron system well because the Hamiltonian operator only contains one and two particle operators and the Pauli Principle prevents three electrons occupying the same spatial orbital.

The Independent Electron Pair Approximation

The simplest electron pair approach is to form correlation wavefunctions from a pair of electrons, and ignore the remaining electrons:

$$\Psi_{ij} = |\Phi_0\rangle + \sum_{a<b} c_{ij}^{ab}|\Phi_{ij}^{ab}\rangle \tag{1.51}$$

Only the electrons labelled i and j are correlated by exciting them from occupied orbitals to virtual orbitals labelled a, b. In so doing, the pair functions are independent of any other electron pairs in the system. The energy for the electron pair ij is given by;

$$E_{ij} = \langle\Phi_0|\hat{H}|\Phi_0\rangle + \sum_{a<b} c_{ij}^{ab}\langle\Phi_0|\hat{H}|\Phi_{ij}^{ab}\rangle \tag{1.52}$$

The first term is just the Hartree-Fock energy. The second term is the pair correlation energy. To find the best possible energy for this pair function, the variational method is

applied, and the equation put into matrix form such that:

$$\begin{pmatrix} 0 & \mathbf{B}_{ij}^{\dagger} \\ \mathbf{B}_{ij} & \mathbf{D}_{ij} \end{pmatrix} \begin{pmatrix} 1 \\ \mathbf{c}_{ij} \end{pmatrix} = E_{ij} \begin{pmatrix} 1 \\ \mathbf{c}_{ij} \end{pmatrix} \tag{1.53}$$

where:

$$(\mathbf{B}_{ij})_{ab} = \langle \Phi_{ij}^{ab} | H | \Phi_0 \rangle \qquad (\mathbf{D}_{ij})_{ab,cd} = \langle \Phi_{ij}^{ab} | H | \Phi_{ij}^{cd} \rangle \qquad (\mathbf{c}_{ij})_{ab} = c_{ij}^{ab} \tag{1.54}$$

This is not the same as CID as the method does not involve any terms such as $\langle \Phi_{ij}^{ab} | H | \Phi_{kl}^{cd} \rangle$ which makes the matrices smaller than for CID. There is a matrix for each electron pair, so the independent electron pair method (IEPA) [5, 20] is equivalent to doing a CID calculation for each pair separately. As the total correlation energy is just the sum of the pair energies the method is size extensive. The method is neither variational, which means it will not give an upper bound to the energy, nor is it invariant to unitary transformations of the occupied spin orbitals. This means if the occupied spin orbitals are transformed among themselves the total energy from the IEPA method will be different.

Coupled Electron Pair Approximation

The Coupled Electron Pair approximation (CEPA) addresses the lack of $\langle \Phi_{ij}^{ab} | H | \Phi_{kl}^{cd} \rangle$ type terms in IEPA that couple the electron pair functionals. These terms add dependence of the remaining electron pairs kl to the pair ij. These coupling terms may be small for well localised electron pairs, but the same is not true for delocalised orbitals. IEPA does not give accurate results for systems with open-shells open shell states as this approximation does not describe delocalised electrons accurately [21, 22]. There are several variants of CEPA where the version is indicated by a number from 0-2. The following pair energy expression is that for CEPA(2) [5, 21]:

$$\langle \Phi_{ij}^{ab} | \hat{H} | \Phi_0 \rangle + \sum_{kl} \sum_{cd} c_{kl}^{cd} \langle \Phi_{ij}^{ab} | H | \Phi_{kl}^{cd} \rangle = E_{ij} c_{ij}^{ab} \tag{1.55}$$

Again, the total correlation energy is given as the sum of the pair energies, therefore CEPA(2) is also size consistent. CEPA equations must be solved iteratively because the equations contain coefficients of the other electron pairs, c_{kl}^{cd}.

The energy expression for the CEPA(1) method is given by [5,21]:

$$\langle\Phi_{ij}^{ab}|\hat{H}|\Phi_0\rangle + \sum_{kl}\sum_{cd} c_{kl}^{cd}\langle\Phi_{ij}^{ab}|H|\Phi_{kl}^{cd}\rangle = \langle\Phi_0|\hat{H}|\Phi_0\rangle c_{ij}^{ab} + \varepsilon_{ij}c_{ij}^{ab} + \frac{1}{2}\sum_{k}(\varepsilon_{ik}+\varepsilon_{kj})c_{ij}^{ab} \quad (1.56)$$

where ε_{ij} is the energy of the pair ij. In this formalism, both the pair energy, and a fraction of the pair energies arising from a pair that have orbitals in common with the pair under consideration are included. CEPA(0) is the same as Linear-CP-MET discussed in Section 1.5.3.

The CEPA series of methods do not give a hierachy of methods that converge to the Full CI method. Just like the IEPA method, the methods are still not invariant to unitary transformations of the occupied orbitals. There has been renewed interest in CEPA type methods [23], because of their simplicity in comparison to other single reference methods such as Coupled Cluster discused below, and because they give numerically quite accurate results for small molecules.

CEPA methods can be viewed from the perspective of modified CISD equations to restore size-consistency. Taking the CI wavefunction Eq. (1.38) truncated to double excitations, the variational equations with respect to the CI expansion coefficients become:

$$E = \langle\Phi_0|H|\Phi_0 + c_D\Phi_D\rangle = E_0 + E_{\text{corr}} \quad (1.57)$$

$$0 = \langle\Phi_D|H - E_0 - E_{\text{corr}}|\Phi_0 + c_D\Phi_D\rangle \quad (1.58)$$

Size-consistency is achieved by replacing E_{corr} by an excitation dependent shift Δ_{ab}^{ij}. This has the effect of restoring the unlinked quadruple contributions. In the case of CEPA(2) this shift is simply $-\Delta_{ab}^{ij} = \varepsilon_{ij}$ [23,24].

1.5.3 Coupled Cluster Ansatz

Separated Pairs

The wavefunction for an even number of N electrons in the separated pair approximation is given by [5]:

$$\Psi(1,2,3,\ldots,N) = \mathscr{A}[\omega_1(1,2)\omega_2(3,4)\ldots\omega_{N/2}(N-1,N)] \quad (1.59)$$

Here, $\mathscr{A}$ is the anti-symmetrisation operator and $\omega_R(i,j)$ are strongly orthogonal geminal or pair functions. Each pair function is expressed as a sum of one-electron approximations to ω_R and a pair correlation function $u_R(i,j)$ as follows:

$$\omega_R(1,2) = c_R \left\{ \phi_R(1)\phi_R(2)\frac{1}{\sqrt{2}}[\alpha(1)\beta(2) - \beta(1)\alpha(2)] + u_R(1,2) \right\} \tag{1.60}$$

By substituting this expression for ω_R into Eq. (1.59) and re-expressing in terms of second quantisation operators, the following wavefunction is obtained:

$$\Psi = c_o \exp\left(\sum_{i=1}^{N/2} \hat{a}_a^\dagger \hat{\bar{a}}_b^\dagger \hat{a}_j \hat{\bar{a}}_i \right) \Phi \tag{1.61}$$

where $\hat{a}^\dagger$ is a creation operator and $\hat{a}$ is an annihilation operator, and where bar denotes β spin.

The correlation energy is then given as the sum of the individual pair correlations energies:

$$E_{\text{corr}} = \sum_R \varepsilon_R \tag{1.62}$$

This wavefunction is capable of rigorously describing systems of electron pairs that are at infinite separation, and scales proportional to N meaning it is size extensive. However, this method does not give a good approximation for calculations involving atoms and molecules because it does not account for all of the electron correlation, and the orthogonality conditions for the pair functionals is too severe.

Coupled Cluster

The coupled cluster pair approximation can be thought of as an extension of the CISD wavefunction with the correct scaling of the energy with the number of electrons established by including 'unlinked' clusters of pair substitutions.

Thus the CCSD wavefunction is given by:

$$|\Psi_{\text{CCSD}}\rangle = \exp(\hat{T})|\Phi_0\rangle = \exp(\hat{T}_1 + \hat{T}_2)|\Phi_0\rangle \tag{1.63}$$

where the operators $\hat{T}_1$ and $\hat{T}_2$ has the form:

$$\hat{T}_1 = \sum_{i,a} t_i^a \hat{a}^\dagger \hat{i} \tag{1.64}$$

$$\hat{T}_2 = \sum_{i<j} \sum_{a<b} t_{ij}^{ab} \hat{a}^\dagger \hat{b}^\dagger \hat{j} \hat{i} \tag{1.65}$$

These operators are given in second quantisation terms, where $\hat{a}^\dagger$ is a creates an electron in the virtual orbital a and $\hat{i}$ is annihilates and electron from the occupied orbital i. The effect of $\hat{T}_1$ is therefore to perform a single excitation relative to the reference Slater Determinant and the amplitudes associated with the generation of these excited determinants ara given by t_i^a.

The expansion of $\hat{T}$ to only contain single and double excitations is a truncation of the more general coupled cluster wavefunction. The exponential form of the wavefunction introduces the unlinked cluster terms leading to contributions from triply, quadruply etc excited determinants compared with the reference Slater Determinant. This ensures that for a system of two non-interacting subsystems the wavefunction is the same as the anti-symmetrised product of the wavefunction of the subsystems, and is therefore size consistent.

The trial exponential wavefunction is substituted into the Schrödinger equation, and to obtain the expression for the energy is projected on the left by the reference wavefunction [25]:

$$\langle \Phi_0 | (\hat{H} - E_0) \exp(\hat{T}) | \Phi_0 \rangle = E_{\text{corr}} \langle \Phi_0 | \exp(\hat{T}) | \Phi_0 \rangle \tag{1.66}$$

By multiplying the Schrödinger equation with $\exp -\hat{T}$ a modified energy expression is obtained;

$$\langle \Phi_0 | \exp(-\hat{T}) \hat{H} \exp(\hat{T}) | \Phi_0 \rangle = E \tag{1.67}$$

The use of this similarity transformed Hamiltonian, $\exp(-\hat{T})\hat{H}\exp(\hat{T})$, decouples the energy expression from the set of equations for determining the cluster amplitudes.

To obtain the cluster coefficients t the Schrödinger equation is instead projected on the left with a manifold of excited states obtained by acting with individual cluster operators on the reference:

$$\langle \Phi_0 | \hat{q}^\dagger \exp(-\hat{T}) \hat{H} \exp(\hat{T}) | \Phi_0 \rangle = 0 \tag{1.68}$$

where $\hat{q}_{ia}$ the cluster operator is given in second quantisation terms as;

$$\hat{q}_{ia} = \hat{a}_a^\dagger \hat{a}_i \tag{1.69}$$

This is the most widely used ansatz for calculating the energy using an exponential wavefunction. It is both size-consistent and invariant to unitary transformation of occupied orbitals. The main obstacle to this method is that it is not variational. This can lead to qualitatively incorrect potential energy curves. Therefore it is desirable to find alternative ansatz to the projection method to determine the energy and properties of molecules. One aim of this thesis is to explore some of the alternative ansatz to the traditional coupled cluster method. A discussion on the different energy functionals can be found in Chapter 2.

Linear Coupled Pair Many Electron Theory

An alternative viewpoint for the coupled cluster approximation is to consider the coefficients for quadruple excitations as being approximated by coupling the coefficients of double excitations. This is not a simple product as there are many ways of obtaining the same quadruple excitation from independent double excitation.

$$c_{ijkl}^{abcd} \approx c_{ij}^{ab} * c_{kl}^{cd} = c_{ij}^{ab} c_{kl}^{cd} - \langle c_{ij}^{ab} * c_{kl}^{cd} \rangle \tag{1.70}$$

By assuming that the last term $\langle c_{ij}^{ab} * c_{kl}^{cd} \rangle$ is zero, the linear Coupled Pair Many Electron Theory (Linear-CPMET) is obtained [25]. The expression for the correlation energy then becomes:

$$\langle \Phi_{ij}^{ab} | \hat{H} | \Phi_0 \rangle + \sum_{kl} \sum_{cd} c_{kl}^{cd} \langle \Phi_{ij}^{ab} | H | \Phi_{kl}^{cd} \rangle = 0 \tag{1.71}$$

The above equation is very similar for that of CEPA(2) energy expression Eq. (1.55) only the correlation energy is set to zero, rather than the pair energy ε_{ij}. Therefore Linear-CPMET is also termed as CEPA(0).

Brueckner Orbitals

Brueckner Theory is a variation of Coupled Cluster theory where the orbitals used for constructing the Slater determinants are optimized in such a way that the contributions

from singles is exactly zero. Brillouin's theorem that single excitations do not mix with the ground state determinant, leads to the contributions from singles arising indirectly via double excitations, therefore the contribution of single excitations to the correlation energy is expected to be small.

The occupied orbitals are iteratively adjusted by the following formula so that the singly substituted configurations do not have any interaction with the correlated wavefunction [26]:

$$\chi_i' = \chi_i + \frac{1}{\sqrt{2}} \sum_a t_i^a \chi_a \tag{1.72}$$

where t_a^i are the expansion coefficients for the singly excited determinants, χ_i is an occupied orbital, and χ_a a virtual orbtial. After this the orbitals are reorthonormalised. This is an iterative process that is repeated until the contributions from singly excited determinants is zero. It has been noted that this process can be very slow to converge [27,28], and so alternatively unitary transformations have been proposed to speed up the convergence [27].

The Brueckner-doubles(BD) [29] equations are given by:

$$\langle \Phi_0 | H | (1 + T_2) \Phi_0 \rangle = E \tag{1.73}$$

$$\langle \Phi_i^a | H | (1 + T_2) \Phi_0 \rangle = 0 \tag{1.74}$$

$$\langle \Phi_{ij}^{ab} | H | (1 + T_2 + \frac{1}{2} T_2^2) \Phi_0 \rangle = t_{ij}^{ab} E \tag{1.75}$$

Here, E is the total energy, Φ_0 is a single determinant composed of Brueckner orbitals, Φ_i^a and Φ_{ij}^{ab} are the singly and doubly excited determinants. The use of Brueckner orbitals in BD simplifies the equations in comparison with CCSD or QCISD and evaluation of the BD energy gradient is simpler [29]. This method has also been extended to include the contributions from triple excitations [30,31]. Another advantage of Brueckner orbitals in the reference wavefunction is that they do not appear to suffer from symmetry-breaking as Hartree-Fock wavefunctions can [28]. Symmetry breaking is when a wavefunction does not transform as a pure irreducible representation of the molecular point group for non-degenerate electronic states.

Quadratic Configuration Interaction

The CISD equations can be expressed as follows using intermediate normalisation:

$$\langle \Phi_0 | H | \hat{C}_2 \Phi_0 \rangle = E_{\text{corr}} \tag{1.76}$$

$$\langle \Phi_i^a | H - E_0 | (\hat{C}_1 + \hat{C}_2 + \hat{C}_1 \hat{C}_2) \Phi_0 \rangle = c_i^a E_{\text{corr}} \tag{1.77}$$

$$\langle \Phi_{ij}^{ab} | H - E_0 | (1 + \hat{C}_1 + \hat{C}_2 + \hat{C}_2^2) \Phi_0 \rangle = c_{ij}^{ab} E_{\text{corr}} \tag{1.78}$$

The right sides of these expressions are quadratic in the c vectors, whereas the left hand sides only contain terms that are linear in the c vectors. This leads to the size inconsistency in the CISD method. Adding terms to the left hand side that are quadratic in the c vectors would be a way to correct this. This is the approach of Quadratic Configuration Interaction (QCISD) [32]. The equations of this method are:

$$\langle \Phi_0 | H | \hat{C}_2 \Phi_0 \rangle = E_{\text{corr}} \tag{1.79}$$

$$\langle \Phi_i^a | H - E_0 | (\hat{C}_1 + \hat{C}_2) \Phi_0 \rangle = c_i^a E_{\text{corr}} \tag{1.80}$$

$$\langle \Phi_{ij}^{ab} | H - E_0 | (1 + \hat{C}_1 + \hat{C}_2) \Phi_0 \rangle = c_{ij}^{ab} E_{\text{corr}} \tag{1.81}$$

This method loses the variational property of Configuration Interaction, but does have the property of size consistency which is regarded as the more important of the two properties. The method can be shown to be the same as CCD if single excitations are omitted from the QCISD equations. In comparison to CCSD, the QCISD misses term arising from $\hat{T}_1^3$ in Eq. (1.80) and $\hat{T}_1 \hat{T}_2$, $\hat{T}_1^3$ and $\hat{T}_1^4$ in Eq. (1.81) [32]. However, numerical results have shown that this method is competitive with CCSD, leading to the conclusion that the omitted terms have small impact on the energy.

1.5.4 Perturbation methods

A different method for finding the correlation energy of the system lies in Rayleigh-Schrödinger perturbation theory, where it is assumed that the problem is only slightly different to the problem that has been solved. The Hamiltonian operator is separated into two parts, the Hamiltonian H_0 for which the eigenvectors and eigenvalues are all ready know, and a perturbation part, $\mathscr{V}$, such that the Schrödinger equation can be expressed

as:

$$H_0 + \mathscr{V}|\Phi_i\rangle = E_i|\Phi_i\rangle \tag{1.82}$$

In order to create a procedure that systematically improves the eigenfunctions and values of H_0, an ordering parameter λ is introduced so that the Hamiltonian becomes:

$$H = H_0 + \lambda\mathscr{V} \tag{1.83}$$

The eigenfunctions Φ_i and eigenvalues E_i are then expressed as a Taylor series expansion in λ

$$E_i = E_i^{(0)} + \lambda E_i^{(1)} + \lambda^2 E_i^{(2)} + \ldots \tag{1.84}$$

$$|\Phi_i\rangle = |\Psi_i^{(0)}\rangle + \lambda|\Psi_i^{(1)}\rangle + \lambda^2|\Psi_i^{(2)}\rangle + \ldots \tag{1.85}$$

By subsituting Eqs.(1.84) and (1.85) into Eq.(1.82) and equating the terms with the same coefficient of λ^n a series of equations is produced for the different nth order of energy $E_i^{(n)}$ and the corrections to the wavefunction:

$$E_i^{(0)} = \langle\Psi_i^{(0)}|H_0|\Psi_i^{(0)}\rangle \tag{1.86}$$

$$E_i^{(1)} = \langle\Psi_i^{(0)}|\mathscr{V}|\Psi_i^{(0)}\rangle \tag{1.87}$$

$$(H_0 - E_i^{(0)})|\Psi_i^{(1)}\rangle = -(\mathscr{V} - E_i^{(1)})|\Psi_i^{(0)}\rangle \tag{1.88}$$

$$E_i^{(2)} = \langle\Psi_i^{(0)}|\mathscr{V}|\Psi_i^{(1)}\rangle \tag{1.89}$$

$$(H_0 - E_i^{(0)})|\Psi_i^{(2)}\rangle = E_i^{(2)}|\Psi_i^{(0)}\rangle - (\mathscr{V} - E_i^{(1)})|\Psi_i^{(1)}\rangle \tag{1.90}$$

$$E_i^{(3)} = \langle\Psi_i^{(0)}|\mathscr{V}|\Psi_i^{(2)}\rangle \tag{1.91}$$

Intermediate normalisation has been included such that $\langle\Psi_i^{(0)}|\Psi_i^{(n)}\rangle$ for $n \neq 0$.

Møller-Plesset Perturbation Theory

In the Møller-Plesset perturbation methods [33], the unperturbed Hamiltonian is the sum of the Fock operators, which counts the average electron-electron repulsion twice:

$$H_0 = \sum_i^N f(i) = \sum_i^N \left(h(i) + \sum_j^N (J_j(i) - K_j(i)) \right) \tag{1.92}$$

The perturbation operator $\mathscr{V}$ is defined as follows:

$$\mathscr{V} = H - H_0 = V_{ee} - \sum_{i}^{N} \sum_{j}^{N} (J_j(i) - K_j(i)) \tag{1.93}$$

where V_{ee} is the exact interelectronic interaction operator. The zero-order wavefunction $\Psi^{(0)}$ is the Hartree-Fock wavefunction, and therefore the zero-ordered energy is the sum of the molecular orbital energies $E_i^{(0)}$, the first order energy $E^{(1)}$ is the Hartree-Fock energy and it is the second-order energy before electron correlation effects are included. To calculate the second order energy $E^{(2)}$ the first order correction to the wavefunction is required. The first-order wavefunction $\Psi^{(1)}$, is expanded as a linear combination of the eigenfunctions of H_0:

$$|\Psi^{(1)}\rangle = \sum_{n} c_n |n\rangle \tag{1.94}$$

By projecting the first order equation Eq.(1.88) with each of eigenfunctions n, the following expression is obtained:

$$\langle i|(H_0 - E^{(0)}) \sum_{n} c_n |n\rangle = -\langle i|(\mathscr{V} - E^{(1)})|\Psi^{(0)}\rangle \tag{1.95}$$

where the sum over the eigenfunctions n does not include the eigenfunction i. The sum of the Fock eigenvalues of each orbital contained in i is E_i, therefore the above equation can be re-arranged to give a set of linear equations for the coefficients c_i:

$$(E_i - E^{(0)})c_i = -\langle i|(\mathscr{V} - E^{(1)})|\Psi^{(0)}\rangle \tag{1.96}$$

The method that includes up to second-order in the energy is termed MP2. The computational cost of MP2 scales as K^4, where K is a measure of the system size. The equations for the series beyond MP2 get increasingly more complicated and the computational costs increase with each order in the MPn series. The MP2 energy includes the correlation of pairs of electrons, whilst the methods beyond include interactions between pairs. Calculations up to MP4 are routine but the computational cost now scales as K^7.

As perturbation methods do not use the variational procedure, there is no guarantee that the energies will be an upper bound to the exact energy. The MP perturbation procedure is size consistent, but this is not necessarily true of all perturbation methods. The method takes the assumption that the Hartree-Fock gives a good approximation to the true ground state wavefunction, which is not necessarily the case, leading to examples where the perturbation expansion is slow to converge to the exact wavefunction limit. This is particularly true for molecules that dissociate to products with unpaired electrons.

Hellmann-Feynman Theorem

Molecular properties can be calculated by derivative techniques. To obtain the nth order property, the analytical gradient of the energy in the presence of a perturbation is differentiated n times, and the perturbation strength set to zero. In the presence of a perturbation, there will be extra terms in the Hamiltonian [34]:

$$H = H_0 + \lambda P_1 + \lambda^2 P_2 \tag{1.97}$$

Here, H_0 is the unperturbed Hamiltonian, P is the perturbation operator, and λ the strength of the perturbation. The energy and the derivative of the energy can be expressed as:

$$E(\lambda) = \langle \Psi(\lambda) | H_0 + \lambda P_1 + \lambda^2 P_2 | \Psi(\lambda) \rangle \tag{1.98}$$

$$\frac{\partial E}{\partial \lambda} = 2 \left\langle \frac{\partial \Psi}{\partial \lambda} \right| H_0 + \lambda P_1 + \lambda^2 P_2 \left| \Psi \right\rangle + \langle \Psi | P_1 + 2\lambda P_2 | \Psi \rangle \tag{1.99}$$

assuming that the wavefunction is real. The wavefunction depends on the perturbation indirectly, through the expansion coefficients $\mathbf{C}$, and in the case of MCSCF basis functions χ. Therefore:

$$\frac{\partial \Psi}{\partial \lambda} = \frac{\partial \Psi}{\partial \chi} \frac{\partial \chi}{\partial \lambda} + \frac{\partial \Psi}{\partial \mathbf{C}} \frac{\partial \mathbf{C}}{\partial \lambda} \tag{1.100}$$

When the strength of the perturbation λ is set to zero, the derivative becomes:

$$\left. \frac{\partial E}{\partial \lambda} \right|_{\lambda=0} = \langle \Psi_0 | P_1 | \Psi_0 \rangle + 2 \left\langle \frac{\partial \Psi_0}{\partial \lambda} \right| H_0 \left| \Psi_0 \right\rangle \tag{1.101}$$

If the wavefunction is variationally optimised with respect to all parameters, as is the case with Hartree-Fock, or MCSCF wavefunctions, then the second term disappears and the wavefunction obeys the Hellmann-Feynman theorem:

$$\frac{\partial}{\partial \lambda} \langle \Psi | H | \Psi \rangle = \langle \Psi | \frac{\partial H}{\partial \lambda} | \Psi \rangle \tag{1.102}$$

For wavefunctions such as those from MP, Coupled Cluster or truncated CI, this theorem is not obeyed because the wavefunction is not completely optimised with respect to all parameters, and instead first order properties must be evaluated as an expectation value. However, for Coupled Cluster if the coefficients t_i are optimised such that $\partial E / \partial t_i = 0$ stationary conditions are obeyed, the generalised Hellmann Feynman theorem is obeyed.

In summary, various different single reference methods have been outlined and the properties they have explained. An ideal single reference method would have all the properties

of being variational, size consistent and extensive, and invariant to orbital transformations. The FCI method has all these properties, but as the cost grows factorially it is only practical for a small number of electrons and a limited basis set size. Truncated CI methods lose the property of size consistency and extensivity. Coupled Cluster method formulated in the most widely used projection ansatz is not variational, neither are the MP series of methods. The CEPA methods are not invariant to orbital transformations. Therefore there is still much interest in the development of new single reference methods.

Chapter 2

Benchmark Calculations of Coupled Cluster Methods for Closed-Shell Molecules

2.1 Coupled Cluster Methods

The Coupled Cluster wavefunction can be expressed as:

$$|\Psi\rangle = \exp(\hat{T})|\Psi_0\rangle \tag{2.1}$$

where Ψ_0 is a suitable reference wavefunction, for example the RHF wavefunction, and $\hat{T}$ is the cluster operator given by:

$$\hat{T} = \sum_{I}^{N} \hat{T}_I \tag{2.2}$$

$$\hat{T}_1 = \sum_{ia} t_a^i \hat{q}_{ai} \tag{2.3}$$

$$\hat{T}_2 = \frac{1}{4} \sum_{ijab} t_{ab}^{ij} \hat{q}_{ai} \hat{q}_{bj} \tag{2.4}$$

where $\hat{q}_{ai}$ is an excitation operator that promotes an electron from an occupied orbital i, to a virtual orbital a, and t_a^i are the cluster amplitudes associated with the expansion coefficients.

The exponential form of this trial wavefunction ensures that it is multiplicatively separable for non-interacting subsystems, and therefore size consistent. If the cluster operator $\hat{T}$ is complete, that is it contains all the possible excitations, then Ψ is capable of converging to the exact wavefunction. In practice, $\hat{T}$ is usually truncated to a given excitation level, for example to single and double excitations only, for reasons of computational cost and complexity.

This trial wavefunction can be used to create expressions for the energy in a variety of ways as discussed below. The way that the different energy expressions are obtained can lead to each of the coupled cluster methods having different desirable properties [35].

2.1.1 Traditional Coupled Cluster

The most widely used ansatz for obtaining the correlation energy, E_{corr}, and the coupled cluster wavefunction is to substitute the trial exponential wavefunction into Schrödinger's

equation and project on the left with the reference wavefunction [25]:

$$\langle\Phi_0|(\hat{H}-E_0)\exp(\hat{T})|\Phi_0\rangle = E_{\text{corr}}\langle\Phi_0|\exp(\hat{T})|\Phi_0\rangle \tag{2.5}$$

where $\hat{H}$ is the Hamiltonian operator, E_0 is the Hartree-Fock energy, and $|\Phi_0\rangle$ is the Hartree-Fock reference Slater determinant. By multiplying the Schrödinger equation with $\exp(-\hat{T})$ a modified energy expression is obtained:

$$\langle\Phi_0|\exp(-\hat{T})\hat{H}\exp(\hat{T})|\Phi_0\rangle = E \tag{2.6}$$

The use of this similarity transformed Hamiltonian, $\exp(-\hat{T})\hat{H}\exp(\hat{T}) = \bar{H}$, decouples the energy expression from the set of equations for determining the cluster amplitudes. To obtain these cluster amplitudes, the Schrödinger equation is projected on the left with the manifold of excited determinants obtained by acting with the individual cluster operators on the reference:

$$\langle\Phi_0|\hat{q}^\dagger\exp(-\hat{T})\hat{H}\exp(\hat{T})|\Phi_0\rangle = 0 \tag{2.7}$$

From this point onwards this method will be refered to as Traditional Coupled Cluster (TCC) as used by Kutzelnigg [36] and the term Coupled Cluster will be used to refer to the whole family of coupled cluster methods that use Eq.(2.1) to generate the trial wavefunction.

Baker-Campbell-Hausdorff Expansion

The exponential operator can be expanded in a Taylor series:

$$\exp(\hat{T}) = 1 + \hat{T} + \frac{1}{2}\hat{T}^2 + \frac{1}{6}\hat{T}^3 + \ldots \tag{2.8}$$

If this expansion is inserted into the energy equation, the following is obtained:

$$\langle\Phi_0|\hat{H}(1+\hat{T}+\frac{1}{2}\hat{T}^2+\frac{1}{6}\hat{T}^3+\ldots)|\Phi_0\rangle = E \tag{2.9}$$

$$\langle\Phi_0|\hat{H}|\Phi_0\rangle + \langle\Phi_0|\hat{H}\hat{T}|\Phi_0\rangle + \langle\Phi_0|\hat{H}\frac{1}{2}\hat{T}^2|\Phi_0\rangle + \langle\Phi_0|\hat{H}\frac{1}{6}\hat{T}^3|\Phi_0\rangle\ldots = E \tag{2.10}$$

An advantage to the TCC formalism is that this expansion can be truncated because of the nature of the Hamiltonian operator being at most a two particle operator. The rules

for determining the value of matrix elements mean that for determinants that differ by more than three or more spin orbitals the matrix element is zero. This means that in the expression above the last term and subsequent terms contains at least a three fold excitation, so the bra and ket will differ by three or more spin orbitals. Thus the energy expression above simplifies to:

$$\langle\Phi_0|\hat{H}|\Phi_0\rangle + \langle\Phi_0|\hat{H}\hat{T}|\Phi_0\rangle + \langle\Phi_0|\hat{H}\frac{1}{2}\hat{T}^2|\Phi_0\rangle = E \tag{2.11}$$

This truncation also holds for the set of equations to determine the amplitudes of the cluster operator, and is independent of the excitations included in the operator $\hat{T}$ and the number of electrons in the system. This also reduces the computational cost so that when TCC is truncated to contain single and double excitations, the method scales as n^6 with system size.

The similarity transformed Hamiltonian can be expanded using the Hausdorff expansion to a linear combination of nested commutators. This expansion can also can be truncated to terms that are fourth order in $\hat{T}$:

$$\begin{aligned}\exp(-\hat{T})\hat{H}\exp(\hat{T}) &= \hat{H} + [\hat{H},\hat{T}] + \frac{1}{2}[[\hat{H},\hat{T}],\hat{T}] + \frac{1}{3!}[[[\hat{H},\hat{T}],\hat{T}],\hat{T}] \\ &+ \frac{1}{4!}[[[[\hat{H},\hat{T}],\hat{T}],\hat{T}],\hat{T}]\end{aligned} \tag{2.12}$$

Calculations using the Traditional Coupled Cluster ansatz and including up to double excitations in the cluster operator are routine and applied to many chemical problems. TCCSD has been used to calculate electron densities [37] which can give useful information about the nature of bonding interactions in molecular systems.

Method of Moments Coupled Cluster

The method of moments approach to Coupled Cluster [38–40] is to find a non-iterative correction to the CCSD energies to recover the FCI energy. The non-iterative correction accounts for contributions from connected higher excitations missing in the CCSD energy. For Coupled Cluster operator $T^{(A)}$ truncated to a excitation level m_A, the energy expression given by:

$$E_0^{(A)} = \langle\Phi_0|[H(1 + T_1 + T_2 + \frac{1}{2}T_1^2)]_C|\Phi_0\rangle \tag{2.13}$$

The energy for any giving excitation level appears to only depend on the single and double excitations because the Hamiltonian at most contains only two particle operators, but the coefficients of these excitations depend on higher excitations, up to hextuple or the number of electrons which ever is the smallest. To obtain the full CI energy, the following non-iterative correction $\delta_0^{(A)}$is added to the Coupled Cluster energy E_0^A:

$$\delta_0^{(A)} = \sum_{n=m_A+1}^{N} \sum_{k=m_A+1}^{n} \frac{\langle \Psi_{\mathrm{FCI}} | Q_n C_{n-k}(m_A) M_k(m_A) | \Phi_0 \rangle}{\langle \Psi_{\mathrm{FCI}} | \exp(T^{(A)}) | \Phi_0 \rangle} \tag{2.14}$$

where Q_n is the projection operator and $C_{n-k}(mA)$ are the $n-k$ body components of the exponential wavefunction operator $\exp(T^{(A)})$. The correction factor $\delta_0^{(A)}$ determined by calculating the individual excitation operators $M_k(m_A)$ for all k greater than m_A. The excitation operators $M_k(m_A)$ are obtained by projecting the single reference Coupled Cluster equations with all the excited configurations that are not included in $T^{(A)}$:

$$M_k(m_A)|\Phi_0\rangle = \sum_{\substack{i_1<\ldots<i_k \\ a_1<\ldots<a_k}} \langle \Phi_{i_1\ldots i_k}^{a_1\ldots a_k} | \bar{H}^{\mathrm{CCSD}} | \Phi_0 \rangle | \Phi_{i_1\ldots i_k}^{a_1\ldots a_k} \rangle \tag{2.15}$$

The values of k range from $m_A + 1$ to $\min(n, 6)$ where n is the number of electrons, and $\bar{H}$ is the similarity transformed Hamiltonian.

Once the wavefunction Ψ_{FCI} is known, the energy correction δ is computed from the higher order moments of the Coupled Cluster equations, by projecting on the left with the $k-$tuply excited configurations with $k > m_A$. The resulting energy will be the exact ground state energy. The correction factor given in Eq.(2.14) has the form of a complete many-body expansion involving a complete set of excitations up to n-tuple. This makes the correction factor impractical for large systems. To make the method less expensive, the values that k can take are truncated to a given excitation level m_B, and the FCI wavefunction is also approximated. Ψ_{FCI} can be replaced with the wavefunction from an approximate ab-inito method such as CI or MBPT methods, with the requirement that the wavefunction contains higher than m_A-tuply excited determinants. This leads to the renormalised and completely renormalised CCSD[T] and CCSD[TQ] approaches.

For example in the completely renormalised CCSD[T] approach the correction factor uses T_1 and T_2 from a CCSD calculation and the Coupled Cluster analogs of the second order many-body perturbation theory contributions to the triple excitations relative to

the reference wavefunction instead of the FCI wavefunction, labelled by $\Psi_{\text{CCSD[T]}}$, and k is truncated to triples:

$$\delta_0^{(A)} = \frac{\langle \Psi_{\text{CSSD[T]}} | Q_3 M_3(2) | \Phi_0 \rangle}{\langle \Psi_{\text{CCSD[T]}} | \exp(T_1 + T_2) | \Phi_0 \rangle} \tag{2.16}$$

The energy expression for the completely renormalised CCSD[T] method is then given by:

$$\Delta E^{\text{CR-CCSD[T]}} = \Delta E^{\text{CCSD}} + \frac{\langle \Psi_{\text{CSSD[T]}} | Q_3 M_3(2) | \Phi_0 \rangle}{\langle \Psi_{\text{CCSD[T]}} | \exp(T_1 + T_2) | \Phi_0 \rangle} \tag{2.17}$$

The term 'renormalised' is used as the energy expression Eq. (2.17) reduces to the CCSD[T]method if the denominator $\langle \Psi_{\text{CCSD[T]}} | \exp(T_1 + T_2) | \Phi_0 \rangle$ is replaced with 1 [38].

These methods have been applied to the potential energy curve of N_2, a particularly challenging problem for single reference methods as a triple bond is broken. The renormalised and completely renormalised CCSD(T) show significant improvements in comparison to CCSD(T) where the triple excitation are approximated from perturbation theory [41]. These methods have also been applied to the potential energy curve of water, where good agreement with mult-reference methods is found [42]. This method has also been extended to the study of electronic excited staes via equations of motion coupled cluster [43].

TCC methods have been developed to include triple excitations either completely [44] or in some approximate manner in the cluster operator. When up to quadruple excitations are included in a complete way the method scales as n^{10} and has been implemented by Bartlett et al [45]. By studying the potential energy curve of H_2O, they found that including quadruple excitations can reduced the error relative to FCI results by 15 to 20 times when compared with TCCSDT results [45]. There have been developments in including quadruple excitations in an approximate manner by using perturbation theory based on TCCSDT [46] that obtain results of a similar accuracy to the full TCCSDTQ.

There are several approaches to approximately including higher excitations in the cluster operator. The method of Bartlett and coworkers [47,48] simplifies the triple contributions by including the dominant terms from perturbation theory, equivalent to $\Psi \approx \exp(T_1 + T_2 + T_3)|\Phi_0\rangle$. The amplitudes from a CCSD calculation are used for the correction to the wavefunction, and the MP4 energy expression is used to calculate the triples contribution. These methods are not good for bond breaking and systems with quasi-degeneracy because of the divergent nature of MBPT when RHF is not a good reference.

Going beyond quadruple excitations in the cluster operator has been investigated previously by Kállay and Surján [49]. They found that the Traditional Coupled Cluster method needs a lower level of excitation in the cluster operator to reach a converged answer to the energy than Configuration Interaction. In the case of N_2 inclusion of quadruple or higher excitations in the cluster operator, gives better results at long distance that are not below the variational limit [49], unlike coupled cluster results truncated to lower excitation levels. Similar studies have also been performed on HF and H_2O at different bond lengths [50], where it was found that convergence in the excitation level is quicker for TCC in comparison to MBPT or CI, but that at stretched and long bond distances higher levels of excitations are required than for equilibrium distances.

The main obstacle to TCC is that it is not variational. It does not provide an upper bound to the exact energy. This means that TCC results can give energies that are significantly below the FCI values. This is seen below in calculations where static correlation is strong, for example breaking the triple bond in N_2. The resulting TCC potential energy curve for this system is qualitatively incorrect. Therefore it is desirable to examine alternative ansatz to the projection method that could potential be more robust.

2.1.2 Variational Coupled Cluster

As discussed in the previous section, the Traditional Coupled Cluster approach is not variational. An alternative ansatz is to calculate the energy as an expectation value:

$$E = \min_T \frac{\langle \Phi_0 | \exp(\hat{T}^\dagger) \hat{H} \exp(\hat{T}) | \Phi_0 \rangle}{\langle \Phi_0 | \exp(\hat{T}^\dagger) \exp(\hat{T}) | \Phi_0 \rangle} \tag{2.18}$$

$$\equiv \min_T \langle \Phi_0 | \exp(\hat{T}^\dagger) \hat{H} \exp(\hat{T}) | \Phi_0 \rangle_L \tag{2.19}$$

where L signifies linked. The two expressions are equivalent, as the disconnected terms in the numerator are cancelled with those in the denominator to create the linked expression. Terms are said to be disconnected if orbitals of a component of the $\hat{T}$ operator and completely independent of the orbitals in the two-electron integral.

This method, termed here as Variational Coupled Cluster (VCC) but also in the literature referred to as Expectation value Coupled Cluster (XCC) [51], provides an upper bound

to the exact energy. It has not been widely implemented because factorial scaling of the computational cost makes it impracticable except for small systems. Unlike TCC there is no convenient truncation of terms in the energy expression. This is because of the presence of the $\exp(\hat{T}^{\dagger})$ to the left of the Hamiltonian operator, which excites the determinant from $|0\rangle$ on the left. Therefore the matrix elements will not vanish to zero for a given excitation level, and so the exponential will only terminate with the number of electrons being correlated for the case that the energy functional is expressed as a quotient, whereas the linked form does not terminate for any finite power of T.

There are several choices for truncating the number of terms in the above expectation value coupled cluster functional to make approximate VCC methods. Bartlett and Noga [51] have truncated the exponential to make a series of methods that are correct to a given perturbation order. This truncation is done so that each approximation satisfies the General Hellmann Feynmann theorem to aid the calculation of molecular properties. This series of truncated methods are still size extensive, but have lost the property of being an upper bound to the correct energy [51]. Pal et al [52] have benchmarked VCC results truncated to cubic and quadratic powers in T and with only double excitations, and compared the results to using T amplitudes from a TCCD calculation subsituted into the VCC energy functional. Both methods give similar results for the correlation energy of hetercyclic compounds, but the methods are no longer an upper bound to the exact energy.

2.1.3 Unitary Coupled Cluster

The Unitary Coupled Cluster (UCC) method uses a unitary operator in the exponential [5, 53–55]; to generate a unitary transformation:

$$|\Psi\rangle = \exp(\hat{\sigma})|\Phi_0\rangle \tag{2.20}$$

$$\hat{\sigma} = \hat{T} - \hat{T}^{\dagger} \tag{2.21}$$

By replacing $\hat{T}$ with anti-Hermitian operator, $\hat{\sigma}$ in the energy expectation value seen in the previous section, the energy expression becomes:

$$E = \min_{T} \frac{\langle\Phi_0|\exp(-\hat{\sigma})\hat{H}\exp(\hat{\sigma})|\Phi_0\rangle}{\langle\Phi_0|\exp(-\hat{\sigma})\exp(\hat{\sigma})|\Phi_0\rangle} \tag{2.22}$$

Since $\exp(\hat{\sigma})$ is unitary, the denominator $\langle\Psi|\Psi\rangle = 1$ provided that the reference wavefunction is normalised. Therefore the energy expression can be written in the following form:

$$E = \min_{T} \langle\Phi_0| \exp(-(\hat{T} - \hat{T}^\dagger))\hat{H} \exp(\hat{T} - \hat{T}^\dagger)|\Phi_0\rangle \tag{2.23}$$

This method has the disadvantage of a non-terminating Taylor series expansion as the unitary operator contains both an excitation operator $\hat{T}$ and a de-excitation operator $\hat{T}^\dagger$, but the series converges rapidly [54], as a Hausdorff expansion will converge exponentially. The convergence of UCC is faster than the convergence of the infinite expansion of the linked VCC expression. If the contributions to the UCC energy are grouped in terms of the powers of $\hat{T}$ then it can be shown that the zero, first and second order terms are similar to Variational Coupled Cluster. Beyond this level, the UCC becomes more complicated in comparison to the VCC energy expressions [36]. If VCC and UCC are truncated to the same order in powers of $\hat{T}$ it is observed that contributions from higher oders in VCC occur lower in the UCC series. Therefore a kth order expansion of UCC will be a better approximation that a kth order expansion of VCC, where k is the order of $\hat{T}$ [36].

An alternative means of creating a truncation hierarchy is to require that the energy is correct through to some order of perturbation theory [56,57]. By choosing this truncation that has Hermitian symmetry in the energy functional, the UCC(4) correct to fourth order in correlation perturbation, can be applied to studying molecular properties [58]. The UCC(4) method is the simplest UCC method in this truncation hierarchy that is different from any other Perturbation Theory method or Coupled Cluster method. Watts et al [58] found that this method gave excellent results for equilibrium properties, where single reference methods are adequate at describing the system, but performed less well for cases such as the symmetric stretch in water.

Hoffmann and Simons [59] have developed a UCC method by truncating the Hausdorff expansion of the Unitary Coupled Cluster energy functional to second order in the t amplitudes:

$$(H + [H, \sigma] + \frac{1}{2}[[H, \sigma], \sigma])|\Phi_0\rangle \approx E|\Phi_0\rangle \tag{2.24}$$

Analytical expression for the energy gradient of this truncated method have also been developed [60]. This method has been used with a MCSCF reference wavefunction on

some challenging computational problems such as the perpendicular insertion pathway of Be into H_2 and the breaking of two bond simultaneously in H_2O [59] where it was found that accurate results compared to experiment and FCI could be obtained if the reference wavefunction is reasonably accurate.

Pal [61] has explored the use of a Unitary Coupled Cluster method to calculate static electronic properties of molecules. By using a unitary cluster operator first order properties can be calculated with respect to the original system wavefunction, and second order properties require only a first order correction to the wavefunction, leading to a simplification in comparison to obtaining static properties from the Traditional Coupled Cluster approach.

2.1.4 Extended Coupled Cluster

The energy expression for the Extended Coupled Cluster (ECC) method [62] again has its starting point from the expression for the expectation value given by Eq. (2.18):

$$E = \frac{\langle\Phi_0|\exp(\hat{T}^\dagger)\hat{H}\exp(\hat{T})|\Phi_0\rangle}{\langle\Phi_0|\exp(\hat{T}^\dagger)\exp(\hat{T})|\Phi_0\rangle} \tag{2.25}$$

$$= \langle\omega|\exp(-\hat{T})\hat{H}\exp(\hat{T})|\Phi_0\rangle \tag{2.26}$$

where ω is given by:

$$\langle\omega| = \frac{\langle\Phi_0|\exp(\hat{T}^\dagger)\exp(\hat{T})}{\langle\Phi_0|\exp(\hat{T}^\dagger)\exp(\hat{T})|\Phi_0\rangle} \tag{2.27}$$

$$= \langle\Phi_0|\exp(\hat{S}^\dagger) \tag{2.28}$$

where $\hat{S}^\dagger$ is a de-excitation operator. This leads to the following equation for the energy:

$$E = \min_{S,T}\langle\Phi_0|\exp(\hat{S}^\dagger)\exp(-\hat{T})\hat{H}\exp(\hat{T})|\Phi_0\rangle \tag{2.29}$$

where $\hat{S}$ and $\hat{T}$ are varied independently.

Arponen has also shown that this energy functional can be expressed in a double-linked form:

$$E_0 = \langle\Phi_0|\exp(\hat{S})[H\exp(\hat{T})]_L|\Phi_0\rangle_{DL} \tag{2.30}$$

where the subscript L indicates direct linking of the $\hat{T}$ amplitudes to the Hamiltonian, and the DL indicates double linked which imposes further restrictions on $\hat{S}$ to link either to the Hamiltonian or two distinct $\hat{T}$ amplitudes. This leads to a termination in the series expansion, though at high order.

Pal [63] has used Arponen's Extended Coupled Cluster formalism to obtain equations for calculating static molecular properties. For first order properties one only needs the T and S amplitudes only, and for second and third order, only the first derivative of T and S. The ECCSD method has been used to calculate molecular properties such as the dipole moment and polarisability of hydrogen fluoride and CH^+ [64], as well as the water dimer, hydrogen fluoride dimer and the water-hydrogen fluoride complex where it was shown that the ECCSD method produces results closer to experimental values than MP2 [65]. Pal [66] has also developed a linearized version of this bivariational response approach for calculating properties of molecules which greatly reduces the complexity of the bivariational response approach. If only double excitations are included in the cluster operator, and the bivariational equations truncated at quadratic powers of T, the average value of a property operator will result in the same result as is obtained from linear coupled cluster approach with only doubles in the T operator [67]. The ECCSD method has also been used to investigate the magnetizability of hydrogen fluorine and carbon monoxide [68].

Piecuch's method of moments approach for correcting the energy from Traditional Coupled Cluster with single double excitations, to recoup the FCI energy has also been extended to Extended Coupled Cluster using the generalised version of method of moments [69]. Whilst in the case of N_2 good results have been obtained for ECCSD(TQ), the method is computationally expensive.

2.1.5 Quadratic Coupled Cluster

The Extended Coupled Cluster method gives a hierarchy of methods can be derived by truncating $\exp(\hat{S}^\dagger)$ to different powers of $\hat{S}^\dagger$. Thus, the traditional Coupled Cluster

energy expression can be written in the form:

$$E = \min_{S,T} \langle \Phi_0 | (1 + \hat{S}^\dagger) \exp(-\hat{T}) \hat{H} \exp(\hat{T}) | \Phi_0 \rangle \tag{2.31}$$

The next higher order of $\exp(\hat{S}^\dagger)$ to a quadratic expression gives the Quadratic Coupled Cluster energy expression [70]:

$$E = \min_{S,T} \langle \Phi_0 | (1 + \hat{S}^\dagger + 1/2\hat{S}^{\dagger 2}) \exp(-\hat{T}) \hat{H} \exp(\hat{T}) | \Phi_0 \rangle \tag{2.32}$$

This method leads to coupled amplitudes equations, that is the cluster amplitudes for both $\hat{S}^\dagger$ and $\hat{T}$ must be solved.

This method has also been extended to approximately include the effects of higher order excitations by a similarity transformed perturbation theory [71].

2.2 Previous Benchmarks of Coupled Cluster methods

Development of efficient algorithms for performing Full Configuration Interaction (FCI) calculations has made it possible to obtaining electron correlation energies and molecular properties on small molecules and in moderate basis sets [13,72–74]. FCI results give the best possible description of the wavefunction and energy of a system, with any errors due to the incompleteness of the basis set only. Therefore, FCI results provide a benchmark for approximate correlation methods to be compared with, that are evaluated in the same basis set.

FCI benchmark calculations have been performed on a variety of chemically interesting systems such as multiply bonded systems [75] and radical molecules [76]. FCI methods have been used to calculate ground state potential energy curves [77,78], potential energy curves for different electronic states, energy separations between states and spectroscopic values [79–82] equilibrium energies [83], ionisation energies and excitation energies [84] as well as reaction energetics [85].

More recently, Evangelisti et al [86] have calculated the FCI potential energy curve of Be_2 using large basis sets, showing that the size of the basis set is essential to obtain

an accurate description of the bonding in the beryllium dimer. It was also shown that TCCSD and CISD results for this molecule give a poor description of the bonding.

The spectroscopic constants of various diatomic molecules have been benchmarked comparing the increasing orders of Møller-Plesset perturbation theory [87].

There are numerous benchmarks available for comparing Traditional Coupled Cluster results with FCI results, for example Halkier et al [88] have compared the accuracies of Møller-Plesset perturbation methods with TCCSD TCCSD(T) and TCCSDT for the one electron properties of BH and HF, as well as systematic variation of the basis set for the electronic properties of BH [89]. The excitation energies of various small molecules have also been benchmarked [90,91]. The potential energy curves of H_2O, F_2 and N_2 have been benchmarked with up to quadruple excitations in the cluster operator, as well as various methods that account for triples and quadruples in approximate ways [92] where it was found, especially for N_2 quadruple excitations are important for equilibrium geometries for systems with multiple bonds, but that up to hextuple excitations are required to give a qualitatively correct potential curve for N_2.

The potential energy curve of water has been studied including up to hextuple excitation in the cluster operator [93] with the conclusion that including up to triple excitations in the cluster operator recovers large static correlation contributions to the energy. Benchmarks on the N_2 molecule [94] have shown that at stretched bond lengths Traditional Coupled Cluster methods perform poorly as the reference wavefunction is no longer a good description of the exact wavefunction.

However, there are few benchmarks in the literature of the alternative ansatz for Coupled Cluster methods. This is because these other Coupled Cluster methods are harder to implement, and are computationally more demanding.

Benchmarks comparing TCCD and VCCD to FCI calculations have been performed previously [95] on the double dissociation of water and N_2 which are particularly challenging systems for approximate electron correlation methods. It was found that VCCD can give qualitatively correct potential energy surfaces in cases of strong static correlation where the TCCD method fails [95].

Benchmarks have also be carried out on the QCCD method for the same small molecules [70]. The QCCD method was found to be a significant improvement over TCCD at giving results much closer to the VCCD results even for cases of strong correlation such as bond breaking.

Vaval and Pal [96] compare Traditional Coupled Cluster and truncated versions of Variational and Extended Coupled Cluster methods for the calculation of molecular properties of small molecules. Here the importance of cubic terms in the truncation of exponential for obtaining accurate properties was investigated, and the ECCSD method was found to be a better choice than stationary-response XCCSD.

2.3 Implementation with the FCI program

For the purpose of benchmarking each of these coupled cluster variants, the methods were implemented within the FCI program in MOLPRO [97]. The FCI method uses a complete set of Slater Determinants that increase exponentially with the number of electrons. Thus, benchmarks are only possible for relatively small systems. This also means the computational cost for each of the coupled cluster methods implemented in this way is at least as expensive as FCI.

The FCI program uses a direct CI approach [98] to finding the lowest, or few lowest eigenvalues and corresponding eigenvectors of the CI secular equations Eq.(1.42), rather than diagonalisation of the matrix. A suitable trial wavefunction can be expressed as a linear combination of all possible n-electron Slater Determinants:

$$|\psi\rangle = \sum_I c_I |I\rangle \tag{2.33}$$

where the expansion coefficients c_I are given by:

$$c_I = \sum_i \alpha_i . v_{Ii} \tag{2.34}$$

and $\underline{v}$ is given by:

$$\underline{v} = \underline{\underline{H}} . \underline{c} \tag{2.35}$$

This vector of coefficients $\underline{c}$ is the used to calculate the residual vector $\underline{r}$;

$$\underline{r} = \underline{\underline{H}}.\underline{c} - E\underline{c} \tag{2.36}$$

The result is unlikely to be zero, so the deviation is used to update the next trial using the following expression:

$$\underline{v_{i+1}} = (\underline{\underline{H_0}} - E)^{-1}\underline{r_i} \tag{2.37}$$

This forms an iterative process for obtaining the coefficients required to obtain a consistent energy. The method does not require the CI matrix explicitly. A set of integrals are read and used directly in the multiplication with the corresponding $\underline{c}$ coefficients. By avoiding the storage of the CI matrix, it becomes possible to perform calculations on larger systems.

$\underline{\underline{H}}.\underline{c}$ is evaluated using resolution-of-the-identity method [73]

$$(\underline{\underline{H}}.\underline{c}) = 1/2 \sum_{KJ} \sum_{ijkl} (ij|kl)\langle I|\hat{E}_{ij}|K\rangle\langle K|\hat{E}_{kl}|J\rangle c_J \tag{2.38}$$

For the purpose of benchmarking coupled cluster theories, the action of the cluster operators on wavefunctions is evaluated in the same way as the Hamiltonian:

$$\hat{T}_2|\psi\rangle = \sum_{IJ} \sum_{ijab} |I\rangle\langle I|\hat{E}_{ai}|K\rangle\langle K|\hat{E}_{bj}|J\rangle c_J T_{ab}^{ij} \tag{2.39}$$

The other required quantity is the projection of the residual vector on the manifold of excited determinants, which has the form of a transition density matrix:

$$V_{ab}^{ij} = \langle\Phi_0|\hat{E}_{ia}\hat{E}_{jb}\hat{H}|\psi\rangle \tag{2.40}$$

With these basic building blocks, each of the coupled cluster variants (TCC, VCC, UCC and ECC) can be constructed.

2.4 Closed-Shell Benchmark Calculations

2.4.1 Preliminary calculations

All of the results in this chapter are on closed-shell systems, where the reference wavefunction used in the calculations was a Restricted Hartree Fock (RHF) wavefunction.

Open-shell benchmarks are discussed in the following chapter.

Each of the Coupled Cluster methods were initially tested with the H_2 molecule and the He atom. These are two electron systems for which each of the Coupled Cluster methods should give the same as the FCI result when double excitations are used in the cluster operator, as the Coupled Cluster wavefunction is exact for this case. They therefore provided initial tests to check that the coding was correct.

- Initial calculations were performed for the Variational and Unitary Coupled Cluster methods, to ascertain how many terms of the Taylor series expansion of the exponential are needed to get a consistent energy out for HF molecule. A sample set of data is given in Table 2.1 for a long bond distance of $r = 5\,\text{Å}$ and with $\hat{T}$ containing only double excitations. The basis set used was a Dunning cc-pVDZ basis set [99], so that further calculations could be compared to previous calculations in the literature.

These calculations show that more terms are needed to converge the Unitary Coupled Cluster method than for Variational Coupled Cluster. The Unitary Coupled Cluster results show that for the example below at least eight terms are need in the expansion to get a consistent result, whereas Variational Coupled Cluster required only four. Similar calculations were also performed at a shorter distance of $r = 1\,\text{Å}$. These had the same convergence pattern for Variational Coupled Cluster. Fewer terms were need for the Unitary Coupled Cluster, for this case six terms were needed, compared to the results at a longer bond length.

Similar convergence data was collected Neon, N_2 and Be_2 which showed the same trends as for HF. Convergence data was also collected for Be_2 in two different basis sets, showing that the size of the basis set did not affect the number of terms required in the expansion.

2.4.2 Ne polarisabilities

The calculated dipole polarisability, α, of Neon using a cc-pVDZ basis set for each of the different coupled cluster methods are shown in Table 2.2. The lowest $1s$ orbital was not correlated, so that there were eight active electrons correlated. The dipole polarisability

Table 2.1: Convergence data for the energies and differences from FCI values for the number of terms included in the exponential to get a consistent result for HF at $r = 5\,\text{Å}$ with double excitations only in the cluster operator.

	VCCD		UCCD	
Number	Energy	Difference	Energy	Difference
1	-99.801588	0.16868809	-99.601799	0.36847714
2	-99.881162	0.08911345	-99.880315	0.08996125
3	-99.881486	0.08878984	-99.881439	0.08883630
4	-99.881487	0.08878915	-99.881459	0.08881686
5	-99.881487	0.08878915	-99.881438	0.08883786
6	-99.881487	0.08878915	-99.881441	0.08883453
7	-99.881487	0.08878915	-99.881442	0.08883416
8	-99.881487	0.08878915	-99.881442	0.08883420
9	-99.881487	0.08878915	-99.881442	0.08883420
10	-99.881487	0.08878915	-99.881442	0.08883420

Table 2.2: Polarisability of Neon in $Å^3$. 1s orbital in the core, 8 active electrons calculated with cc-pVDZ basis set.

Method	Polarisability	Difference from FCI
FCI	0.07156318	-
TCCSD	0.07160974	4.656E-05
CISD	0.07163581	7.264E-05
VCCSD	0.07161503	5.178E-05
UCCSD	0.07161872	5.551E-05
KCCSD	0.07161355	5.035E-05
ECCSD	0.07161366	5.045E-05
QCCSD	0.07161364	5.043E-05
CCSD(T)	0.07157406	1.085E-05

of the Neon atom was calculated numerically from the second derivative of the energy:

$$\alpha = 2(e_0 - e_1)/df^2 \tag{2.41}$$

where e_0 is the energy with no electric field applied, e_1 is the energy with the field applied, and df is the strength of the dipole moment.

Table 2.2 shows that all of the different Coupled Cluster methods give very similar values for the dipole polarisability of Neon, approximately $\alpha = 0.0716\,Å^3$. The errors for each of the different methods, with single and double excitations included in the cluster operator, when compared with the FCI value are between 4-6x10^{-5} $Å^3$. However, there is a significant improvement on including triples excitations in the cluster operator, as is shown by the CCSD(T) result where the error compared with FCI decreases to 1x$10^{-5}Å^3$. In this method, triple excitations are only included in an approximate way by using perturbation theory. These results indicate that it is the level of truncation of the excitation included in $\hat{T}$ operator that is more important than which cluster ansatz is used.

2.4.3 Potential energy curve of Be_2

The correct bonding description for the beryllium dimer is a challenge for computational methods. Experimental results [100] have shown that there is a minima at $r = 2.45\,\text{Å}$, with an energy of 2.26 ± 0.09 kcal mol^{-1}. This is at a shorter distance than most van der Waals bonds, but still a very weak bond.

Previously, Traditional Coupled Cluster results have been performed on this molecule [86, 101], where it was found that TCCSD cannot give a qualitative description of the potential energy curve in Be_2, this method predicted a very shallow minimum beyond 8 Bohr. A large basis set is needed to gain a good qualitative description with the inclusion of triple excitations in the cluster operator [83, 86, 101]. It has also been shown that contributions to the energy from quadruple excitations are small [102].

The potential energy of this system provides an interesting case for benchmarking the different Coupled Cluster methods, so that it can be determined whether higher excitations or a variational ansatz is more important to give a qualitatively accurate description of the bonding in Be_2.

Calculations were performed on the beryllium dimer in the cc-pVDZ(p) basis set, with four electrons correlated. For each of the Coupled Cluster methods single and double excitations were included in the cluster operator. Table 2.3 shows the FCI values and the errors in the Coupled Cluster methods as a difference from the FCI for energy calculated in the range of 2.0 to 5.0 Å along the potential energy surface. The potential energy curves for FCI and each of the coupled cluster methods are shown in Fig 2.1 as well as the differences from FCI values.

The potential energy curves for all of the methods, including the FCI results, with this basis set are repulsive energy curves. This is qualitatively not what is expected as the beryllium dimer has been shown to have a minimum around $r = 2.45\,\text{Å}$. These errors are due to deficiencies in the basis set as it only includes s and p functions, whereas d functions have been shown to be essential for describing the bond between two beryllium atoms correctly [86]. This matters little for the purpose of benchmarking the Coupled Cluster methods as it is more interesting to compare results to the FCI values in the

same basis set.

The results show that all of the Coupled Cluster methods for this system give essentially the same results, the potential energy curves are all close together and have the same shape. The largest errors are seen at short range where there is strong dynamic correlation. For this small test system Quadratic Coupled Cluster results give exactly the same as the Extended Coupled Cluster method.

Fig 2.1 also shows Traditional Coupled Cluster results with the inclusion of triple excitations, TCCSDT, and the CCSD(T) method where triple excitations are estimated using perturbation theory. These pair of curves are much closer to the FCI values, with complete inclusion of triples giving the best results with comparison to FCI for the beryllium dimer. This shows that for this system higher excitations are needed to better describe the dynamic correlation rather than a Coupled Cluster method that is more variational.

Fig 2.2 shows the potential energy curve obtained with each of the Coupled Cluster methods for Be_2 in a larger basis set, cc-pVTZ which includes up to f functions. This is the largest basis set that can be used with this system before the computational cost becomes too large. With this larger basis set the FCI results show a minimum at $r = 2.5$ Å with a binding energy of 0.00284302 Hartrees or 1.784kcal mol^{-1}. In contrast the TCCSD result shows a purely repulsive graph, whilst the other Coupled Cluster methods have a shallow minimum around $r = 4.5$ Å. Each of the Coupled Cluster methods with single and double excitations are failing to accurately describe the bonding region of the potential energy curve. Again it is only with triple excitations with either the TCCSD(T) method or the TCCSDT from MRCC code [103–106] that are able to describe the potential energy curve more accurately. These two curves follow the FCI more closely, and find the deeper minimum at $r = 2.5$ Å.

These results indicate that for systems with strong dynamic correlation the inclusion of higher excitations are require to obtain a qualitatively correct description potential energy curve rather than moving to a Coupled Cluster method that is more variational.

Table 2.3: The potential energy curve of Be_2, FCI energies in Hartrees, and Coupled Cluster methods as differences from FCI values in Hartrees.

R/ Å	FCI	TCCSD	VCCSD	UCCSD	ECCSD	QCCSD
2.1	0.0192097	3.510E-03	3.256E-03	3.527E-03	3.290E-03	3.290E-03
2.3	0.0112796	2.902E-03	2.705E-03	2.930E-03	2.731E-03	2.731E-03
2.5	0.0078136	2.268E-03	2.100E-03	2.252E-03	2.113E-03	2.113E-03
2.7	0.0060307	1.701E-03	1.558E-03	1.640E-03	1.557E-03	1.557E-03
2.9	0.0047436	1.253E-03	1.138E-03	1.172E-03	1.127E-03	1.127E-03
3.1	0.0036026	9.20E-04	8.32E-04	8.41E-04	8.15E-04	8.15E-04
3.4	0.0021457	5.80E-04	5.22E-04	5.17E-04	5.04E-04	5.04E-04
3.7	0.0011092	3.69E-04	3.25E-04	3.18E-04	3.10E-04	3.10E-04
4.0	0.0004840	2.39E-04	1.99E-04	1.94E-04	1.89E-04	1.89E-04
4.5	0.0000527	1.16E-04	8.6E-05	8.4E-05	8.2E-05	8.2E-05
5.0	-0.0000238	5.9E-05	3.8E-05	3.6E-05	3.6E-05	3.6E-05

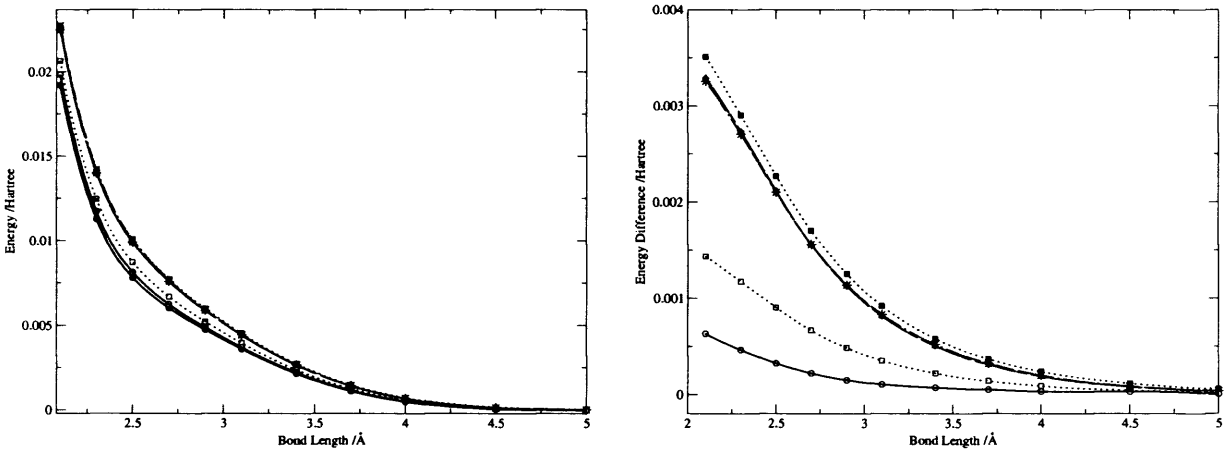

Figure 2.1: Potential energy curve of Be_2 in Hartrees, with errors from FCI on the left, obtained with cc-pVDZ(p) basis set. FCI ● TCCSD ■ QCCSD ◆ ECCSD ▲ UCCSD × VCCSD ✻ CCSD(T) ❑ TCCSDT ○

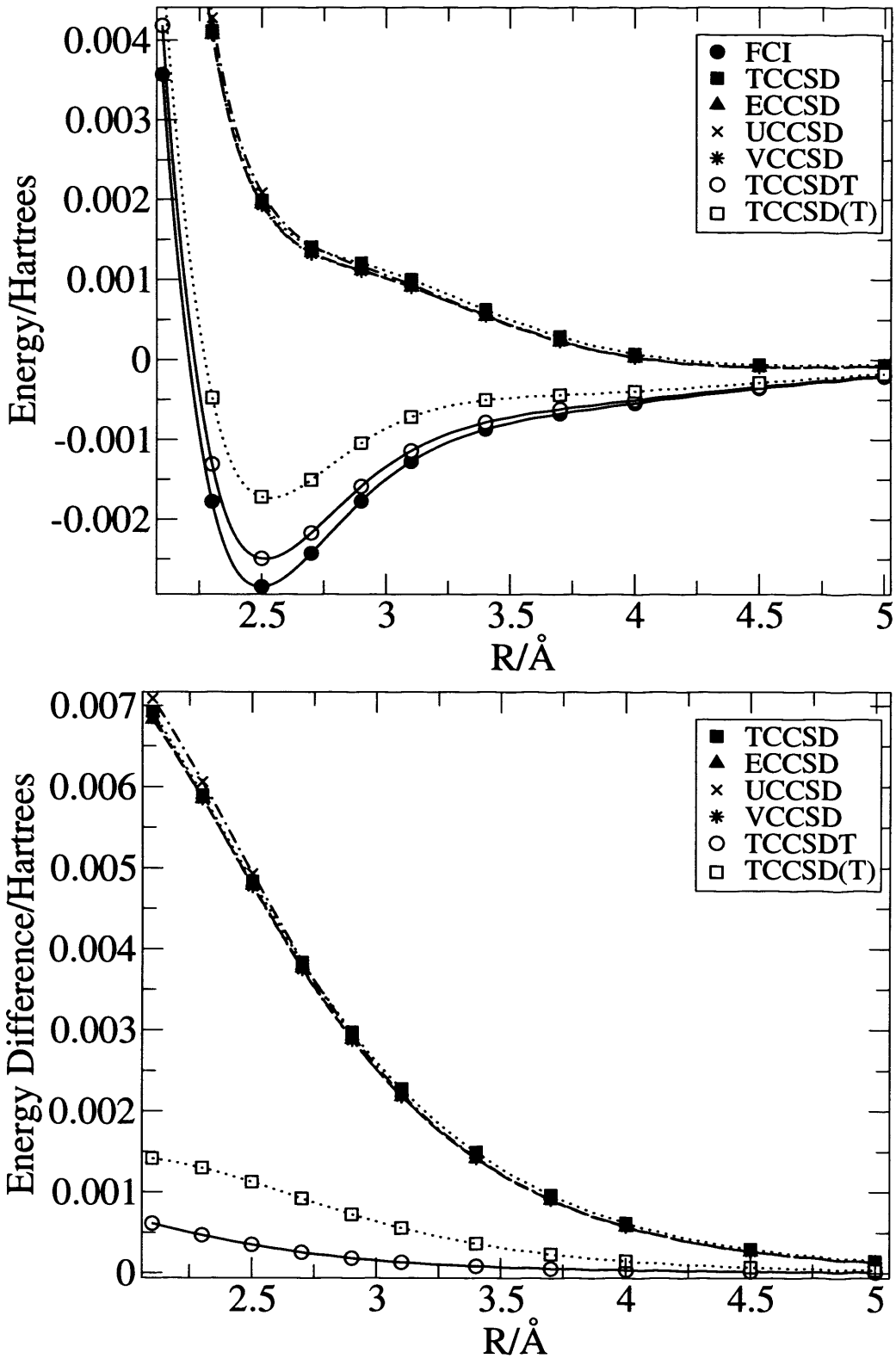

Figure 2.2: Potential energy curve of Be_2 in Hartrees, with errors from FCI below.

2.4.4 Hydrogen Fluoride

The potential energy curve of hydrogen fluoride was investigated, as an example of single bond breaking. This molecule is interesting because it has low lying excited states and an avoided crossing at a stretched bond length of $1.5r_e$, that can effect convergence as has been seen with many body perturbation calculations [107]. Calculations performed on HF with Traditional Coupled Cluster including up to octuple excitations have shown that as the bond length is increased higher orders of excitation are need to accurately describe the potential energy curve [49,50]. The renormalised and completely renormalised CCSD(T) and CCSD(TQ) approaches give potential energy curves for HF that are more accurate than CCSD or CCSDT results [108]. Previous calculations on hydrogen fluoride comparing Traditional, Variational and Quadratic Coupled Cluster methods with only double excitations have shown that there is little difference between these methods [70].

Calculations were performed on the single bond breaking in hydrogen fluoride, using a cc-pVDZ basis [99] and with all ten electrons correlated. Table 2.4 gives the results of these calculations with the FCI energy given as differences from the asymptotic energy, and the Coupled Cluster with single and double excitations in the cluster operator, results given as differences from the FCI values. Fig. 2.3 shows the potential energy curve of HF for each of the Coupled Cluster methods between the range of $r = 1$ to $r = 3\,\text{Å}$, as well as differences from FCI values over this range.

The results show that each of the coupled cluster methods perform comparably with Variational Coupled Cluster for single bond breaking. At short distances and equilibrium distance there is little difference between the coupled cluster methods, each of which have small errors from FCI of 1-3 mHartrees. At the longer bond lengths differences start to be seen between the different coupled cluster methods, where Traditional Coupled Cluster (TCCSD) performs least well with errors ten times larger than at the equilibrium bond length. In contrast Variational Coupled Cluster (VCCSD) performs significantly better with an error of 7 mHartrees in comparison with the FCI values. VCCSD performs better than Unitary, Extended or Quadratic Coupled Cluster. Also, there again is little difference between QCCSD and ECCSD and is a significant improvement over TCCSD results.

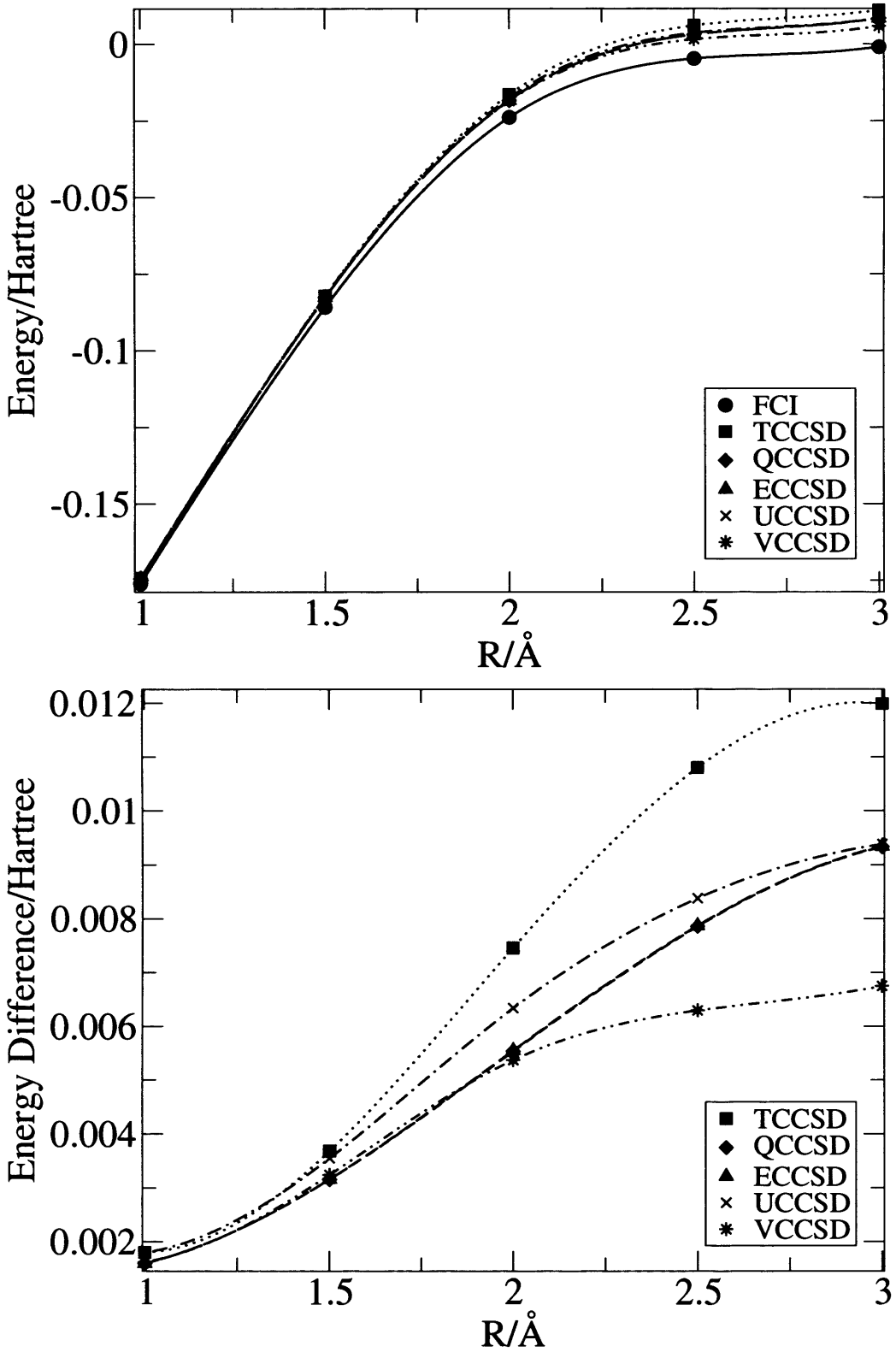

Figure 2.3: Potential energy curve for Hydrogen Fluoride with energy differences from the FCI below, calculated with cc-pVDZ basis set

Table 2.4: The potential energy curve of HF, FCI energies in Hartrees, and Coupled Cluster methods as differences from FCI values in Hartrees. Calculations performed with cc-pVDZ basis set.

R/ Å	FCI	TCCSD	VCCSD	UCCSD	ECCSD	QCCSD
3.0	-0.00085170	0.01198966	0.00674861	0.00938450	0.00934278	0.00933284
2.5	-0.00468178	0.01080213	0.00629561	0.00838082	0.00787201	0.00785850
2.0	-0.02385873	0.00745902	0.00537323	0.00634060	0.00555201	0.00553644
1.5	-0.08575842	0.00368028	0.00324017	0.00354676	0.00315680	0.00315373
1.0	-0.17603913	0.00180043	0.00162110	0.00179730	0.00159555	0.00159471

2.4.5 Symmetric stretch in water

The double dissociation of water has been studied numerous times previously [44, 50, 70, 78, 83, 95]. As both bonds are simultaneously, this provides a more challenging case than single bond breaking. Results using the renormalised and completely renormalised CCSD(T) approach have shown this method to have increased accuracy in the bond breaking region in comparison to CCSD or CCSD(T) with perturbative triples [109]. Previously [70,95] benchmarks have been performed on H_2O with Variational and Quadratic Coupled Cluster methods with only double excitations in the cluster operator. These results showed much better agreement with FCI results and both were a considerable improvement over TCCD results. Here these are extended upon to included both single and double excitations and also compared with Unitary and Extended Coupled Cluster methods.

Energy calculations were performed at three points along the symmetric stretching mode of a water molecule. The points were at the equilibrium bond length r_e, $1.5r_e$ and $2r_e$. The calculations were performed in the 6-21G basis set, with all the electrons correlated, and single and double excitations in the cluster operator.

The results of these calculations are shown in Table 2.5 where the FCI values are given relative to the asymptotic energy of an oxygen atom and two hydrogen atoms, and the

Table 2.5: The potential energy curve of H_2O, FCI energies in Hartrees, and Coupled Cluster methods as differences from FCI values in Hartrees calculated with 6-21G basis set.

R/ Å	FCI	TCCSD	VCCSD	UCCSD	ECCSD	QCCSD
0.967	-0.35181309	0.00164550	0.00140510	0.00143941	0.00140111	0.00140122
1.450	-0.23241210	0.00585200	0.00491824	0.00509404	0.00491480	0.00491435
1.933	-0.12453404	0.00922161	0.00991359	0.01037255	0.01002517	0.01003273

Coupled Cluster values are again differences from the FCI values. Fig. 2.4 shows the potential energy curves associated with the symmetric stretching mode of a water molecule as well as differences from FCI values.

In this region all the Coupled Cluster methods perform well at the equilibrium bond length with errors between 1.4 and 1.7 mHartrees in comparison with the FCI values. At this bond length, Traditional Coupled Cluster has larger errors than Variational, Unitary, Extended and Quadratic Coupled Cluster. At a slightly stretch bond length of $r = 1.450$ Å, the errors in comparison with FCI are all ready showing a significant increase, as the errors are 3.5 times greater. Again, TCCSD has larger errors in comparison with the other Coupled Cluster methods at this point. On further stretching the molecule to twice the equilibrium bond length, the errors are doubled in comparison to the previous point. This is because as the bonds are stretched the static correlation increases, and therefore it becomes harder for approximate correlation methods to account for all the static correlation present.

Interestingly, TCCSD has smaller errors in comparison with VCCSD for the last point. This is likely to be as a result of TCCSD not giving an upper bound to the exact energy, and upon further stretching it may be found that TCCSD results go below the FCI values.

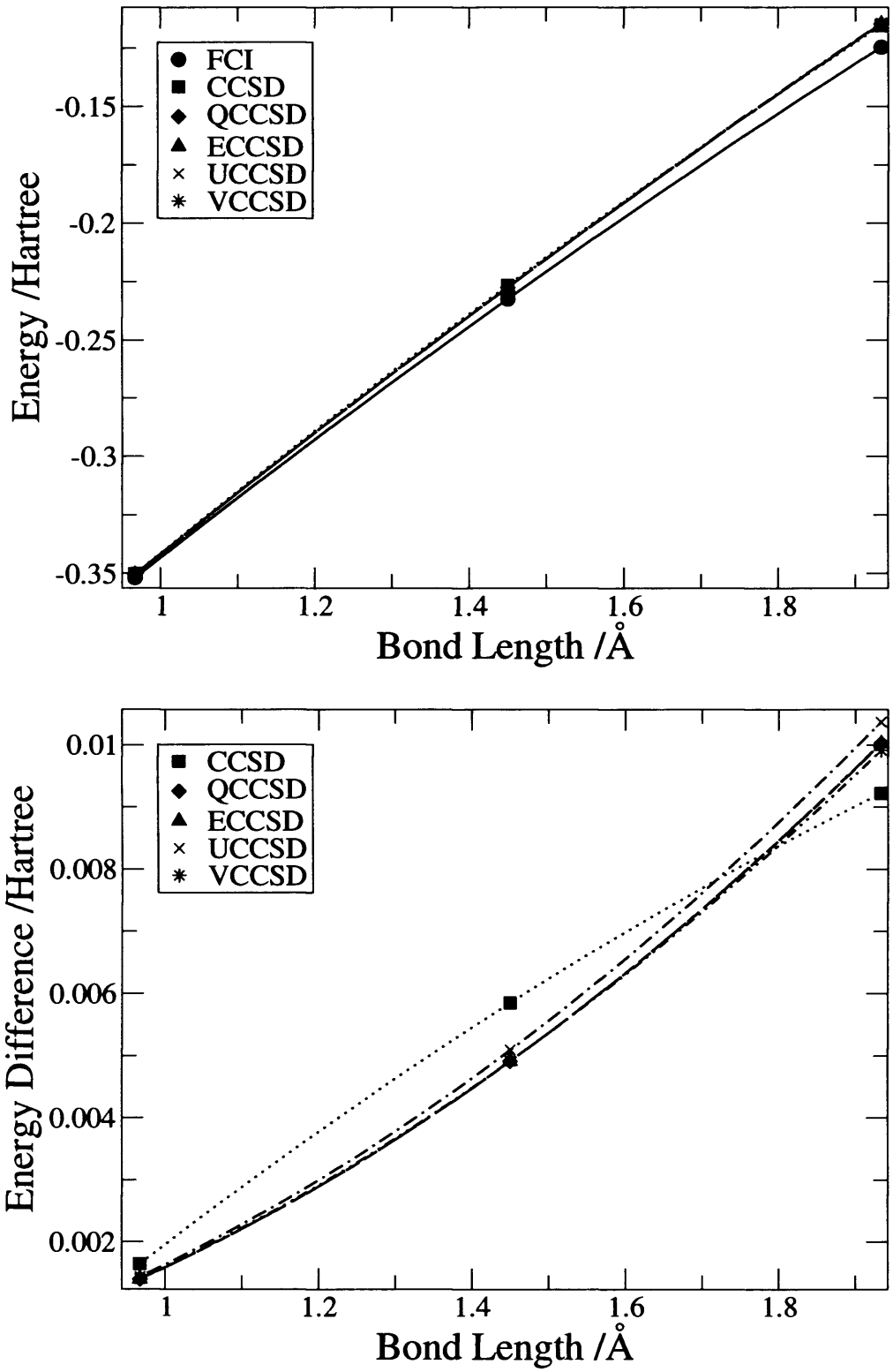

Figure 2.4: Potential energy curve for the symmetric stretch of water with differences from FCI below calculated with 6-21G basis set.

2.4.6 Potential energy curve of N_2

The potential energy curve for the dissociation of N_2 is frequently studied [75, 110, 111], as it involves the breaking of a triple bond. This is a extremely challenging problem for approximate methods for calculating correlation energies as it is an example where there is strong static correlation at stretched bond lengths. This molecule will therefore provide a difficult test for each of the Coupled Cluster methods benchmarked.

Previous benchmarks with Traditional Coupled Cluster using a single reference wavefunction have shown that this method does not accurately describe the breaking of the triple bond [94]. TCCSD calculations at stretched bond lengths lie below the FCI values and the magnitude of the error can be more than 100 mHartrees [112]. Multi-reference methods such as MRCISD and MRCCSD perform much better across the potential energy curve in comparison with their single reference counterparts, and give more accurate equilibrium properties such as vibrational frequencies for N_2 [110, 113]. Methods that included triple excitations approximately by perturbation methods have been shown to perform poorly for the potential energy curve of N_2 as the effect of triples is overestimated at large bond lengths [41, 92]. The renormalised and completely renormalised CCSD(T) and CCSD(TQ) coupled cluster approaches are much better at describing the potential energy curve of N_2 [41]. The Extended and Quadratic Coupled Cluster approaches, and generalised method of moments approach to account for triple and quadruple contributions for these methods have been shown to be able to give a qualitatively correct description of the potential energy curve of Nitrogen, and not suffer from the non-variational collapse of Traditional Coupled Cluster methods for this system [69]. Previous benchmarks comparing Variational and Quadratic Coupled Cluster with only double excitations show that these two methods perform significantly better than Traditional Coupled Cluster at describing the breaking of the nitrogen bond [70].

The potential energy curve for N_2 has been examined using the minimal STO-3G basis set. The lowest two orbitals were included in the core and not correlated. The potential energy curves obtained when single and double excitations were included in the cluster operator are shown in Fig. 2.5 and errors from FCI values shown in Table 2.6. Fig. 2.6 shows the potential energy curve with quadruple excitations in the cluster operator, as

well as VCCSD and VCCSDT for comparison. Table 2.7 shows the errors in comparison with FCI for Traditional and Variational Coupled Cluster methods with increasing level of excitation included in the cluster operator up to quadruple excitations.

The results show that with single and double excitations included in the cluster operator each of the Coupled Cluster methods perform well at equilibrium bonds lengths, with errors in the range of $1 - 4$ mHartrees. However, Fig. 2.5 shows the dramatic failure of TCCSD in breaking the triple bond in nitrogen. The energies beyond $r = 1.7\,\text{Å}$ lie below the FCI values and the TCCSD energy curve shows an energy barrier to forming the nitrogen triple bond. The TCCSD method gives errors at stretched bond lengths of tens and even hundreds of mHartrees.

In contrast the VCCSD curve follows the FCI energy curve more closely, and as expected does not dip below the FCI results. The errors in comparison with FCI values for VCCSD stay in the order of mHartrees, even when the bond is quite stretched at $r = 2.1\,\text{Å}$ the error is only 6.55 mHartrees. ECC an QCC also show better agreement with the FCI, and give similar curves to the VCCSD method, with errors again a few mHartrees. QCCSD performs considerably better than TCCSD, with the maximum error in the range tested of 14.99 mHartrees, and the values for the energies do not go below the FCI values. Unfortunately, there was no convergence beyond $r = 2.1\,\text{Å}$ for any of the methods, and UCCSD fails to converge after $r = 1.5\,\text{Å}$.

Fig. 2.6 where up to quadruple excitations are included in the cluster operator for each of the Coupled Cluster methods, shows that all the methods now give a qualitatively correct potential energy curve. There are no more fictitious barriers to the formation of a triple bond. VCCSDTQ still outperforms TCCSDTQ, as the errors from FCI are still smaller for VCCSDTQ, and the last point for TCCSDTQ still lies below the FCI value although the error is now in the tens of mHartrees rather than over a hundred.

Table 2.7 compares the effect of including higher excitations in the TCC and VCC methods. From this data, the inclusion of triple excitations is clearly not enough to improve the quality of the TCC or VCC energy curves produced. Whilst the errors at equilibrium are reduced by a factor of around 4 in the VCC case, at long bond lengths the errors are comparable with those obtained with the inclusion of up to double excitations only.

Table 2.6: The potential energy curve of N_2, FCI energies in Hartrees, and Coupled Cluster methods as differences from FCI values in mHartrees calculated with STO-3G.

R/ Å	FCI	TCCSD	VCCSD	UCCSD	ECCSD	QCCSD
0.9	0.14530804	1.70	1.23	1.24	1.22	1.22
1.1	-0.21580695	3.92	2.19	2.24	2.11	2.12
1.3	-0.22113309	8.54	3.60	3.96	3.30	3.31
1.5	-0.14346261	13.78	4.43	5.60	3.93	4.01
1.7	-0.07061097	3.75	3.47	-	3.43	3.71
1.9	-0.02803802	-59.09	3.70	-	5.90	6.58
2.1	-0.01058371	-135.75	6.53	-	13.43	14.99

For VCCSDT the error at $r = 2.1$ Å is just 0.56 mHartrees smaller than with single and double excitations only. Further inclusion of quadruple excitations however, leads to a dramatic reduction in the errors for both methods. At equilibrium errors are on the μHartree scale with quadruple excitations included, however at long bond lengths the errors are much increased. With the inclusion of quadruple excitations TCCSDTQ performs comparably with VCCSD.

These results shows that for cases with strong static correlation methods that are more towards a Variational Coupled Cluster method are required or one has to go to much higher levels of excitations in the cluster operator to achieve potential energy curves that are qualitatively correct. QCCSD is a significant improvement on TCCSD for cases with strong static correlation and as it has been previously shown that a QCCD method scales with the system size as n^7 [70], whereas inclusion of up to quadruple excitations in TCC method scales as n^{10} [45] using a method that is on the way to being more variational is more preferable than including higher levels of excitation.

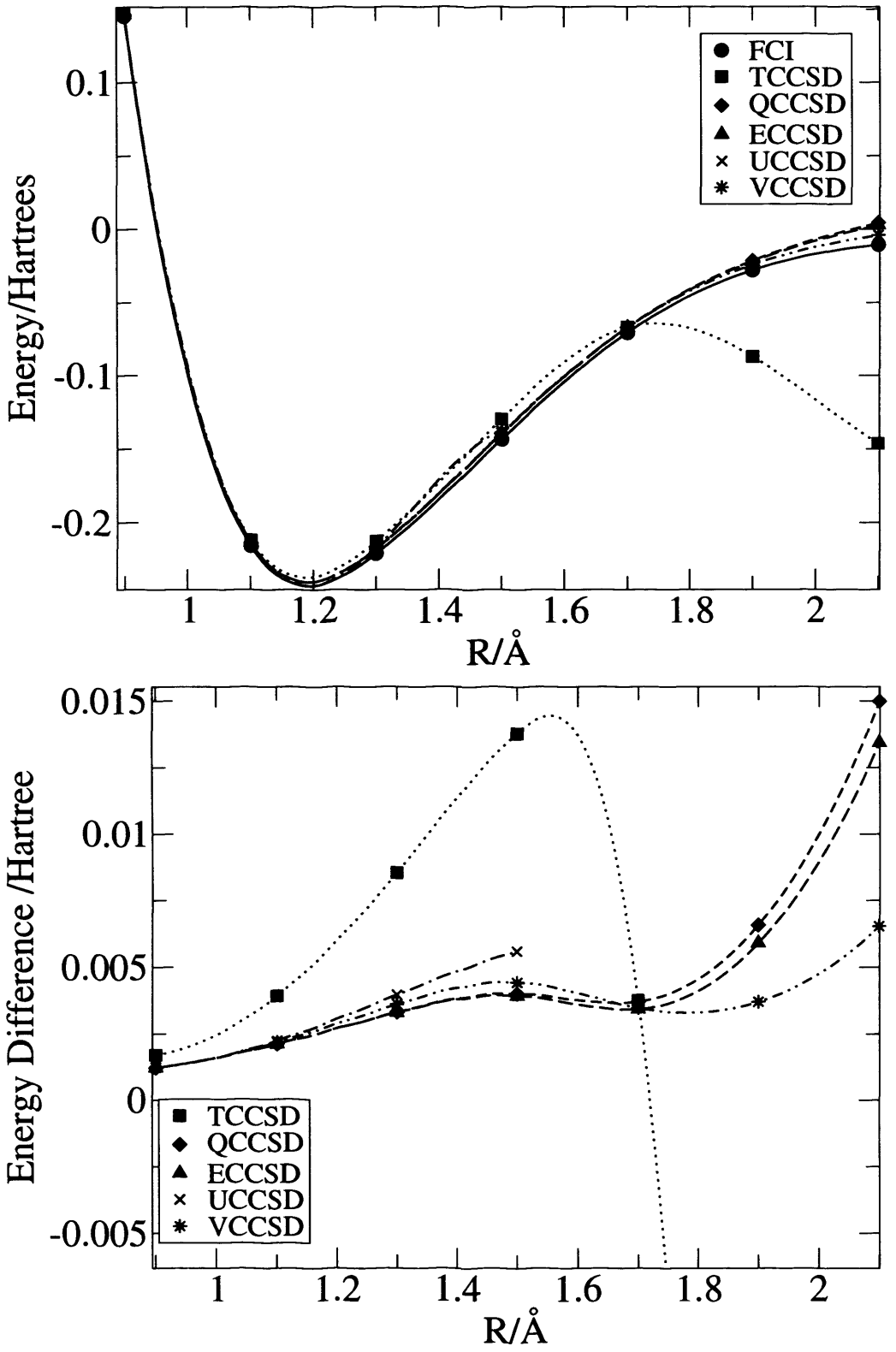

Figure 2.5: Potential energy curve and differences from FCI for N_2 in Hartrees, with single and double excitations in the cluster operator, calculated with STO-3G basis set.

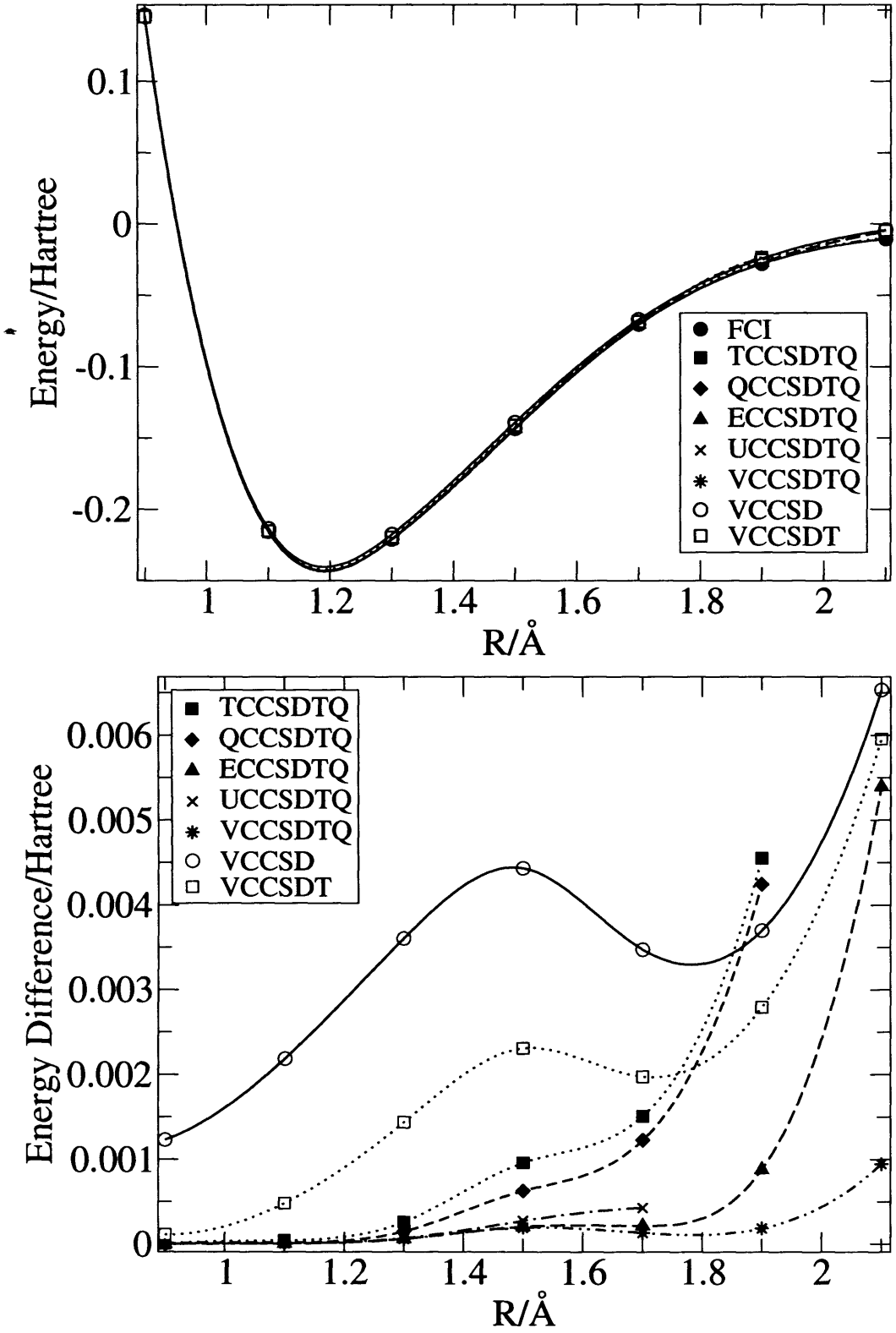

Figure 2.6: Potential energy curve and differences from FCI for N_2 in Hartrees, with up to quadruple excitations in the cluster operator calculated with STO-3G basis set.

Table 2.7: Differences from FCI in mHartree for Traditional and Variational Coupled Cluster methods with triple and quadruple excitations in the cluster operator for N_2 with two cored orbitals.

R/ Å	TCCSD	TCCSDT	TCCSDTQ	VCCSD	VCCSDT	VCCSDTQ
0.9	1.70	0.49	0.01	1.23	0.11	7.5E-04
1.1	3.92	2.05	0.04	2.19	0.48	8.1E-03
1.3	8.54	6.15	0.26	3.60	1.44	0.06
1.5	13.78	11.62	0.96	4.43	2.31	0.19
1.7	3.75	3.06	1.51	3.47	1.97	0.13
1.9	-59.09	-59.84	4.55	3.70	2.79	0.19
2.1	-135.72	-136.42	-14.01	6.52	5.96	0.95

2.5 Conclusions

Benchmark calculations were performed on various closed shell systems for each of the Coupled Cluster methods. Calculations on the polarisability of Neon showed there was little difference between the different energy formalisms. The potential energy curves of the beryllium dimer also showed little difference between the Coupled Cluster methods, and that the largest errors were seen at short bond lengths where the dynamic correlation is strong. Calculations performed in a larger basis set, cc-pVTZ, showed that both Variational Coupled Cluster and Traditional Coupled Cluster methods with single and double excitations were unable to account for the strong dynamic correlation leading to a qualitatively incorrect potential energy surface, as the FCI minima at $r = 2.5\,\text{Å}$ was not reproduced. For both neon and the beryllium dimer, inclusion of triple excitations in the cluster operator lead to superior results being obtained. With triple excitations more of the dynamic correlation energy was recovered in the potential energy of Be_2.

However, large differences were seen in the different Coupled Cluster methods for systems where static correlation is important. The calculations on Hydrogen Fluoride showed that Variational Coupled Cluster (VCC) gave superior results for single bond breaking in comparison with Traditional Coupled Cluster (TCC). Quadratic Coupled Cluster results

were very similar to Extended Coupled Cluster results and a significant improvement over TCC results.

When multiple bonds are broken, the differences between each of the Coupled Cluster methods becomes more apparent. Calculations on water and nitrogen molecules showed that all the Coupled Cluster methods work well at equilibrium bond lengths, but that errors increase significantly when multiple bonds are stretched or broken. When breaking the triple bond in Nitrogen, Traditional Coupled Cluster with singles and doubles fails to produce an accurate qualitative description of the potential energy curve, it has a fictitous barrier to forming the triple bond. The Variational Coupled Cluster method is far superior as it follows the potential curve of FCI more closely, with a similar error throughout the potential energy curve, in the order of a few mHartrees. All ready Quadratic Coupled Cluster, the next step between TCC and Extended Coupled Cluster, is significantly better at describing the potential energy curve of N_2. Inclusion of quadruple excitations are required to reduce the errors to tens of mHartree at long bond lengths for TCC.

Chapter 3

Benchmark Calculations of Coupled Cluster Methods for Open-Shell Molecules

3.1 Introduction

3.1.1 Hartree Fock Methods for Open-Shell systems

The spin Restricted Hartree Fock (RHF) method becomes inappropriate when a molecule dissociates to open shell products, as is the case with N_2 or H_2. This is because pairs of electrons are placed in the same spatial orbital, but with different spins. As a molecule such as H_2 dissociates it becomes more energetically favourable for the two electrons to break symmetry and localise on one nuclei or the other. This cannot happen in the spin Restricted HF method, which requires both electrons to stay in the same spatial orbital leading to ionic H^+ and H^- products at dissociation.

In the Unrestricted HF (UHF) method [114], there are two sets of spatial orbitals, those with alpha spin and a set with beta spin, each singly occupied. This allows the electrons to localise onto one nuclei or the other when the molecule dissociates, therefore giving the correct neutral species as the products.

The disadvantage of the UHF method, is that it is often spin contaminated with electronic states of a higher multiplicity. The wavefunction therefore is not an eigenfunction of the $\hat{S}^2$ spin operator.

The UHF molecular orbitals for H_2 can be expressed in terms of a linear combination of RHF molecular orbitals as follows [115]:

$$\begin{aligned} \psi_o^\alpha &= \cos(\theta)\phi_o + \sin(\theta)\phi_u \\ \psi_u^\alpha &= -\sin(\theta)\phi_o + \cos(\theta)\phi_u \\ \psi_o^\beta &= \cos(\theta)\phi_o - \sin(\theta)\phi_u \\ \psi_u^\beta &= \sin(\theta)\phi_o + \cos(\theta)\phi_u \end{aligned} \tag{3.1}$$

If these unrestricted molecular orbitals are substituted into the single determinant for

the ground state, the following is obtained [116]:

$$\begin{aligned} |\Phi_0\rangle &= |\psi_o^\alpha \psi_o^\alpha\rangle \\ &= \cos^2\theta|\phi_o^\alpha\phi_o^\beta\rangle - \sin^2\theta|\phi_u^\alpha\phi_u^\beta\rangle - \cos\theta\sin\theta[|\phi_o^\alpha\phi_u^\beta\rangle - |\phi_u^\alpha\phi_o^\beta\rangle] \\ &= \cos^2\theta|\phi_o^\alpha\phi_o^\beta\rangle - \sin^2\theta|\phi_u^\alpha\phi_u^\beta\rangle - 2^{1/2}\cos\theta\sin\theta|^3\Psi_1^2\rangle \end{aligned} \tag{3.2}$$

Here the term $|^3\Psi_1^2\rangle$ is a singly excited triplet configuration. The other two terms in the equation are singlet terms. The triplet contribution increases as the bond length in H_2 is increased, until at the limit of dissociation at $R \longrightarrow \infty$ when it makes up fifty percent of the total wavefunction.

The General Hartree Fock method (GHF) has no restrictions on spin orbitals used other than the set of orbitals are chosen to be orthonormal. This method was termed unrestricted Hartree-Fock by Fukutome [117, 118], but this term has later been used to describe molecular orbitals restricted to have either α or β spin. In the GHF theory, the spin orbitals, $\psi_i(r,\zeta)$, are a linear combination of α and β spins:

$$\psi_i(r,\zeta) = u_k(r)\alpha(\zeta) + v_k(r)\beta(\zeta) \tag{3.3}$$

The GHF method is difficult to implement because the general spin orbitals contain twice as many orbital functions as there are in the UHF method. Both RHF and UHF methods are a special case of GHF where additional restrictions are placed on the form of the spin orbitals. There can be multiple solutions to the GHF method because of the non-linear character of the Hartree-Fock equations. The work of Mayer and Lowdin [119] has shown that there are up to six GHF solutions for the BH molecule, one of which is RHF, three are UHF and two are genuine GHF solutions.

Fukutome [118] classified the possible solutions to the General Hartree-Fock equations using group theory to determine the possible types of broken-symmetry HF solutions. There are eight classes associated with all the ways that spin and time reversal symmetries can be broken and if the solution is invariant to the magnetic operator. For example, RHF solutions fall into one of two classes for closed shell systems, time invariant closed shell (TICS) which are spin invariant and time-reversal invariant, and charge current wave (CCW) which are spin invariant but neither time-reversal invariant nor magnetic operator invariant. CCWs form complex solutions, therefore if real basis functions with real coefficients are used the RHF solutions fall into the TICS class only.

The GHF wavefunction is not necessarily an eigenfunction of $\hat{S}_z$ or $\hat{S}^2$ spin operators, unless the GHF solution coincides with the RHF solution which is a eigenfunction of both, or UHF solution which is an eigenfunction of $\hat{S}_z$ but not $\hat{S}^2$. However it does produce qualitatively correct descriptions of the ground state potential energy curves that are continuous with respect to nuclei position as has been shown for a non-symmetric arrangement of four hydrogen atoms [120].

There are methods that project out spin from the UHF wavefunction, for example Projected Unrestricted Hartree Fock (PUHF) where the spin projection operator [115] $\hat{P}_S$ is used to annihilate the next highest order multiplicity:

$$\hat{P}_s = \prod_{k \neq s} \frac{\hat{S}^2 - k(k+1)}{s(s+1) - k(k+1)} \tag{3.4}$$

This method of projecting out the spin in UHF is done after convergence. Alternatively, the spin contamination can be removed in a more self consistent manner by eliminating the first spin contaminant before the Fock matrix is constructed and the energy is calculated at each cycle during the SCF procedure. This method is known as Annihilated Unrestricted Hartree Fock (AUHF).

3.1.2 Perturbation Theory Methods for Open-Shell Systems

There have been many developments to create a perturbation method that is suitable for open-shell systems. The simplest implementation is the Unrestricted Møller-Plesset (UMP) based on the UHF wavefunction, and where the unperturbed Hamiltonian is a sum of the α and β Fock operators.

It has been shown previously [121] that this UMP series is slow to converge in comparison to the closed shell variant and UMP2 gives poor agreement in comparison to experiment. The slow convergence of the UMP series has been rationalised by spin contamination in the wavefunction [122].

Spin projection can be applied to the UMP wavefunctions. In the work of Schlegel [123] the first spin contaminant is removed from the reference wavefunction using Lowdin's

spin projection operator [115], and the resulting energy difference used to estimate the projected MP2 to MP4 energies. The projected MP4 energies for the potential energy curves of LiH and CH_4 are found to be in good agreement with FCI values [123]. The spin projection operator has also been applied to the correlation corrected wavefunction to remove the first spin contaminant [124] [125], and also the first two spin contaminants to UMP2 [126]. Only if the complete spin projection operator is used is the method size consistent, but Knowles and Handy [126] found that results from this PMP(2) method greatly improves accuracy in cases where spin contamination is significant.

The AUHF wavefunction has also been used to make an MP2 method [127] [128]. This method is relatively easy to implement as the AUHF wavefunction is used as the reference in the perturbation expansion, and so there is no need to project out the spin contamination at each order of the perturbation series [128]. AUMP has been shown to give better convergence properties when going to higher orders of perturbation theory in comparison to UMP for diatomics with large spin contamination such as the cyano radical ($CN^{\bullet}$) [127]. This is because the AUMP wavefunction contains less spin contamination than the UMP. Similarly electron affinities are more accurate with AUMP in cases where the spin contamination is large. When spin contamination is low, AUMP can give poorer electron affinities because the electron correlation is described better in the anion than the neutral species, as well as higher energies than UMP as the UHF reference can be lower than the AUHF reference wavefunction. The other draw back of this method is that it is only applicable to the region of the minimum as the AUHF wavefunction does not describe bond dissociation well [128].

In the ROHF wavefunction the open-shell orbitals all have like spin, i.e. they are all α spins. Restricted Open-Shell MP (ROMP) [129] is based around the ROHF wavefunction where the α and β orbitals are not the same. The ROHF space is partitioned into singly, doubly and unoccupied space for both α and β. This method has been shown to have much better convergence properties in comparison to UMP [129].

Restricted MP theory for open shell molecules (RMP) [130] differs from ROMP in that the distinction between singly occupied and doubly occupied *alpha* spin orbitals is lost. There are no spin contamination effects in the expression for the energy for ROHF MBPT. RMP2 can still give results little better than UMP2 as is highlighted in the case of the

formaldehyde radical cation ($H_2CO^{+\bullet}$) and the isomer hydroxymethylene radical cation ($HCOH^{+\bullet}$) where both UMP2 and RMP2 predicting the $H_2CO^{+\bullet}$ as higher in energy than $HCOH^{+\bullet}$, whereas the reverse is expected [131].

Z-Averaged Perturbation Theory (ZAPT) uses standard RHF α and β orbitals for the doubly occupied and unoccupied orbitals spin functions, but singly occupied orbitals have spin functions that are a linear combination of α and β as follows [132]:

$$\sigma^+ = \frac{1}{\sqrt{2}}(\alpha + \beta) \tag{3.5}$$

$$\sigma^- = \frac{1}{\sqrt{2}}(\alpha - \beta) \tag{3.6}$$

A perturbation theory [133] based around these orbitals in the reference will be cheaper computationally than using RHF wavefunction because the orbitals are symmetric with respect to interchanging α or β spins, and so identical spatial parts for the α and β spin orbitals can be used. Schaefer [134] gives a good comparison between ZAPT series and RMP ROMP methods.

3.1.3 Coupled Cluster Methods for Open-Shell Systems

The are three main approaches for coupled cluster theory for open shell systems. Firstly a UHF reference wavefunction or ROHF wavefunction is used as the reference wavefunction. These coupled cluster methods are still spin contaminated [135], and the computational cost of such schemes is much higher than the equivalent closed shell case. The single reference spin-restricted method of Rittby and Bartlett [136] uses an ROHF reference wavefunction and different orbitals for different spins to create an open shell coupled cluster method. The energy for this method is not spin contaminated, but $\langle \Psi_{CC} | \hat{S}^2 | \Psi_{CC} \rangle \neq s(s+1)$, the wavefunction is still contaminated which may effect the calculation of molecular properties.

Alternatively, the spin restricted approach uses the following equations to apply constraints on the cluster operator, $\hat{T}$ [137]:

$$s(s+1) = \langle \Phi_0 | \exp(-\hat{T}) \hat{S}^2 \exp(\hat{T}) | \Phi_0 \rangle \tag{3.7}$$

$$0 = \langle \Phi_0 | \hat{q}^\dagger \exp(-\hat{T}) \hat{S}^2 \exp(\hat{T}) | \Phi_0 \rangle \tag{3.8}$$

Spin projections on the Schrödinger equation on configurations that yield $s(s+1)$ are used to determine the independent amplitudes. This is used to reduce the number of independent amplitudes to the number of spin-adapted configurations used in the truncated subspace. This method has the advantage that the $\hat{T}$ operator can still be truncated to single and double excitations, and the computational cost is reduced in comparison to UHF-CCSD method.

The unitary group approach (UGA) to a spin-adapted coupled cluster method for open shell [138] uses a spin-free spatial reference configuration, and a spin-free cluster operator T and the number of independent unknowns in the cluster amplitudes is minimal. The resulting wavefunction however is not antisymmetric, but is spin-free. The correlation energy is determined using a spin-independent Schrödinger equation. This approach has been applied to the excited states of ozone, where good agreement with experiment and FCI results were obtained [139].

A fully spin adapted approach was also developed by Janssen and Schaefer [140]. The disadvantage of this method is in the complexity of the equations making them difficult to implement. The spin-adapted coupled cluster formalism of Nooijen and Bartlett [141] uses spin orbital based equations, rather than the spatial orbital approach of UGA, and a similarity transformed Hamiltonian where the exponential operators are normal ordered.

A less rigorous, but computationally more efficient method is partially spin-adapted coupled cluster methods [142]. The spin contamination is not completely removed, but the effect on the calculated energies is much reduced compared to unrestricted coupled cluster methods. In the partially spin-adapted method of Neogrády [143], only the largest class of excitation are spin-adapted, the double excitation between doubly occupied and virtual orbitals. Since only one class of excitations is spin adapted, the implementation is simpler, and the results are very similar to those obtained through full spin-adaption.

Similarly to the ZAPT method, symmetric spin orbitals [132] based on an open shell RHF can be used as the reference wavefunction for a coupled cluster approach. The advantage of this is that the reference wavefunction will be an eigenfunction of S^2, but not of S_z. The Open-shell Coupled Cluster method(OCCSD) [144] based on these spin orbitals has more symmetry in the spin indices, leading to fewer independent parameters,

and therefore a reduction in the computational cost.

3.2 Benchmark Coupled Cluster results with a UHF reference wavefunction

When an RHF wavefunction is used as the reference wavefunction to calculate the potential energy curves of each of the coupled cluster methods for N_2, poor results were seen at stretched bond lengths, and there is a great difficulty to get points further out than $r = 1.7\,\text{Å}$. This is because N_2 dissociates to open shell products, and for this the RHF wavefunction becomes a poor reference. By changing the reference wavefunction to an UHF wavefunction, it is hoped that the long range correlation will be described better for each of the coupled cluster methods.

Fig.3.1 illustrates the results of each of the coupled cluster methods for N_2 with a UHF reference wavefunction. Calculations were performed with the minimal STO-3G basis set. At long bond lengths all the coupled cluster methods give better results, with the right dissociation products, in comparison to the results in the previous chapter where a RHF wavefunction was used. This is also seen in the methods having small errors compared to FCI in the region longer than $r = 2\,\text{Å}$.

From these results it is clear that the largest errors are seen at short bond lengths, between $1 - 2\,\text{Å}$. The smallest errors are seen with VCCSD and ECCSD with TCCSD performing considerably poorer. There are missing data points in the UCCSD and ECCSD graphs as in this region the points failed to converge.

This region, after $r = 1\,\text{Å}$, is the start of the onset of the UHF solution. Therefore, the large errors maybe arising from the coupled cluster wavefunctions still containing spin contamination.

The potential energy curves of N_2 calculated using both RHF and UHF wavefunctions are shown in Fig 3.2. From this it can be seen that UHF and RHF give exactly the same results at short bond lengths, but that there is a discontinuity in the second derivative

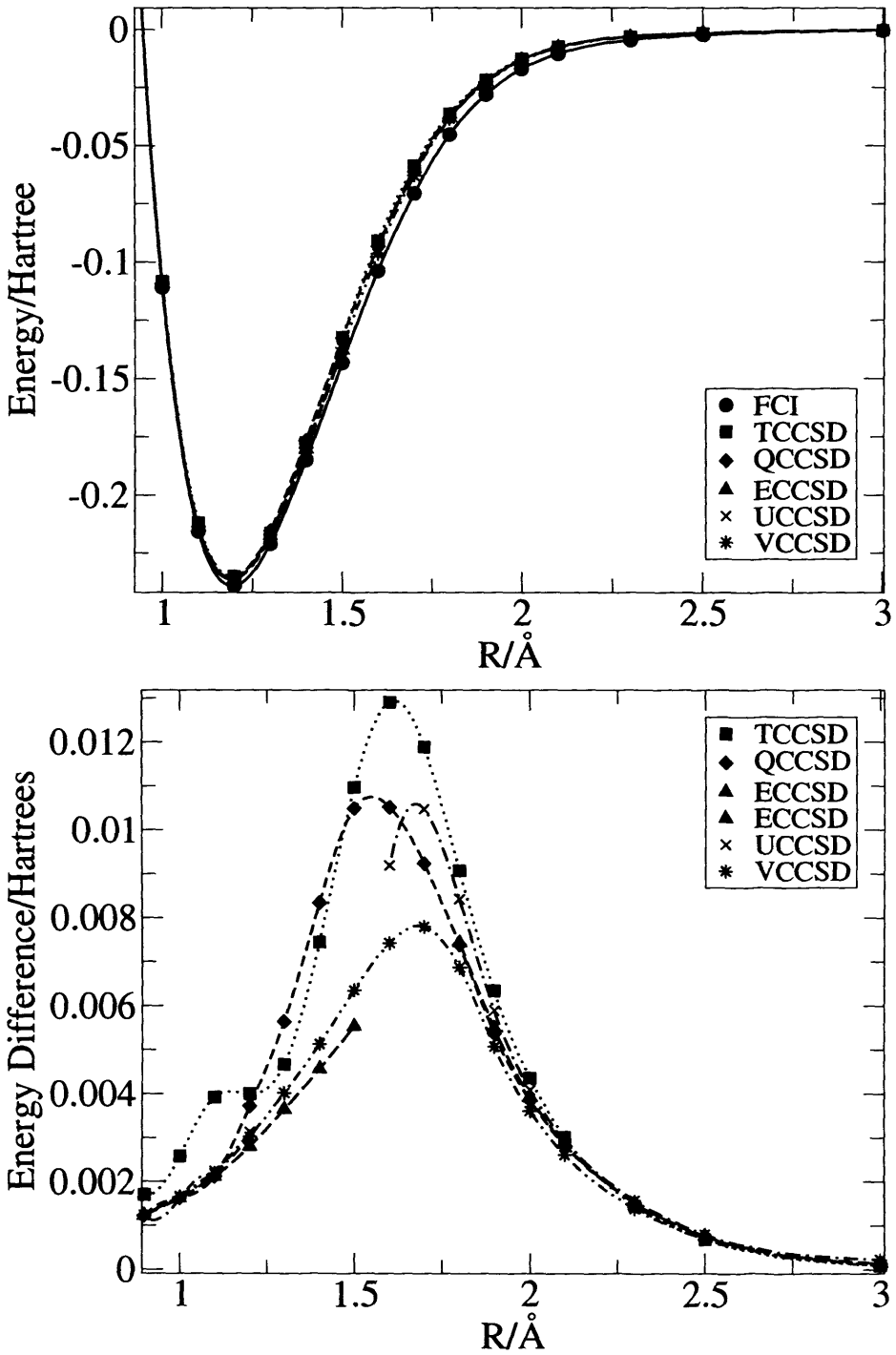

Figure 3.1: Potential energy curves for each of the Coupled Cluster method using a UHF reference function for N_2,and differences from FCI below

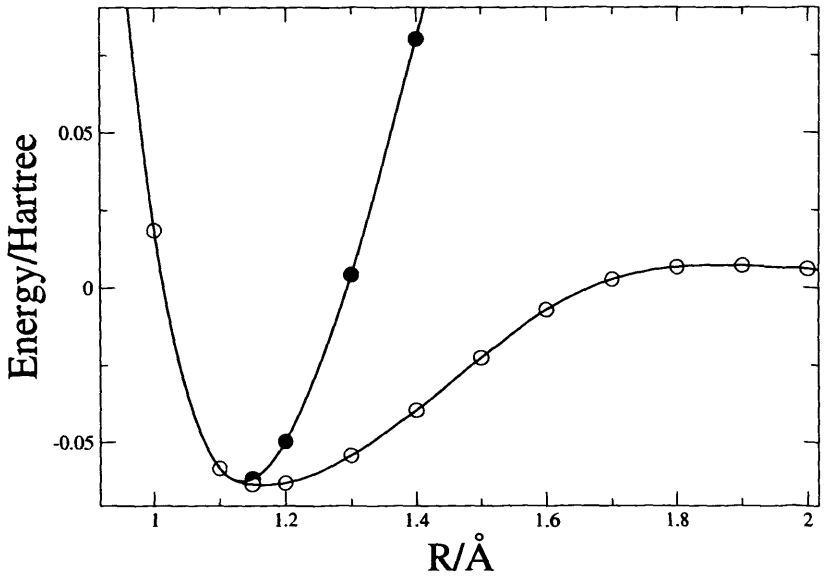

Figure 3.2: The potential energy curves for N_2 with the RHF ● and UHF ○ methods with STO-3G basis set.

of the energy in the UHF method, resulting in the UHF method giving the correct dissociation products of two neutral N atoms. The magnitude of this discontinuity in the derivative of the energy can give a measure of the spin contamination, as is set out in the following section.

3.3 Size of the Discontinuity in the Second Derivative of the Energy

3.3.1 Theory

The UHF molecular orbitals can be expressed in terms of a linear combination of atomic orbitals, for example the alpha spin orbitals are expressed as follows [115]:

$$\psi_o^\alpha = \cos(\theta)\,\phi_o + \sin(\theta)\,\phi_u \tag{3.9}$$

$$\psi_u^\alpha = -\sin(\theta)\,\phi_o + \cos(\theta)\,\phi_u \tag{3.10}$$

where the subscripts o and u indicate occupied and virtual orbitals, and θ is the symmetry breaking parameter. When $\theta = 0$, this corresponds to completely delocalised orbitals. This is the case for bond lengths smaller than r_{root}, where r_{root} is the location of the discontinuity in the energy derivative. This is also the point where UHF and RHF orbitals are equivalent. When $\theta = \pi/4$ this corresponds to completely localised orbitals, i.e. at infinite separation of the two atoms.

The electronic energy of the unrestricted single determinant of the wavefunction can be expressed as a function of θ, the symmetry breaking parameter, and in terms of the molecular integrals of the restricted problem, as follows [116]:

$$E_0(\theta) = 2\cos^2\theta\, h_{11} + 2\sin^2\theta\, h_{22} + \cos^4\theta\, J_{11} + \sin^4\theta\, J_{22} + 2\sin^2\theta\,\cos^2\theta\,(J_{12} - 2K_{12}) \tag{3.11}$$

The derivative of the energy with respect to θ can be expressed as:

$$\frac{\partial E}{\partial \theta} = 4\sin\theta\,\cos\theta\,[h_{22} - h_{11} + \sin^2\theta\, J_{22} - \cos^2\theta\, J_{11} + \cos^2\theta\,\sin^2\theta\,(J_{12} - 2K_{12})] \tag{3.12}$$

From the above equation it can the seen that there are two possible solutions for a stationary point in the energy. Firstly, $4\sin\theta\,\cos\theta$ could be zero which is the restricted solution. The second unrestricted solution is given by the following expression:

$$h_{22} - h_{11} + \sin^2\theta\, J_{22} - \cos^2\theta\, J_{11} + \cos^2\theta\,\sin^2\theta\,(J_{12} - 2K_{12}) = 0 \tag{3.13}$$

There is only an unrestricted solution when $\cos^2\theta = \eta$ where η is given by:

$$\eta = \frac{h_{22} - h_{11} + J_{22} - J_{12} + 2K_{12}}{J_{11} + J_{22} - 2J_{12} + 4K_{12}} \tag{3.14}$$

At dissociation, the energies of the occupied and virtual orbitals become degenerate, i.e. $h_{22} \rightarrow h_{11}$, and using the above equation $\eta = 1/2$. As R, the bond length, is decreased and the atoms are brought together, the separation in the energies of the occupied and virtual orbitals increases and so η will increase. At $\eta = 1$ there is a saddle point in the energy, and when the bond length is further decreased there is no unrestricted solution and the restricted $\theta = 0$ solution is the true minimum. The gradient with respect to R at $\eta = 1$ will be finite as there are no restrictions on the value that η can take.

The derivatives with respect to R of the general energy expression as a function of both θ and R can be expressed as:

$$E(\theta, R) = g(\theta)f(R) \tag{3.15}$$

$$\frac{dE}{dR} = g'(\theta)f(R)\frac{d\theta}{dR} + g(\theta)\frac{df(R)}{d(R)} \tag{3.16}$$

$$\frac{d^2E}{dR^2} = g''(\theta)f(R)(\frac{d\theta}{dR})^2 + 2g'(\theta)\frac{df(R)}{dR}\frac{d\theta}{dR} + g'(\theta)f(R)\frac{d^2\theta}{dR^2} + g(\theta)\frac{d^2f(R)}{dR^2} \tag{3.17}$$

where θ is a function of R. At convergence, the derivative of the energy with respect to θ is zero, as this is a variational condition. Therefore the first term in Eq. (3.16) will disappear, and at the critical point the first derivative will be the same as the RHF derivative. The first derivative of the energy with respect to R will therefore be continuous. In the second derivative Eq. (3.17) the third term only disappears. The terms that contain $\frac{d\theta}{dR}$ are discontinuous. The discontiunity occurs at the onset of the UHF solution. By replacing $\sin(\theta)$ in Eq. (3.11) with x, and grouping terms with the same power of x together, the energy can be expressed as:

$$E(x) = a(R) + x^2b(R) + x^4c(R) \tag{3.18}$$

with:

$$a(R) = 2h_{11} + J_{11} \tag{3.19}$$

$$b(R) = -2(h_{11} - h_{22} + J_{11} - J_{12} + 2K_{12}) \tag{3.20}$$

$$c(R) = J_{11} + J_{22} - 2(J_{12} - 2K_{12}) \tag{3.21}$$

The derivative of the energy with respect to x becomes:

$$\frac{\partial E(x)}{\partial x} = x(2b(R) + 4c(R)x^2) \tag{3.22}$$

The RHF solution is given by $x = 0$ and the UHF solution is $x = \sqrt{-b(R)/2c(R)}$. This means there is only a real solution when $b(R)/c(R)$ is negative. The functions $b(R)$ and $c(R)$ are continuous, therefore there must be a discontinuity in the derivative dx/dR. In the limit of $R \rightarrow$ inf, $h_{22} \rightarrow h_{11}$ and the integrals J_{11}, J_{22} J_{21} and K_{12} are all the same, J. The UHF solution is real, because $b(R) = -4J$ and $c = +4J$. In the bonded limit, taking values from a calculation on H_2 in a minimal basis set, $c(R)$ remains positive. When the energy gap between the σ_g and σ_u is large, h_{22} becomes much larger than h_{11} and the sign in $b(R)$ will flip to being positive. The UHF solution will fall in the complex plane.

In the exact wavefunction there will be no discontinuities. Therefore the size of the discontinuity in approximate wavefunction methods can give a means of assessing how close the approximate wavefunction is to the exact wavefunction, as well as an idea of the magnitude of the spin contamination remaining in the method. It is therefore interesting to consider the size of the discontinuity for each of the coupled cluster methods when a UHF wavefunction is used as the reference function.

3.3.2 Calculation of the size of the discontinuity in the energy derivative

The magnitude of the discontinuity in UHF was calculated for the N_2 molecule by first evaluating numerically the second derivative of the energy between 1.11 and 1.13Å, a range that includes the location of the root, using the following formula:

$$\frac{\delta^2 E}{\delta r^2} = \frac{E_1 + E_3 - 2E_2}{(r_2 - r_1)^2} \tag{3.23}$$

The step size used between points was 0.001 Å. The step size was chosen such that there was a large enough difference in the values of the energy calculated at each point for the subtraction operations to have enough significant figures remaining, whilst small enough that the results would still be accurate. To this end the convergence thresholds were set to be 10^{-12} to increase the number of significant figures that were reliable.

Table 3.1: The size of the discontinuity in the first and second derivatives of the energy for each of the coupled cluster methods, with single and double excitations in the cluster operator

Method	First Derivative	Second Derivative
FCI	-0.0003	0.00168
HF	-0.0004	5.1612
TCC	0.0207	
VCC	-0.0022	
UCC	0.0	
ECC	-0.0011	
QCC	-0.0152	
MP2	1.3455	
MP4	-0.5333	

This large difference between the size of the discontinuity in the energy for TCCSD and VCCSD can be seen in Fig. 3.3. There is a clear break in the TCCSD energy derivative when the UHF wavefunction is used, and there is a significant lowering of the value of the energy derivative after the onset of the UHF solution. In comparison, the difference is much smaller, with the RHF and UHF VCCSD results being very similar over the range of the onset of the UHF solution.

The Unitary Coupled Cluster result indicates that there is no spin contamination remaining in this method, and that the wavefunction is very close to the exact wavefunction.

Table 3.1 also shows that there is much less spin contamination in all the coupled cluster methods in comparison to the Møller-Plesset perturbation methods, MP2 and MP4. This can also be seen in Fig.3.4, which shows the potential energy curve for N_2 calculated with MP2 and TCCSD with both RHF and UHF reference wavefunction in the region of the onset of the UHF solution. The large amount of spin contamination in the UMP2 method leads to a minima in the potential energy curve at the onset of the UHF solution, rather than indicating the equilibrium structure. It has been shown [145] that UMP exhibits the same failure in accurately describing the potential energy surface of O_2^{+2}, which is isoelectric with N_2. In comparison, the TCCSD results are much better as they the

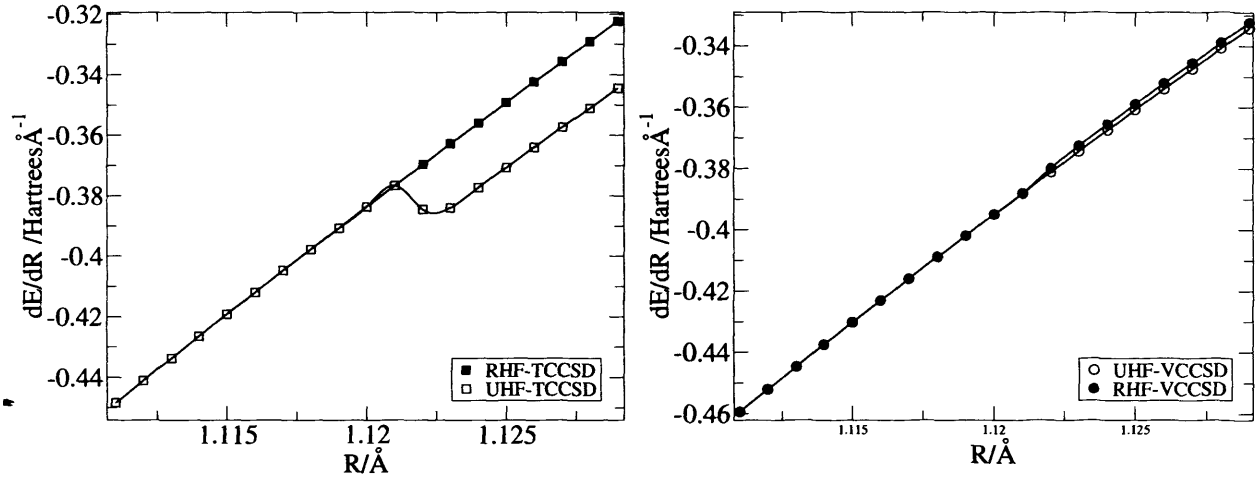

Figure 3.3: The values of the derivative of the energy as the bond length is changed, TCCSD left and VCCSD right for N_2.

minima is at the equilibrium structure, and the potential energy curve is much smoother through out this region.

In order to support these results, the values of S^2 have been evaluated for each of the Coupled Cluster methods for N_2.

3.4 Evaluation of S^2 for N_2

The evaluation of S^2 has been shown to be a useful diagnostic tool in determining the quality of calculations [125]. Chen and Schlegel show that the UMP, UCC and UCI methods using the UHF reference wavefunction, have lower values for S^2 than UHF at the same bond lengths for single bond breaking, because these post-SCF methods are nearer to the exact wavefunction than UHF. They also show that all the single reference methods based on UHF reference have an S^2 value at dissociation that is the same as the UHF result.

The usefulness of the expectation value of S^2 when a UHF reference wavefunction is used with CCSD for analysing the quality of the energy has been examined by Yuan and Cremer [146]. They analysed the components of $\langle \hat{S} \rangle$ by separating it into terms arising from the fact that the CCSD wavefunction does not satisfy the Hellman-Feynman theorem,

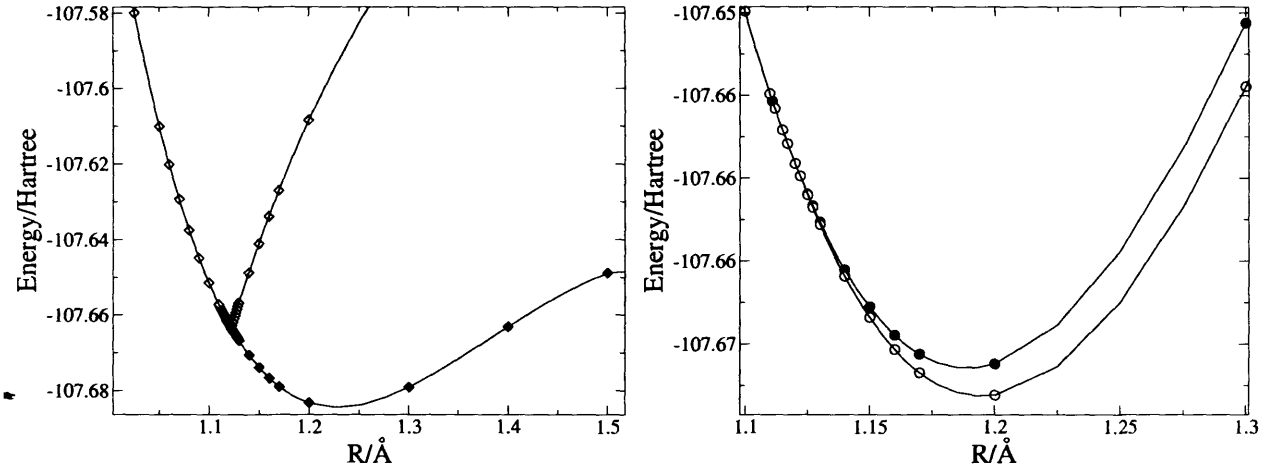

Figure 3.4: The energies curves for N_2 with the MP2 method, left with UHF ◊ and with RHF ♦ and TCCSD to the right, UHF reference ○, and RHF reference●

i.e. the perturbation $\lambda\hat{S}$ affects the cluster amplitudes, and those that relate to the form of the energy operator. They conclude that UHF-CCSD is free from $S+1$ contaminant, and therefore is good at describing homolytic single bond breaking. However, the large values of $\langle\hat{S}\rangle$ seen at large R, bond length, are due to wavefunction not satisfying the Hellman-Feynman theorem and the spin contamination making up a significant portion of the wavefunction, and so $\langle\hat{S}\rangle$ is no longer a good diagnostic tool for assessing the quality of the energy. They also conclude that when the UHF wavefunction has large spin contamination the S^2 value for CCSD will be large, and the energy less accurate if more than one bond is broken, as the wavefunction will have higher multiplicity spin contaminants.

In a many electron system, the total spin-squared angular momentum operator, $\hat{S}^2$, can be represented in the following way, using second quantisation notation [126]:

$$\hat{S}^2 = \hat{S}_z^2 + \hat{S}_z + N_\beta - \sum_{pq\bar{r}\bar{s}} S_{p\bar{s}} S_{q\bar{r}} \hat{E}_{pq} \hat{E}_{\bar{r}\bar{s}} \tag{3.25}$$

where $\hat{E}_{pq}$ and $\hat{E}_{\bar{r}\bar{s}}$ are annihilation-creation operators for alpha and beta spins, and $S_{p\bar{s}}$ is the overlap matrix:

$$S_{p\bar{s}} = \langle\phi_p|\bar{\phi}_{\bar{s}}\rangle \tag{3.26}$$

An estimation for the spin contamination in each of the coupled cluster methods can be evaluated using the following equations:

Traditional

$$S^2 = \langle\Phi_0|\hat{S}^2 \exp(\hat{T})|\Phi_0\rangle \tag{3.27}$$

Variational

$$S^2 = \frac{\langle\Phi_0| \exp(\hat{T}^\dagger)\hat{S}^2 \exp(\hat{T})|\Phi_0\rangle}{\langle\Phi_0| \exp(\hat{T}^\dagger) \exp(\hat{T})|\Phi_0\rangle} \tag{3.28}$$

Unitary

$$S^2 = \langle\Phi_0| \exp(-(\hat{T} - \hat{T}^\dagger))\hat{S}^2 \exp(\hat{T} - \hat{T}^\dagger)|\Phi_0\rangle \tag{3.29}$$

Extended

$$S^2 = \langle\Phi_0| \exp(\hat{\Lambda}^\dagger) \exp(-\hat{T})\hat{S}^2 \exp(\hat{T})|\Phi_0\rangle \tag{3.30}$$

where $|\Phi_0\rangle$ is the UHF reference function and $\hat{T}$ is the cluster operator, specified as a linear combination of a manifold of excitation operators:

$$\hat{T} = \sum_q T_q \hat{q} \tag{3.31}$$

3.4.1 Results

Fig 3.5 shows the value of S^2 for each of the coupled cluster methods as the bond length is varied. This shows that for each of the coupled cluster methods the value of S^2 approaches the UHF value of 3 at dissociation. This follows the work of Chen and Schlegel [125]. S^2 takes a non-zero value from the onset of the UHF solution.

The graph shows that the derivative of S^2 with respect to bond length, is greater for UHF than for the coupled cluster methods at the onset of the UHF solution. TCCSD has a significantly different graph than the other coupled cluster methods. UCCSD gives a plot similar to VCCSD indicating that these methods have similar behaviour with respect to spin contamination. These two methods have S^2 values closer to zero over a much larger range of bond lengths, out to $r = 1.3$ Å before the value of S^2 rises steeply. ECCSD and QCCSD curves are also similar to each other.

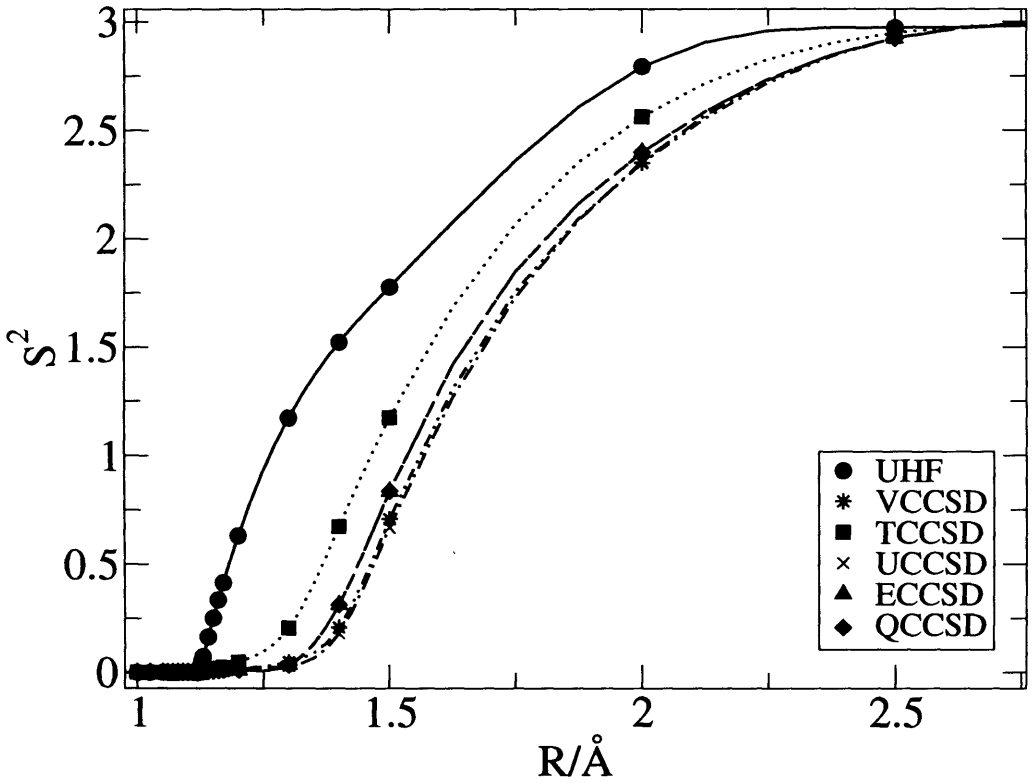

Figure 3.5: Plot of the values of S^2 for each of the Coupled Cluster method using a UHF reference function for N_2

Table 3.2: Values of the derivative of S^2 with respect to bond length at the onset of the UHF solution

Method	$\frac{d}{dr}S^2$
UHF	9.67
TCCSD	1.58
VCCSD	0.23
UCCSD	0.50
ECCSD	1.39
QCCSD	1.37

Table 3.2 shows the values of the derivative of S^2 for each of the coupled cluster methods at the onset of the UHF solution. From these results it can again be seen that VCCSD and UCCSD are giving similar results. TCCSD has a significantly higher value for the derivative in comparison to VCCSD and UCCSD. ECCSD and QCCSD have values closer to TCCSD than VCCSD. This is not in agreement with the values for the derivative of the energy, which would suggest that ECCSD should be closer to VCCSD.

3.4.2 Electron Affinity for CN

The UHF wavefunction for the cyano radical (CN•) is heavily spin contaminated even at the equilibrium geometry. Previously, [121] it has been found that the UMP series for the cyano radical converges slowly, thus UMP2 electron affinities for this species give poor agreement compared to experiment. The slow convergence of the UMP series has been rationalised by spin contamination in the wavefunction [122]. It has also been shown that there is small but negligible spin contamination in UHF-CCSD and ROHF-CCSD wavefunctions, even in cases where the spin contamination in the UHF reference is high when considering molecules at the equilibrium structures [135].

Spin contamination can also give very large errors in the vibrational frequencies of diatomic molecules [147] [148], with the errors related to the geometric derivative of $\langle S^2 \rangle$. As the wavefunction gets contaminated with higher energy states the potential energy surface will rise too steeply, giving rise to large values of $d\langle S^2 \rangle / dR$, and thus the vi-

Table 3.3: Frequencies, bond lengths and energies for CN with RHF used as the reference wavefunction.

Method	$\omega_e(cm^{-1})$	r_e(Å)	E_{CN}(Hartree)	ZPE(Hartree)
RHF	2534.21	1.16490	-90.99754272	0.005773
FCI	2043.74	1.22936	-91.18012786	0.004656
TCCSD	2136.90	1.22573	-91.17273177	0.004868
VCCSD	2081.27	1.22569	-91.17461223	0.004741
UCCSD	2091.46	1.22486	-91.17358654	0.004765
ECCSD	2077.77	1.22486	-91.17492818	0.004734
QCCSD	2079.04	1.22586	-91.17490053	0.004736

brational energies will be too high. The equilibrium bond length can be too short, and the energy too high in molecules with a large amount of spin contamination, and these properties related directly to the difference in $\langle S^2 \rangle$ and $s(s+1)$.

It is therefore interesting to study the electron affinity of the cyano radical with each of the coupled cluster methods. All calculation were performed with the STO-3G minimal basis set. The energies were calculated for each of the methods at five points around the minimum. A quartic fit through the points was used to calculate the equilibrium bond length, r_e and the equilibrium energies. The derivative of the fit at the minimum gives the force constant, k, and from this the vibrational frequencies, ω_e can be calculated using the following expression;

$$\omega_e = \frac{1}{2\pi}\sqrt{\frac{k}{\mu}} \tag{3.32}$$

where μ is the reduced mass. The electron affinity was calculated as follows;

$$EA = E_{CN^-} - E_{CN} \tag{3.33}$$

with the energies corrected with the zero point energies.

Tables 3.3, 3.4 and 3.5 show vibrational frequencies ω_e, equilibrium bond lengths, r_e, energies, and the zero point energy for CN and CN^- for each of the coupled cluster methods, with both RHF and UHF reference wavefunctions.

Table 3.3 shows that the RHF method gives a large difference in the equilibrium structure

Table 3.4: Frequencies, bond lengths and energies for CN with UHF used as the reference wavefunction.

Method	$\omega_e(cm^{-1})$	r_e(Å)	E_{CN}(Hartree)	ZPE(Hartree)
UHF	1562.01	1.23455	-91.02639017	0.003559
FCI	2043.74	1.22936	-91.18012786	0.004656
TCCSD	2098.21	1.22640	-91.17602468	0.004780
VCCSD	2063.81	1.22732	-91.17553805	0.004702
UCCSD	2095.91	1.22479	-91.17394511	0.004775
ECCSD	2063.78	1.22700	-91.17547305	0.004702
QCCSD	2087.52	1.22562	-91.17503282	0.004756

Table 3.5: Frequencies, bond lengths and energies for CN- with RHF used as the reference wavefunction.

Method	$\omega_e(cm^{-1})$	r_e(Å)	E_{CN^-}(Hartree)	ZPE(Hartree)
RHF	2559.70	1.16225	-90.93767006	0.005831
FCI	2134.05	1.21166	-91.08317942	0.004862
TCCSD	2189.06	1.20658	-91.07801051	0.004987
VCCSD	2170.68	1.20818	-91.07935757	0.004945
UCCSD	2179.31	1.20752	-91.07897878	0.004965
ECCSD	2167.64	1.20841	-91.07949275	0.004938
QCCSD	2167.65	1.20841	-91.07949384	0.004938

for the cyano radical in comparison to FCI. This is seen in both the equilibrium bond length being shorter, by 0.064 Å and in the large difference in the frequency, which is 490 cm^{-1} greater than the FCI frequency. The coupled cluster methods overestimate the frequencies, and underestimate the equilibrium bond lengths, in comparison to FCI, indicating that these methods are over binding.

TCCSD has larger errors in each of the properties in comparison to the other coupled cluster methods. TCCSD gives the largest error in the equilibrium energy with a difference from FCI of 0.0074 Hartree, whereas VCCSD has an error of 0.0055 Hartree for this quantity. TCCSD also has a large error in the equilibrium frequency, with an error of 93 cm^-1 greater than the FCI value, whereas the error in VCCSD is much smaller, 38 cm^-1. UCCSD, ECCSD and QCCSD all give similar results to VCCSD.

Table 3.4 shows that the UHF result overestimates the bond length in the cyano radical, in comparison to the FCI result by 0.005 Å. This is a much lower error than for RHF. The equilibrium bond length with UHF is longer than the bond length in RHF because the UHF wavefunction includes some electron correlation and because of the spin contamination. The equilibrium energy is also closer to the FCI result than RHF, but still too high. Again a lower energy is expected with a UHF wavefunction than with RHF because of the inclusion of electron correlation and the variational principle guarantees that the lowering effect of electron correlation is more than the rising of the energy due to inclusion of higher spin states. The error in the frequency for UHF is comparable to that in RHF, 482 cm^{-1}, but is underestimated rather than overestimated. Again this is expected because of the spin contamination in the wavefunction.

All the Coupled Cluster methods overestimate ω_e and underestimate the equilibrium bond lengths, which indicates that they are still over binding when a UHF wavefunction is used as the reference wavefunction. TCCSD has larger errors in each of the properties in comparison to the other Coupled Cluster methods. The errors in the equilibrium energy are all similar ranging form 0.0045-0.0051 Hartree. The errors in the energies are smaller with the UHF reference wavefunction than when the RHF reference function is used, suggesting that the effects of including electron correlation are still outweighing the spin contamination.

Table 3.6: Electron Affinities for CN with each of the coupled cluster methods, with RHF and UHF reference wavefunctions

Method	EA_{RHF} (eV)	EA_{UHF} (eV)
HF	1.631	2.476
FCI	2.644	2.644
TCCSD	2.581	2.673
VCCSD	2.598	2.624
UCCSD	2.580	2.589
ECCSD	2.602	2.618
QCCSD	2.602	2.605

Table 3.7: Values of S^2 and the derivative of S^2 with respect to bond length at the equilibrium bond length for each method

Method	S^2	$\frac{d}{dr}S^2$
UHF	1.563	4.48
TCCSD	0.110	1.44
VCCSD	0.054	0.41
UCCSD	0.018	0.2
ECCSD	0.034	0.41
QCCSD	0.035	0.41

Table 3.5 shows that the RHF method gives large differences for the equilibrium structure of the cyano anion, compared to the FCI results. It predicts a bond length similar to the of the cyano radical, and 0.049 Å shorter than the FCI bond length. The Coupled Cluster methods again overestimate the frequency, and underestimate the bond lengths, indicating that these are still consistently over binding, and therefore it is expected that there will be a cancelation of errors when the electron affinity is calculated.

TCCSD again has larger errors than the other coupled cluster methods. ECCSD and QCCSD give results very similar to those of VCCSD. The error in the energy in comparison to FCI is 0.0052 Hartree for TCCSD compared to VCCSD, ECCSD and QCCSD which give errors between 0.0038-0.0037 Hartree.

Table 3.6 shows the calculated electron affinities for each of the methods with an RHF and UHF wavefunctions. Each of the coupled cluster methods gives results very similar to FCI due to cancelation of errors, in that both the CN radical and CN anion results were over binding. The electron affinities when a UHF reference wavefunction was used for the radical for each of the coupled cluster methods, are closer to the FCI values in comparison to when an RHF wavefunction was used.

The results show that there is a greater difference in the values obtained using TCCSD with RHF and UHF references, of 0.082 eV compared to the other coupled cluster methods, where the differences are between, 0.026 and 0.003 eV. TCCSD with a UHF reference wavefunction overestimates the electron affinity of CN•, whereas the other coupled cluster methods underestimate the electron affinity, in comparison to the FCI values. The smallest errors are seen with VCCSD, ECCSD and QCCSD with both types of reference wavefunction.

Table 3.7 shows the value of S^2 and the derivative of S^2 with respect to bond length at the equilibrium bond length for each of the coupled cluster methods. S^2 was evaluated at the same five geometry points as the energies, and the results were extrapolated to find the value at the minimum.

The results for S^2 and $\frac{dS^2}{dR}$ again show that VCCSD, ECCSD and QCCSD have a similar amount of spin contamination. This concurs with the similar results found in the equilibrium properties of CN•with VCCSD, ECCSD and QCCSD. TCCSD has greater values for for S^2 and $\frac{dS^2}{dR}$ than the other coupled cluster methods, although there is still a significant improvement in comparison to the UHF wavefunction. This indicates that the TCCSD is more spin contaminated than the other coupled cluster methods, and explains the poorer results seen in the cyano radical with TCCSD and a UHF reference wavefunction.

UCCSD has the smallest values forS^2 and $\frac{dS^2}{dR}$ indicating that there is little spin contamination in this method, and that the wavefunction is nearer the exact wavefunction than the other methods. This can also be seen in the properties of the cyano radical calculated with UCCSD where there is little difference between the results calculated with an RHF wavefunction compared with those calculated with a UHF wavefunction.

3.5 Conclusion

The potential energy curves for N_2 with UHF reference wavefunction show large errors for each of the coupled cluster methods in the region of the onset of the UHF solution. However, the asymptotic region is well described by each of the coupled cluster methods, with the correct neutral species for the products. TCCSD performs considerably poorer than VCCSD or ECCSD in the region of the onset of the UHF solution.

It has also been shown that the TCCSD wavefunction, when a UHF wavefunction is used as the reference, has more spin contamination remaining in the wavefunction in comparison to the other coupled cluster methods. This is shown in both the analysis of the discontinuity in the energy derivative, and the evaluation of S^2 for N_2. However, the amount of spin contamination is much less than in UHF wavefunction, and considerably less than in the perturbation methods MP2 and MP4 methods.

The remaining spin contamination has been shown to be ten times smaller for variational coupled cluster methods in comparison to TCCSD, for the N_2 case in both the size of the discontinuity in the energy as well as S^2 values.

These results are also reflected in the CN•case. TCCSD results are again furthest away from the FCI values, and show the most change when a UHF reference wavefunction in comparison to RHF wavefunction. TCCSD equilibrium energies are lowered and bond lengths increased when UHF wavefunction is used as the reference. The same trends are true for the other coupled cluster methods, but the differences are much smaller.

TCCSD and has the largest values of S^2, in comparison to the other coupled cluster methods, but the value is much smaller than for UHF suggesting that the amount of spin contamination in the TCCSD wavefunction is more than ten times smaller than in the UHF reference wavefunction. The vibrational frequencies are lower when a UHF wavefunction is used in comparison to RHF wavefunction as the reference. The largest change is again seen with TCCSD which is supported by this method also having the largest $\frac{dS^2}{dR}$ at the equilibrium point.

Chapter 4

Quasi-Degenerate States

4.1 Introduction

Quasi-degeneracy is a non-dynamical type of electron correlation that arises when more than one configuration is needed to describe the electronic system correctly. This is particularly significant for dissociative process and to studies of reactions. In cases of strong quasi-degeneracy quantum chemical methods based around a single reference are often qualitatively incorrect because the Hartree-Fock reference wavefunction becomes a poor description of the ground state wavefunction. Multi-reference methods can perform much better, as the configurations that are important can be include in the optimisation of the molecular orbitals in the reference wavefunction. However, the main disadvantage of multi-reference methods is that they are not black box, care has to be taken about choosing the correct active space.

It is therefore interesting to benchmark the various Coupled Cluster methods on systems known to have strong quasi-degeneracy to see if using a variational energy functional can correctly describe the ground state potential energy curve without the need for a multi-reference wavefunction. The H_4 and BeH_2 systems are extensively studied, as the degree of quasi-degeneracy in the system can be continuously varied, and because the systems are small enough that FCI calculations can be performed for comparisons.

4.2 The perpendicular insertion of Be into H_2

The Be atom has quasi-degenerate 2s and 2p orbitals. Therefore both the $1s^2 2s^2$ and $1s^2 2p^2$ configurations are important when considering the formation of the BeH_2 molecule. It is the $2p$ orbitals that have the correct symmetry to allow the formation of BeH_2 bonds to be formed. The reaction coordinate is further complicated by the hydrogen orbitals. The σ_u and σ_g in the H_2 molecule become degenerate as the H-H bond is broken. It is therefore difficult for single reference methods to describe the perpendicular insertion of a Be atom into an H_2 molecule.

The perpendicular insertion of Be atom into H_2 following a C_{2v} reaction path has previously been studied by Purvis et al [149]. Coupled cluster results were found to be in good

agreement with FCI when the single reference function was changed during the reaction pathway. For geometries starting from the non-bonded Be atom and H_2 molecule to the transition state the $1a_1^2 2a_1^2 3a_1^2$ configuration was used as the reference and beyond the transition state to the bonded BeH_2 geometry the $1a_1^2 2a_1^2 1b_2^2$ reference configuration was used.

The above approach is ambiguous as it is unclear at which value of R, the distance between the Be atom and the H_2 molecule, the reference configuration should be changed. Hanrath [150] has shown that by taking the switching point to be where the dominant configuration changes, there can be a discontinuity in the energy by as much as 10% of the total correlation energy for the SRMRCC (a coupled cluster method where the excitations within T are chosen to span a multi-reference CI space) method [151] which is clearly unacceptable.

To describe the ground state energy surface of the C_{2v} reaction path for this system, more configurations are needed than just the $1a_1^2 2a_1^2 3a_1^2$ and $1a_1^2 2a_1^2 1b_2^2$. Banerjee [152] found that other configurations, the triplet and singlet states are needed near the transition geometry when constructing a MCSCF reference wavefunction for coupled cluster calculations. This system is frequently used to test multi-reference methods such as the the state-selective multi-reference coupled cluster methods [104, 153, 154].

Banerjee *et al* [152] showed that traditional coupled cluster results based on a single RHF reference wavefunction, follow the energy of the reference state. For example when the RHF reference is the $1a_1^2 2a_1^2 1b_2^2$ coupled cluster results are reasonable at short distance of Be-H_2, but dissociate to the wrong products - the ground state Be atom and the excited state of H_2, whereas results for $1a_1^2 2a_1^2 3a_1^2$ reference wavefunction gives good agreement to FCI for the fragments, but not beyond the transition state to the bonded species.

This problem will therefore provide an interesting test problem for each of the Coupled Cluster methods that have been studied. From previous results it is expected that the TCCSD results will follow the RHF results, but it will be interesting to see if the same is true for a the variational method, VCCSD.

4.2.1 Results

Calculations followed a C_{2v} reaction path of insertion of a Be atom between an H_2 molecule in the same manner as Purvis *et al* [149]. The distance between Be atom and the centre of the H_2 molecule was varied between 0.1 and 4 Bohr. The distance between H atoms was varied according to the following expression [152]:

$$r_{HH} = 2(2.54 - 0.46 * r_{Be\text{-}H_2}) \tag{4.1}$$

where r_{HH} is the distance between the two hydrogen atoms, and r_{BeH_2} is the distance between Be and the centre point between the two hydrogen atoms. While this is not the true reaction path, it does cover a range of geometries over which many configurations are required to accurately describe the ground state energy surface. Calculations were performed in the cc-pVDZ(p) basis set, which is small enough that FCI calculations on the system are possible for comparison. An RHF reference wavefunction was used as the reference wavefunction for each of the coupled cluster methods, and with the coupled cluster methods truncated at single and double excitations in the cluster operator.

Fig. 4.1 shows the potential energy curve generate with each of the coupled cluster methods for BeH_2. All of the coupled cluster methods reproduce the FCI results in the range between the bonded molecule, $r_{Be\text{-}H_2} = 0$ to just before the transition point at $r_{Be\text{-}H_2} = 2.6$ Bohr. Throughout this range the RHF reference wavefunction gives a qualitatively correct description of the ground state energy surface.

At the transition point, $r_{Be\text{-}H_2} = 2.8$ Bohr, the quasi-degenerate effects become important, as there is an avoided crossing of the energies of the $1a_1^2 2a_1^2 1b_2^2$ and the $1a_1^2 2a_1^2 3a_1^2$ states. At this point there are differences between the energies seen with the coupled cluster results compared to the FCI values, but there is still not much to distinguish between any of the different formulations of coupled cluster methods.

Beyond $r_{Be\text{-}H_2} = 2.8$ Bohr the $1a_1^2 2a_1^2 3a_1^2$ is the dominant configuration, and as such the RHF reference used becomes a poor description of the ground state energy surface. At this point Fig. 4.1 shows that the best results are seen with the Variational Coupled Cluster method (VCCSD) which gives a potential energy curve that is similar to the FCI curve, although the errors in the energies are still much larger in comparison to the

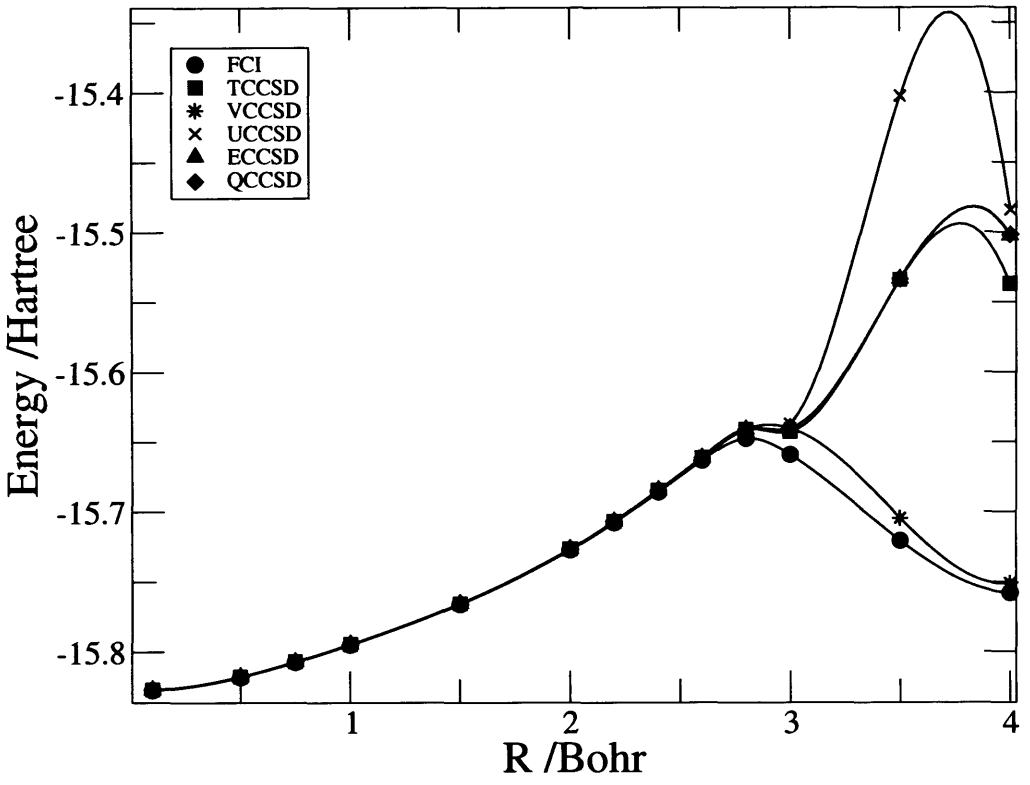

Figure 4.1: Potential energy curve for the C_{2v} reaction pathway for the insertion of Be into H_2.

VCCSD results obtained before the transition point. This is in contrast to the results obtained with Traditional Coupled Cluster (TCCSD), Unitary Coupled Cluster (UCCSD), Extended Coupled Cluster (ECCSD) and Quadratic Coupled Cluster (QCCSD) which all give a qualitatively incorrect potential energy surface after the transition point. These curves reproduce the RHF reference energy curve, and have large energy differences from the FCI results.

4.3 The H_4 model system

The H_4 system has been extensively studied because of its simplicity, and because the relative amount of quasi-degeneracy of the states involved can be continuously varied over a large range.

Here, three reaction coordinates are examined. Firstly in the P4 two hydrogen bonds are broken simultaneously. In the H4 model a single bond is broken as the conformation changes from square planar to a linear structure. Finally, a further reaction coordinate where two hydrogen molecules at infinite separation are brought to a square planar conformation, and then separated again in a perpendicular direction so that the atoms involved in the bonds are different from the original configuration, was also studied. This model has been termed Q4 as a quadratic is fitted through the transition structure and the start and end points.

4.3.1 P4 model

In the P4 model, two parallel hydrogen molecules are separated by the distance α. The hydrogen molecules have a fixed bond length of 2 Bohr. When $\alpha = 2.0$ Bohr, the system is in a square planar arrangement, and there is strong quasi degeneracy. As the distance is increased the amount of quasi degeneracy reduces as two bonds are being broken. At bond lengths $\alpha < 2$ Bohr the system is compressed.

In the square planar D_{4h} geometry the ground state wavefunction can be describe by a linear combination of the two degenerate determinants [155]:

$$|\Psi_1\rangle = |(1a_{1g})^2(1e_{ua})^2\rangle \tag{4.2}$$

$$|\Psi_2\rangle = |(1a_{1g})^2(1e_{ub})^2\rangle \tag{4.3}$$

These determinants in the non-degenerate D_{2h} geometries become:

$$|\Psi_1\rangle = |(1a_1)^2(1b_{3u})^2\rangle \tag{4.4}$$

$$|\Psi_2\rangle = |(1a_1)^2(1b_{2u})^2\rangle \tag{4.5}$$

The P4 model [156] system has been studied by Evangelista *et al.* [155] and Hanrath [150], comparing multi-reference coupled cluster methods with a single reference coupled cluster method with CAS(2,2) optimised orbitals for the reference. They found that whilst multi-reference coupled cluster methods perform better than single reference coupled cluster in the quasi-degenerate region, multi reference coupled cluster methods have larger errors in

the non-degenerate regions. They also found that inclusion of triplet excitations improved the potential energy surfaces in the quasi degenerate region.

Coupled pair methods have also been used to calculate the potential energy surface of the P4 model [156] as well as multi-reference coupled pair methods [157]. CPMET performs well for quasi-degenerate systems even in regions where the quasi degeneracy is strong, whereas linear approximations to this method, L-CPMET and ACP, break down in the region where quasi degeneracy is strong, due to the linear elements of CPMET becoming singular when the orbital energies between doubly excited configurations become degenerate.

Calculations were performed on this model system for each of the coupled cluster methods. The parameter α was varied from 10 Bohr to 1 Bohr, an RHF reference wavefunction was used and the cluster operator included single and double excitations only.

Fig 4.2 shows the potential energy curves obtained for each of the coupled cluster methods following the P4 model for H_4, with the differences in the energy from the FCI values on the right. The plots show that there is little difference between the coupled cluster methods for this model. Each method gives a qualitatively accurate potential energy surface compared to the FCI results.

The graph of the energy differences show that the errors are very small across the range of bond lengths given. At long bond lengths the errors disappear to zero which is expected as all the methods will be exact for two separated hydrogen molecules. The differences from the FCI values however indicates that in the quasi-degenerate region the errors in the coupled cluster methods increase quite dramatically although the errors are still less than 2 mHartrees.

4.3.2 H4 model

The H4 model [156] consists of four hydrogen molecules arranged in an isosceles trapezoidal geometry. The bond lengths between each of the hydrogen atoms is fixed a 1.06Å, and the angle ϕ is varied between $\phi = 90$ square planar geometry to $\phi = 180$ linear

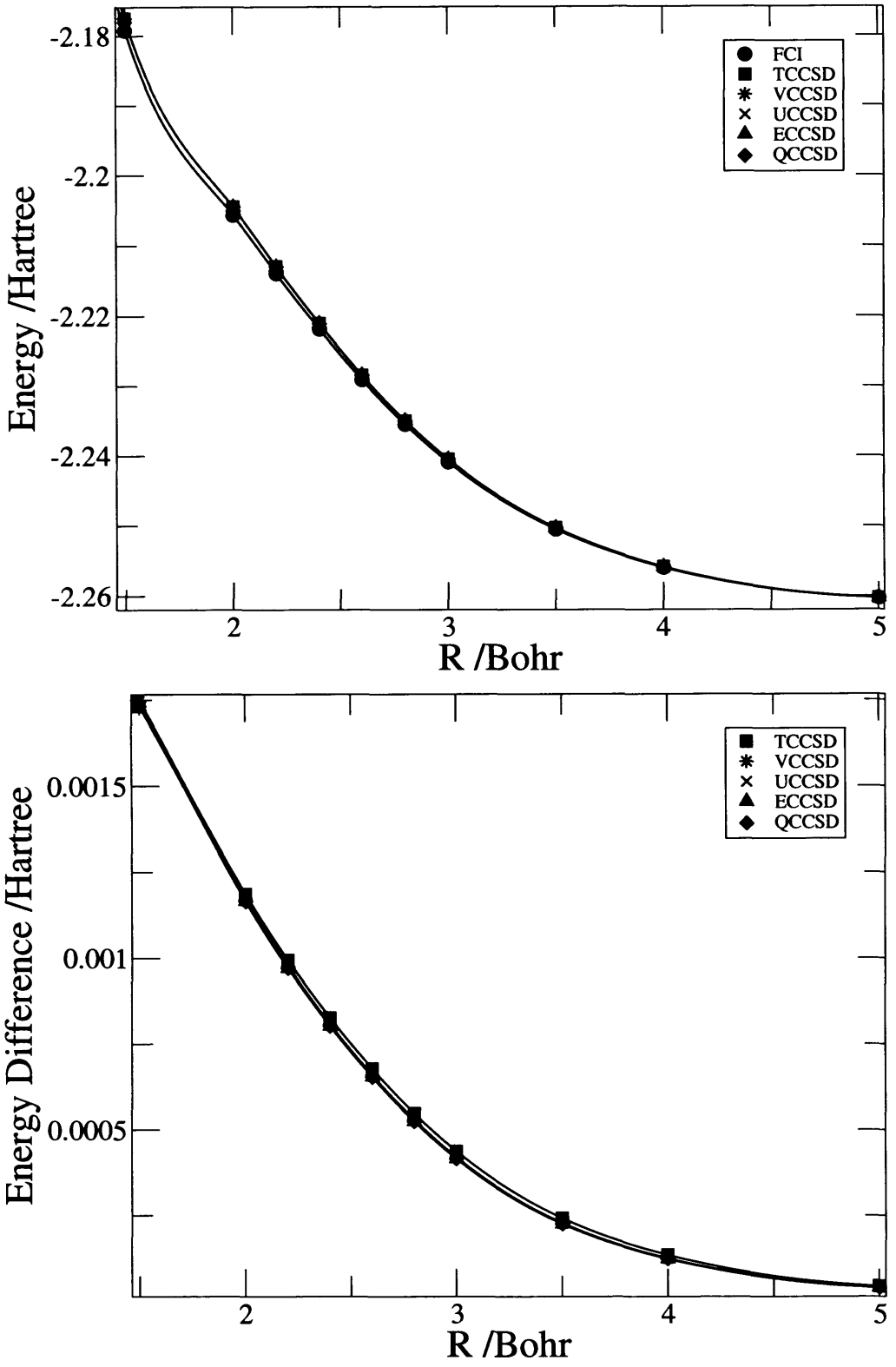

Figure 4.2: Potential energy curve for the P4 model for each of the coupled cluster methods, and differences from FCI below.

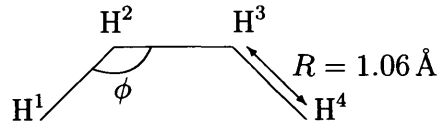

Figure 4.3: Diagram of the arrangement of the four hydrogen atoms in the H4 model.

structure. This model represents a single bond breaking. It is expected that the coupled cluster methods will perform well in the linear and trapezoidal geometries where a single determinant is dominant, but less well in the quasi-degenerate square planar region, where the following two determinants become degenerate:

$$|\Psi_1\rangle = |(1a_{1g})^2(1e_{ua})^2\rangle \tag{4.6}$$

$$|\Psi_2\rangle = |(1a_{1g})^2(1e_{ub})^2\rangle \tag{4.7}$$

Previous calculations on this system comparing single reference coupled cluster methods with multi-reference coupled cluster methods [155] [150] again show that the single reference coupled cluster performs poorly in the quasi degenerate region as expected whilst multi reference methods give a qualitatively accurate potential energy curves with small deviations from FCI values across the range of geometries tested. Errors are again reduced when triple excitations are used in the cluster operator [155]. Previously it has been shown [156] that CPMET calculations perform well for this model system whereas the linear approximations do not. This model system has also been used to study the multiple solutions that result from CCD [158], and test multi-reference methods [153, 159, 160].

In the H4 model, the angle ϕ is varied from the square-planar geometry to a linear conformation:

$$\phi = 90 + \alpha * 180 \tag{4.8}$$

where the parameter α is varied between 0, the square-planar structure, and 0.5 the linear structure. The remaining geometry parameters were kept fixed at 1.06Å. Calculations were performed using the cc-pVDZ(p) basis set. For each of the coupled cluster methods a RHF reference wavefunction was used, and the cluster operator truncated at single and double excitations.

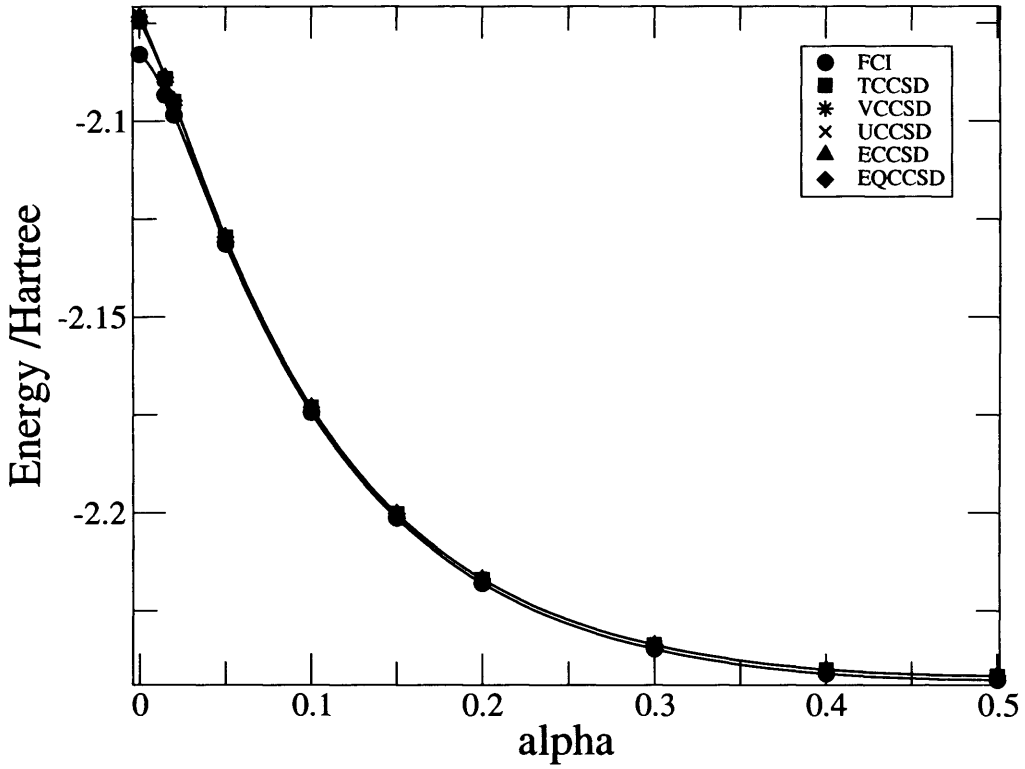

Figure 4.4: Potential energy curve for H_4, where a single bond is broken following the H4 model

Fig 4.4 shows the potential energy curves generated for each of the coupled cluster methods. The graph shows that all the coupled cluster methods for this model system give very similar potential energy curves. As expected the largest errors are seen around $\alpha = 0$, where the amount of quasi-degeneracy is strongest.

4.3.3 Q4 model

In this model two infinitely separated hydrogen molecules are brought together to a square planar intermediate, and then dissociated again so that the molecules are composed of different hydrogen atoms than at the start. Fig. 4.5 demonstrates this reaction path.

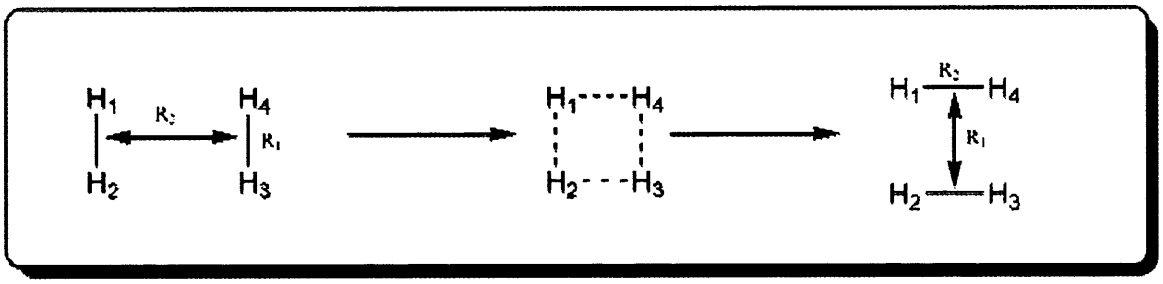

Figure 4.5: Diagram to show the reaction path for H_4, in the Q4 model.

The bond lengths at each point were calculated using the following expressions:

$$r_e = .75 \tag{4.9}$$

$$r_{\text{trans}} = 1.3 \tag{4.10}$$

$$r_1 = r_e + \sqrt{(r_{\text{diff}}^2/4 + (r_e - r_{\text{trans}})^2)} + r_{\text{diff}}/2 \tag{4.11}$$

$$r_2 = r_1 - r_{\text{diff}} \tag{4.12}$$

where r_{trans} is the bond length in Angstroms of the transition state square planar geometry, r_{diff} is the difference between the two sets of bond lengths, r_1 is the distance between H^1 and H^2, and between H^3 and H^4, and r_2 is the distance between H^1 and H^4, as well as H^2 and H^3. The difference between the molecules, r_{diff}, was varied between -10 and 0.5Å. Calculations were performed in the cc-pVDZ(s) basis set, the RHF reference wavefunction was used and the cluster operator was again truncated at the singles and doubles level of excitations.

In this model a wide range of geometries are again explored. When $r_{\text{diff}} = 0$ the arrangement of atoms is again square planar, and the amount of quasi-degeneracy is strong. At negative values of r_{diff} the RHF wavefunction is a suitable reference wavefunction, whereas when the values of r_{diff} are positive, there has been an avoided crossing, and a different configuration has become the lowest in energy. It is therefore expected that the coupled cluster methods will perform well for negative values of r_{diff}, but poorly after $r_{\text{diff}} = 0$.

Fig. 4.6 shows the potential energy curves generated with each of the coupled cluster methods for H_4. As the FCI curve shows, the potential energy curve goes through a maxima at $r_{\text{diff}} = 0$, and is symmetric about this point. Fig. 4.6 shows that as expected

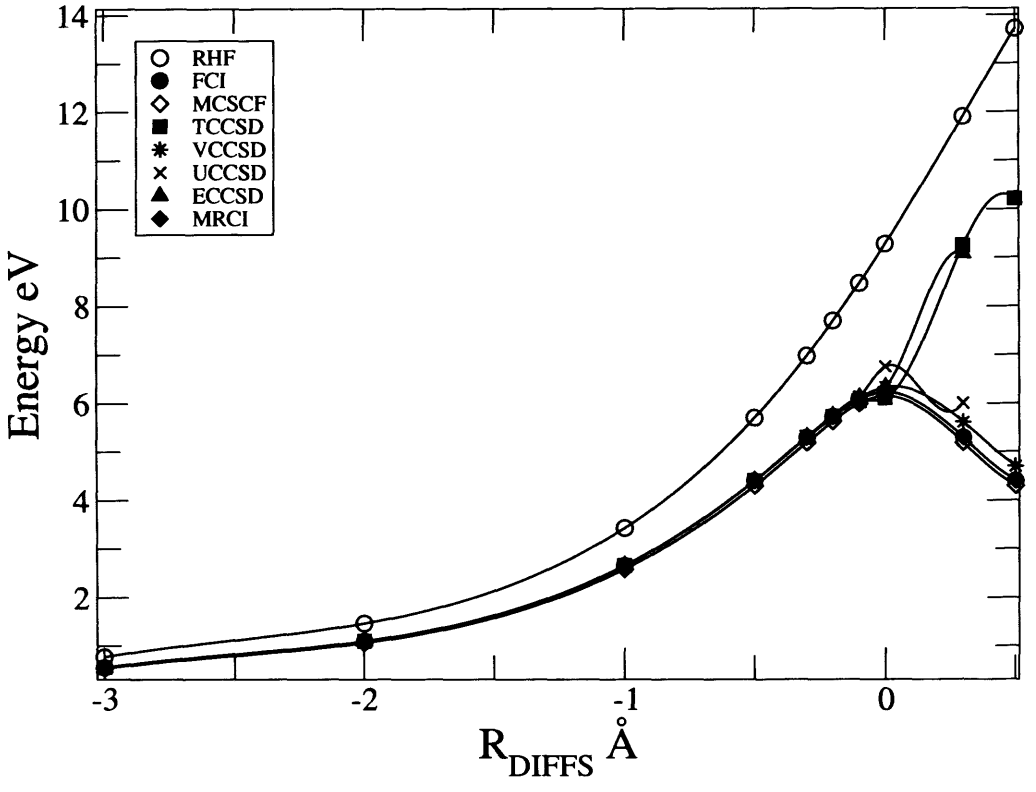

Figure 4.6: Potential energy curve for H_4 following the Q4 model.

all the coupled cluster methods work well in the region $r_{\text{diff}} < 0$. As r_{diff} approaches zero the errors get larger as the amount of quasi degeneracy increases.

After $r_{\text{diff}} = 0$ the RHF reference wavefunction becomes a poor reference as is shown by the RHF curve. Instead of a maxima at $r_{\text{diff}} = 0$, the RHF curve keeps rising as r_{diff} increases. This is because a different configuration has become lower in energy. Of the coupled cluster methods, TCCSD and ECCSD follow the RHF results in that they are qualitatively incorrect after $r_{\text{diff}} = 0$. In comparison, both the VCCSD and UCCSD qualitatively perform much better, these curves have a maxima, but the errors are much larger at positive values of r_{diff}.

The multi-reference methods MCSCF [7, 8] and MRCI give results closest to the FCI values at all points in the graph. The multi-reference methods perform well as they include both the important configurations needed to describe the whole of the potential energy curve. It is therefore interesting that VCCSD performs almost as well as these methods at positive R_{diff} bond lengths.

The UCCSD method also appears to work remarkably well for positive values of r_{diff} but unfortunately does not converge beyond $r_{\text{diff}} = 0.3$. It is difficult to get converged results for any of the coupled cluster if r_{diff} is increased beyond 0.5Å.

4.4 Analysis of the Q4 model system for H_4

4.4.1 The Ground State wavefunction

The H_4 system was looked at in more detail with the aim of understanding why Traditional Coupled Cluster is much poorer at accurately representing the potential energy curve of this model system in comparison to Variational Coupled Cluster. To do this, two hydrogen molecules at infinite separation are studied in a minimal basis set. Fig. 4.7 indicates the orientation of the four hydrogen atoms, showing that H^1 is bonded to H^2 and parallel with H^4.

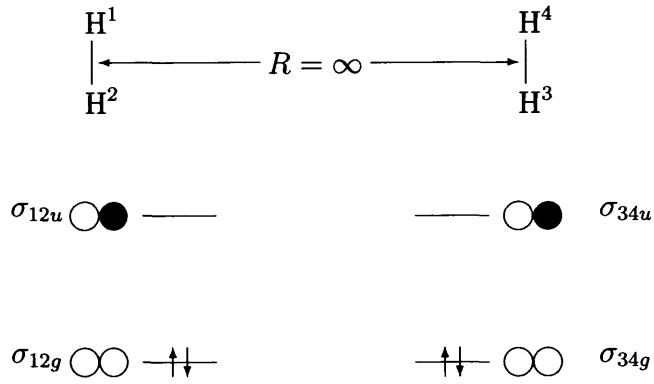

Figure 4.7: Diagram of the molecular orbitals of two hydrogen molecules at infinite distance, showing that H^1 is bonded to H^2, and H^3 to H^4.

Firstly, the orbital between H^1 and H^4 are expressed in terms of the orbitals between H^1-H^2 and H^3-H^4, and the same basis is used to describe the orbitals between H^2 and H^3. This is equivalent to the end point of the calculation where the reference wavefunction used has become a poor description of the ground state. The bonding and anti-bonding molecular orbitals can be written as a linear combination of atomic orbitals as follows:

$$\sigma_{ijg} = \frac{1}{\sqrt{2(1+S_{ij})}}(\phi_i + \phi_j) \tag{4.13}$$

$$\sigma_{iju} = \frac{1}{\sqrt{2(1-S_{ij})}}(\phi_i - \phi_j) \tag{4.14}$$

where S_{ij} is the overlap integral and ϕ_i are atomic orbitals. For the orbitals between H^1 and H^4 there is an infinite distance between the atomic orbitals, and also for H^2 and H^3, so $S_{14} = S_{23} = 0$:

$$\sigma_{14g} = \frac{1}{\sqrt{2}}(\phi_1 + \phi_4) \quad \sigma_{23g} = \tfrac{1}{\sqrt{2}}(\phi_2 + \phi_3) \tag{4.15}$$

$$\sigma_{14u} = \frac{1}{\sqrt{2}}(\phi_1 - \phi_4) \quad \sigma_{23u} = \tfrac{1}{\sqrt{2}}(\phi_2 - \phi_3) \tag{4.16}$$

However, these orbitals do not form an orthonormal set. Therefore, linear combinations of these orbitals were used:

$$G = \frac{1}{\sqrt{2(1+S)}}(\sigma_{14g} + \sigma_{23g}) \quad U = \tfrac{1}{\sqrt{2(1-S)}}(\sigma_{14u} + \sigma_{23u}) \tag{4.17}$$

$$F = \frac{1}{\sqrt{2(1+S)}}(\sigma_{14g} - \sigma_{23g}) \quad V = \tfrac{1}{\sqrt{2(1-S)}}(\sigma_{14u} - \sigma_{23u}) \tag{4.18}$$

These orbitals can then be expressed in terms of the orbitals between H^1-H^2 and H^3-H^4 as follows:

$$\begin{aligned} G &= \frac{1}{\sqrt{2(1+S)}}(\frac{1}{\sqrt{2}}(\phi_1+\phi_4)+\frac{1}{\sqrt{2}}(\phi_2+\phi_3)) \\ &= \frac{1}{2\sqrt{(1+S)}}(\phi_1+\phi_4+\phi_2+\phi_3) \\ &= \frac{1}{2\sqrt{(1+S)}}(\sqrt{2(1+S)}\sigma_{12g}+\sqrt{2(1+S)}\sigma_{34g}) \\ &= \frac{1}{\sqrt{2}}(\sigma_{12g}+\sigma_{34g}) \end{aligned} \tag{4.19}$$

The remaining orbitals become:

$$F = \frac{1}{\sqrt{2}}(\sigma_{12u}-\sigma_{34u}) \tag{4.20}$$

$$U = \frac{1}{\sqrt{2}}(\sigma_{12g}-\sigma_{34g}) \tag{4.21}$$

$$V = \frac{1}{\sqrt{2}}(\sigma_{12u}+\sigma_{34u}) \tag{4.22}$$

The ground state wavefunction can now be expressed in terms of the bonding and anti-bonding orbitals, as follows:

$$|G^\alpha G^\beta F^\alpha F^\beta\rangle = \frac{1}{4}(\sigma_{12g}+\sigma_{34g})^\alpha(\sigma_{12g}+\sigma_{34g})^\beta(\sigma_{12u}-\sigma_{34u})^\alpha(\sigma_{12u}-\sigma_{34u})^\beta \tag{4.23}$$

This can be expanded and written in terms of spin eigenfunctions:

$$\begin{aligned} |G^\alpha G^\beta F^\alpha F^\beta\rangle &= \frac{1}{4}|\sigma^2_{12g}\sigma^2_{12u}-\sigma^2_{12g}\sigma_{12u}\sigma_{34u}(\alpha\beta-\beta\alpha)+\sigma^2_{12g}\sigma^2_{34u}+\sigma_{12g}\sigma^2_{12u}\sigma_{34g}(\alpha\beta-\beta\alpha) \\ &+ \sigma_{12g}\sigma_{34g}\sigma^2_{34u}(\alpha\beta-\beta\alpha)+\sigma^2_{12u}\sigma^2_{34g}-\sigma_{12u}\sigma^2_{34g}\sigma_{34u}(\alpha\beta-\beta\alpha)+\sigma^2_{34g}\sigma^2_{34u} \\ &+ \sigma_{12g}\sigma_{12u}\sigma_{34g}\sigma_{34u}(\alpha\alpha\beta\beta-\frac{1}{2}(\alpha\beta+\beta\alpha)^2+\frac{1}{2}(\alpha\beta-\beta\alpha)^2+\beta\beta\alpha\alpha)\rangle \end{aligned} \tag{4.24}$$

This wavefunction can be analysed in terms of the electronic states of H_2, for example the first term is the H_2^{2-} with term symbol $^1\Sigma_g^+$, and the second term is the H_2^+ state of one of the hydrogen molecules with the corresponding H_2^- state of the other hydrogen molecule. There are eighteen possible combinations of electronic states. In the above ground state wavefunction, the $\sigma^2_{12g}\sigma^2_{34g}$ state which would correspond to the two electron ground states for each of the hydrogen molecules does not appear, and neither does the quadruply excited state $\sigma^2_{12u}\sigma^2_{34u}$.

From this analysis it is possible to obtain a vector of coefficients of each of the states for the ground state wavefunction. It is also possible to analyse each of the excited states of the model system in a similar manner.

4.4.2 Excitation Operators

It is also possible to express the excitation operators in terms of creation and annihilation of the G, F, U and V orbitals:

$$\hat{E}_{UG} = |\sigma_{12g} - \sigma_{34g}\rangle\langle\sigma_{12g} + \sigma_{34g}| \tag{4.25}$$

This single excitation operator destroys a G orbital and creates a U orbital. This can be expressed in terms of the excitations between the normal orbitals:

$$\begin{aligned} \hat{E}_{UG} &= |\sigma_{12g}\rangle\langle\sigma_{12g}| + |\sigma_{12g}\rangle\langle\sigma_{34g}| - |\sigma_{34g}\rangle\langle\sigma_{12g}| - |\sigma_{34g}\rangle\langle\sigma_{34g}| & (4.26)\\ &= \hat{E}_{12g12g} + \hat{E}_{12g34g} - \hat{E}_{34g12g} - \hat{E}_{34g34g} & (4.27)\end{aligned}$$

When this operator acts on the ground state wavefunction, the following is obtained:

$$t_U^G \hat{E}_{UG}|GGFF\rangle = t_U^G(|UGFF\rangle + |GUFF\rangle) \tag{4.28}$$

Where t_U^G is the amplitude of this single excitation. In the H_4 model system, singly excited states do not mix with the ground state. It is only the double and quadruple excitations that are needed to model the system completely.

The double excitations can be built in much the same way. For example when the $\hat{E}_{UG}\hat{E}_{UG}$ operator acts on the ground state wavefunction, the following is obtained:

$$\begin{aligned} t_{UU}^{GG}\hat{E}_{UG}\hat{E}_{UG}|GGFF\rangle &= t_{UU}^{GG}\hat{E}_{UG}(|UGFF\rangle + |GUFF\rangle)\\ &= 2t_{UU}^{GG}|UUFF\rangle & (4.29)\end{aligned}$$

Where t_{UU}^{GG} is the amplitude of this excitation.

There are six possible double excitation: $\hat{E}_{UG}\hat{E}_{UG}$, $\hat{E}_{VG}\hat{E}_{VG}$, $\hat{E}_{UF}\hat{E}_{UF}$, $\hat{E}_{VF}\hat{E}_{VF}$, $\hat{E}_{UG}\hat{E}_{VF}+\hat{E}_{UF}\hat{E}_{VG}$ and $\hat{E}_{UG}\hat{E}_{VF}-\hat{E}_{UF}\hat{E}_{VG}$. The quadruple excitation is expressed as $\hat{E}_{UG}\hat{E}_{UG}\hat{E}_{VF}\hat{E}_{VF}$. From these a vector T can be built containing all the amplitudes associated with these excitations.

4.4.3 The Hamiltonian Matrix

Finally, the Hamiltonian matrix is built with the eigenvalues of the electronic states of a hydrogen molecule.

In the exact ground state there is mixing between σ_g^2 and σ_u^2:

$$\Psi_1 = \cos\theta|\sigma_g^2\rangle - \sin\theta|\sigma_u^2\rangle \tag{4.30}$$

$$\Psi_2 = \sin\theta|\sigma_g^2\rangle + \cos\theta|\sigma_u^2\rangle \tag{4.31}$$

where θ gives the degree of mixing of the orbitals σ_g^2 and σ_u^2.

The Hamiltonian matrix component for $\langle\Psi_1|\hat{H}|\Psi_1\rangle$ is the ground state energy, which will be set to zero. The components $\langle\Psi_1|\hat{H}|\Psi_2\rangle$ and $\langle\Psi_2|\hat{H}|\Psi_1\rangle$ will also be zero, and the value of $\langle\Psi_2|\hat{H}|\Psi_2\rangle$ will be given the symbol α and is twice the orbital energy of the excited state.

Eq.(4.30) and Eq.(4.31) can be rearranged to give σ_g^2 and σ_u^2 in terms of Ψ_1 and Ψ_2:

$$|\sigma_g^2\rangle = \cos\theta\Psi_1 + \sin\theta\Psi_2 \tag{4.32}$$

$$|\sigma_u^2\rangle = -\sin\theta\Psi_1 + \cos\theta\Psi_2 \tag{4.33}$$

Using the Hamiltonian components above it is possible to obtain the Hamiltonian components for the states involving σ_{12g}^2, σ_{12u}^2, σ_{34g}^2 and σ_{34u}^2 for the H_4 model system in terms of θ and α:

$$\langle\sigma_{12g}^2\sigma_{34g}^2|\hat{H}|\sigma_{12g}^2\sigma_{34g}^2\rangle = 2\alpha\sin^2\theta \tag{4.34}$$

$$\langle\sigma_{12u}^2\sigma_{34u}^2|\hat{H}|\sigma_{12u}^2\sigma_{34u}^2\rangle = 2\alpha\cos^2\theta \tag{4.35}$$

$$\langle\sigma_{12g}^2\sigma_{34u}^2|\hat{H}|\sigma_{12g}^2\sigma_{34u}^2\rangle = \alpha\sin^2\theta + \alpha\cos^2\theta \tag{4.36}$$

$$\langle\sigma_{12g}^2\sigma_{34g}^2|\hat{H}|\sigma_{12u}^2\sigma_{34g}^2\rangle = \alpha\sin\theta\cos\theta \tag{4.37}$$

$$\langle\sigma_{12g}^2\sigma_{34g}^2|\hat{H}|\sigma_{12u}^2\sigma_{34u}^2\rangle = 0 \tag{4.38}$$

The remaining values of the Hamiltonian matrix are more straightforward as these states do not mix. The remaining terms of the Hamiltonian matrix can all be expressed in terms of singlet and triplet energies, ionisation potentials, electron affinities and orbital energies. For example:

$$\langle\sigma_{12g}\sigma_{12u}\sigma_{34g}\sigma_{34u}\frac{1}{2}(\alpha\beta-\beta\alpha)^2|\hat{H}|\sigma_{12g}\sigma_{12u}\sigma_{34g}\sigma_{34u}\frac{1}{2}(\alpha\beta-\beta\alpha)^2\rangle = 2S \tag{4.39}$$

where S is the energy of the singlet.

Table 4.1: The values obtained for the electronic states of the hydrogen molecule in STO-3G basis set.

Quantity	Symbol	Energy $/E_h$
Twice the energy of the first unoccupied orbital	α	1.71950
Degree of mixing	θ	0.05243
Energy of the singlet	S	1.01574
Energy of the triplet	T	0.65774
First ionisation energy	IP	0.61430
Second ionisation energy	IP^+	1.27785
First Electron Affinity	A	-0.73301
Second Electron Affinity	A^-	-1.41927
Orbital energy in the ion	Δ^+	0.82955
Orbital energy in the anion	Δ^-	0.85227

Calculations were performed on H_2 in the minimal STO-3G basis set to obtain the values required for the hamiltonian matrix. These values are shown in Table 4.1.

At this point, all the tools that are needed for the analysis of the H_4 system have been constructed. The ground state and excited states describing the orbitals between the H_2 molecules have been constructed and expressed in terms of the original basis. A T vector containing the amplitudes for the different possible excitations has been built, and there is a Hamiltonian matrix expressed in terms of the energies of the electronic states of H_2.

4.4.4 Results

Using the above tools it is possible to evaluate the FCI energy and the exact amplitudes of each of the states by solving the eigenvector problem. The lowest eigenvalue was found to be 0 Hartrees as the problem is posed such that the exact answer for the ground state will be zero. The eigenvector associated with the lowest eigenvalue gives the exact amplitudes. The eigenvector shows that for the exact answer to the ground state, the coefficient for the $|GGFF\rangle$ state tends to zero, whereas the $|GGUU\rangle$ coefficient tends to 1. This is expected because the two bases are related by symmetry. After dividing each

of the exact amplitudes by the result for $|GGUU\rangle$ the following vector is obtained for the exact amplitudes:

$$T|\Psi\rangle = \begin{pmatrix} -0.02624 \\ -0.02624 \\ -0.02624 \\ 0.00275 \\ 1. \\ 0.02624 \\ 0.04545 \\ -0.02624 \end{pmatrix} \begin{matrix} |GGFF\rangle \\ |UUFF\rangle \\ |GGVV\rangle \\ |VVFF\rangle \\ |GGUU\rangle \\ |GUVF + UGFV + VGFU + GVUF\rangle \\ |2UGVF + GUVF + UGFV + 2GUFV - VGFU - GVUF\rangle \\ |UUVV\rangle \end{matrix} \tag{4.40}$$

It is also possible to analyse how the amplitudes depend on the CI mixing parameter θ. For the exact exponential wavefunction the T amplitudes the dependence should be as $1, 1, 1, \theta, \theta^{-1}, 1, 1, 1$.

The Variational Coupled Cluster (VCC) method and the Traditional Coupled Cluster have also been examined in this way. The quadruple excitation coefficient was constructed from the contributions arising from $\frac{1}{2}\hat{T}^2$ where $\hat{T}$ contains the double excitation operators:

$$\begin{aligned} \frac{1}{2}\hat{T}^2 &= 4t_{uu}^{ff}t_{vv}^{gg}\hat{E}_{UF}\hat{E}_{UF}\hat{E}_{VG}\hat{E}_{VG} + 4t_{vv}^{ff}t_{uu}^{gg}\hat{E}_{VF}\hat{E}_{VF}\hat{E}_{UG}\hat{E}_{UG} \\ &+ 2(t_{uv}^{gf+})^2(\hat{E}_{UG}\hat{E}_{VF} + \hat{E}_{UF}\hat{E}_{VG})^2 + 6(t_{uv}^{gf-})^2(\hat{E}_{UG}\hat{E}_{VF} - \hat{E}_{UF}\hat{E}_{VG})^2 \end{aligned} \tag{4.41}$$

The variational energy was formulated from the following expression:

$$E = \frac{\langle 0|(1 + \hat{T}_2 + \frac{1}{2}\hat{T}_2^2)\hat{H}(1 + \hat{T}_2 + \frac{1}{2}\hat{T}_2^2)|0\rangle}{\langle 0|(1 + \hat{T}_2 + \frac{1}{2}\hat{T}_2^2)(1 + \hat{T}_2 + \frac{1}{2}\hat{T}_2^2)|0\rangle} \tag{4.42}$$

This functional can be minimised to determine the value of the energy, and the $\hat{T}$ amplitudes. The VCCSD energy is calculated as an an error from the correct value given by the FCI result. The error in the energy was found to be 0.6 mHartrees.

The dependence of the T amplitudes on θ can approximately be given by $1, 1, 1, \theta, \frac{2}{\theta}, 1, 1, 1$. There are small errors in the resulting amplitudes in comparison to the FCI case, due to higher orders of θ. There is a deviation from the exact amplitudes for dependence on θ for the T amplitude associated with the $|GGUU\rangle$ state which is the dominant configuration for the system.

In a similar manner the energy for the Traditional Coupled Cluster formalism can be found by finding the root of the following expression for the residual:

$$r = (\hat{H} - E)(1 + \hat{T}_2 + \frac{1}{2}\hat{T}_2^2)|0\rangle \tag{4.43}$$

This converges to a poor value of the energy of 0.550 Hartree above the FCI value if the initial vector given is the reference wavefunction $1, 0, 0, 0, 0, 0, 0, 0, 0, 0$. This might be expected from the poor results shown in the previous section for TCCSD results in comparison to VCCSD or FCI results. By giving different starting points, taken from the VCCSD result, the FCI result, or by using the dependence of theta seen in the other calculations, better energies can be obtained in that they are closer to zero, but the points are not able to converge. When the FCI result is given as the initial vector, the TCCSD solution moves away from this and the dominant configuration $|GGUU\rangle$ has a coefficient that is four times too small. It therefore becomes difficult to analyse how the T amplitudes in TCCSD depend on θ or why such poor results are seen.

4.5 Conclusions

In this chapter calculations have been performed on BeH_2 and H_4 as examples of systems where the amount of quasi-degeneracy can be varied with geometric parameters. Both the results on the perpendicular insertion of Be into a hydrogen molecule, and the Q4 model system of H_4 showed significantly better results were obtained with Variational Coupled Cluster (VCCSD) than with Traditional Coupled Cluster (TCCSD). Whilst the errors with each of the coupled cluster methods increased in the areas of the potential energy curves where quasi-degeneracy is strongest, the VCCSD method gave qualitatively accurate curves in regions where the Hartree-Fock reference is far from the true ground state wavefunction. These are region where another electron configuration has become lower than the configuration that the Hartree-Fock wavefunction describes. TCCSD on the other hand gave qualitatively incorrect potential energy curves, following more closely the Hartree-Fock reference function than the true ground state wavefunction.

The further analysis of the H_4 system again showed that Variational Coupled Cluster is capable of giving an energy close to the FCI energy, at the extremity of the potential

energy curve for the Q4 model system where the dominant configuration is $|GGUU\rangle$ rather than the Hartree-Fock reference $|GGFF\rangle$. For VCCSD the resulting vector of T amplitudes showed very similar dependence on the mixing parameter θ as the FCI result. However, the analysis for the TCCSD method proved inconclusive as the equation struggled to converge for this test system. Even when the initial vector was the FCI result, the TCCSD equations failed to converge, and moved away from the correct answer. It is difficult therefore to assess the dependence of T amplitudes with the mixing parameter θ.

Chapter 5

A Linked Electron Pair Functional

5.1 Introduction

The Configuration Interaction wavefunction is a linear combination of configuration state functions (CSFs) built from spin orbitals:

$$\Psi = \psi_0 + \sum_{Px} C_{Px}\psi_{Px} \tag{5.1}$$

where ψ_0 is the reference wavefunction, x labels the external parts that is $x = a$ for singles and $x = a, b, p$ for doubles where a and b denote external molecular orbitals and p denotes the spin coupling, P is the internal parts of the remaining CSFs. If Ψ contains all the possible CSFs of the correct symmetry, then the wavefunction is complete, and will solve the the Schrödinger equation exactly.

The energy functional for the CI method can be expressed as follows:

$$E_{CI} = \frac{\langle \psi_0 + \psi_c | H - E_0 | \psi_0 + \psi_c \rangle}{1 + \langle \psi_c | \psi_c \rangle} \tag{5.2}$$

Where ψ_c is given by;

$$\psi_c = \sum_P \psi_P \tag{5.3}$$

$$\psi_P = \sum_x C_{Px}\psi_{Px} \tag{5.4}$$

Full CI can only be used when the system size is small enough, as the computational cost grow with the number of electrons and the size of the basis set factorially. Therefore the CI method is usually truncated to CSFs that only differ from the reference wavefunction by single or double excitations (CISD). Unfortunately, truncating the number of CSFs used, leads to an energy that is not size consistent.

The Langhoff-Davidson correction [161] is perhaps the simplest method that corrects a posteriori the CISD energy so that it more size consistent. The contribution of up to quadruple excitations is estimated using the following formula:

$$\Delta E_Q = (1 - c_0^2)(E_{\text{CISD}} - E_{\text{HF}}) \tag{5.5}$$

where c_0 is the coefficient of the HF wavefunction in the CI expansion, E_{CISD} is the CISD energy, and E_{HF} is the HF energy. However, using the Langhoff-Davidson correction does not lead to the correct answer for a two-electron system.

Alternatively, the CISD energy functional can be modified to approximately include contributions from higher excitations and so have the property of size consistency. As was seen in Chapter 1, the CEPA methods fall into this category. CEPA methods can be viewed as shifted CISD calculations where the contributions from quadruple excitations are approximated by coupled pair energies.

5.1.1 Coupled Pair Functional and Average Coupled Pair Functional

The Coupled Pair Functional (CPF) of Ahlrichs *et al.* [162] uses topological factors, T_{PQ} in the denominator of the CI energy functional, so that the functional only includes partial normalisation. The CPF correlation energy functional is given by the following:

$$F_c[\psi_c] = 2\sum_P \frac{\langle\psi_0|H - E_0|\psi_P\rangle}{N_P} + \sum_{P,Q} \frac{\langle\psi_p|H - E_0|\psi_Q\rangle}{M_P M_Q} \tag{5.6}$$

where, $N_P = 1 + \sum_Q T_{PQ}\langle\psi_Q|\psi_Q\rangle$ and $M_{PQ} = \sqrt{N_P}$. When $T_{PQ} = 1$ then $N_P = 1 + \langle\psi_c|\psi_c\rangle$ and the energy functional becomes the same as the CI energy functional. When $T_{PQ} = 1$ then $N_P = 0$ and the linear CP-MET energy functional is obtained. For a single reference and the inclusion of single and double excitations, $P = (ijp)$ for doubles and $P = i$ for singles where p labels spin coupling.

The choice of T_{PQ} are defined so that the energy functional is correct for systems of separated electron pairs, and invariant with respect to unitary transformations of equivalent orbitals of identical subsystems. This leads to T_{PQ} being given by:

$$T_{PQ} = \frac{\delta_{ik} + \delta_{il}}{2n_i} + \frac{\delta_{jk} + \delta_{jl}}{2n_j} \tag{5.7}$$

where n_i is the occupation number of the ith orbital of the reference, for $P = (ijp)$ and $Q = (klq)$ where p and q label the different spin couplings. T_{PQ} corresponds to an averaging over all occupied spin orbit pairs which differ only in the spin. This CPF functional can account for the effects on the energy of unlinked triples and quadruple contributions, but linked triples and quadruples are missed. The drawback of this approach of individual partially normalised denominators is that the electron pairs are no longer unambiguously defined. This makes the method difficult to extend to a multi-reference method.

Averaged Coupled Pair Functional(ACPF) [163] is closely related to CPF but the individual partial denominators are replaced with a single averaged denominator:

$$F_c[\Psi_c] = \frac{\langle \Psi_0 + \Psi_c | H - E_0 | \Psi_0 + \Psi_c \rangle}{1 + g\langle \Psi_c | \Psi_c \rangle} \tag{5.8}$$

The choice of the parameter g is obtained by considering two electron systems and systems with non-interacting pairs of electrons. This leads to the choice that $g = 2/n$ where n is the number of electrons correlated in order that the method is size extensive. This method can be extended to the multi-reference case by partitioning the CSFs:

$$\Psi_c = \Psi_a + \Psi_e \tag{5.9}$$

where Ψ_a contains the CSFs that have the same orbital occupation as the reference outside of the active space, and Ψ_e contains all the remaining CSFs. This leads to two factors in the denominator, $g_e = 2/n$ to ensure that the method is extensive for separated electron pairs and g_a which is set to 1 as cluster corrections do not occur for these CSFs. More recently [164], the MR-ACPF functional has been modified to treat single excitations differently to double excitations by choosing different g factors.

5.1.2 Parametric Variational Second Order Reduced Density Matrix

Kollmar [165] has also taken the approach to change the normalisation condition by using a topological factor. The CID energy expression can be partitioned into three parts:

$$\begin{aligned} E = \langle \Psi | \hat{H} | \Psi \rangle &= E_0 + 2E_1 + E_2 && (5.10) \\ E_0 &= \langle \Psi_0 | \hat{H} | \Psi_0 \rangle \\ E_1 &= b_0 \langle \Psi_0 | \hat{H} | \Psi_c \rangle \\ E_2 &= \langle \Psi_c | \hat{H} | \Psi_c \rangle && (5.11) \end{aligned}$$

where the CID wavefunction is given by:

$$\begin{aligned} \Psi &= b_0 \Psi_0 + \sum_i b_i \Psi_i \\ &= b_0 \Psi_0 + \Psi_c && (5.12) \end{aligned}$$

Ψ_i is any wavefunction that differs from the reference by a double excitation. The CID normalisation condition is given by:

$$b_0^2 + \sum_i |b_i|^2 = 1 \tag{5.13}$$

The lack of size extensivity can be shown to arise from E_1 [165]. If $b_0 = 1$ the linear CP-MET or CEPA(0) method is obtained, and the method would be size extensive.

Kollmar [165] modifies the prefactor b_0 so that is does not contain coefficients b_i^j for $j \neq i$. This leads to the modified energy functional:

$$E = E_0 + \sum_{\substack{i<j \\ a<b}} 2b_{0,ij}^{ab} \langle \Psi_0 | \hat{H} | \Psi_{ij}^{ab} \rangle b_{ij}^{ab} + \sum_{\substack{i<j \\ a<b}} \sum_{\substack{k<l \\ c<d}} b_{kl}^{cd} \langle \Psi_{kl}^{cd} | \hat{H} | \Psi_{ij}^{ab} \rangle b_{ij}^{ab}. \tag{5.14}$$

A constrained optimisation is performed where the constraint is given by the normalisation condition with a topological factor, f_{ijkl}^{abcd} introduced:

$$|b_{0.ij}^{ab}|^2 + \sum_{\substack{k<l \\ c<d}} |b_{kl}^{cd}|^2 f_{ijkl}^{abcd} = 1 \tag{5.15}$$

The topological factor f_{ijkl}^{abcd} is chosen so that the method is size extensive, and by considering the N-representability conditions of second order reduced density matrix (2-RDM). The 2-RDM can be computed from the differential of the energy functional with respect to the corresponding elements of the reduced Hamiltonian ${}^2K$ [166]:

$${}^2D_{ij}^{kl} = \frac{\partial E}{\partial ({}^2K_{ij}^{kl})} \tag{5.16}$$

The N-representability conditions restrict 2-RDM so that they represent an N-particle system. This leads to the following choice for the topological factor:

$$\begin{aligned} f_{ijkl}^{abcd} &= \frac{1}{4}(\delta_{ik} + \delta_{il} + \delta_{jk} + \delta_{jl} + \delta_{ac} + \delta_{ad} + \delta_{bc} + \delta_{bd}) \\ &- \frac{1}{16}(\delta_{ik} + \delta_{il} + \delta_{jk} + \delta_{jl})(\delta_{ac} + \delta_{ad} + \delta_{bc} + \delta_{bd}) \end{aligned} \tag{5.17}$$

Here, the topological factors involve both occupied and virtual orbitals in contrast to Ahlrich et al CPF method [162] which only involves occupied orbitals. This method termed parametric variational 2-RDM method has been extended to include single excitations explicitly [166, 167].

The constraints on the normalisation coefficients, Eq.(5.15) can be incorporated directly into the energy functional [168]. The $b^{ab}_{0,ij}$ coefficients can be expressed as:

$$b^{ab}_{0,ij} = \sqrt{1 - \sum_{c,k} |b^c_k|^2 f^{abcc}_{ijkk} - \sum_{c<d//k<l} |b^{cd}_{kl}|^2 f^{abcd}_{ijl}} \tag{5.18}$$

This can then be substituted directly into the energy expression Eq.(5.14). The advantage of this is that an unconstrained optimisation can then be performed. The disadvantage of these methods is that unless all the factors f^{ijkl}_{abcd} are chosen to be one, the method is no longer a wavefunction approach.

5.2 A Linked Electron Pair Functional

The drawbacks of the previous functionals are that they require a particular choice of molecular orbital function so that the partitioning of the of the unlinked cluster contributions is uniquely defined. Here, a new functional the Linked Electron Pair Functional (LPF) has been derived with a fully-linked tensor expression so that it is invariant to orbital transformations.

The starting point is the configuration interaction energy expression:

$$E_{\mathrm{CI}} = \frac{\langle \Phi_0 | (1 + \hat{T}^\dagger) \hat{H} (1 + \hat{T}) | \Phi_0 \rangle}{1 + \langle \Phi_0 | \hat{T}^\dagger \hat{T} | \Phi_0 \rangle} \tag{5.19}$$

where $|\Phi_0\rangle$ is a single Slater determinant reference wavefunction and the $\hat{T}$ excitation operator will contain only double excitations from occupied orbitals in the reference wavefunction, labelled $\psi_i = 1, 2...N$, to virtual orbitals denoted ψ_a:

$$\hat{T} = \sum_{ijab} T^{ij}_{ab} a^\dagger b^\dagger j i \tag{5.20}$$

The CI denominator can be written in terms of the One- (η^m_n) and Two- (η^{mp}_{nq}) hole density matrix;

$$1 + \langle \Phi_0 | \hat{T}^\dagger \hat{T} | \Phi_0 \rangle = 1 + \frac{1}{4} T^{ij}_{ab} T^{ij}_{ab} = 1 + \sum_i \eta^i_i - \sum_{i>j} \eta^{ij}_{ij} \tag{5.21}$$

where the one- and two-hole hole density matrices are given by:

$$\eta_n^m = \langle \hat{T}^\dagger n m^\dagger \hat{T} \rangle = \frac{1}{2} T_{ab}^{mj} T_{ab}^{nj} \tag{5.22}$$

$$\eta_{nq}^{mp} = \langle \hat{T}^\dagger n q p^\dagger m^\dagger \hat{T} \rangle = \frac{1}{2} T_{ab}^{mp} T_{ab}^{nq} \tag{5.23}$$

This can be used to define a matrix $\mathbf{\Delta}$ that is a two-index matrix, where the rows and columns are labelled by composite indices $ij, i = 2, ..., N; j = 1, ..., i-1$:

$$\begin{aligned} \Delta_{kl}^{ij} &= \eta_k^i \delta_l^j + \eta_l^j \delta_k^i - \eta_l^i \delta_k^j - \eta_k^j \delta_l^i - \eta_{kl}^{ij} \\ &= \frac{1}{2}(\delta_l^j T_{ab}^{im} T_{ab}^{km} + \delta_k^i T_{ab}^{jm} T_{ab}^{lm} - \delta_k^j T_{ab}^{im} T_{ab}^{lm} - \delta_l^i T_{ab}^{jm} T_{ab}^{km} - T_{ab}^{ij} T_{ab}^{kl}) \end{aligned} \tag{5.24}$$

Using this, a transformation matrix is defined as:

$$U_{kl}^{ij} = \delta_{kl}^{ij} + \Delta_{kl}^{ij} \tag{5.25}$$

The above definition of U_{kl}^{ij} Eq.(5.25) allows matrix powers to have the form:

$$(\mathbf{U^2})_{kl}^{ij} = \frac{1}{2} U_{mn}^{ij} U_{mn}^{kl} \tag{5.26}$$

The $\mathbf{U}$ is then used to transformed T amplitudes and introduce partial normalisation into the numerator of the CI energy expression:

$${}_qT_{kl}^{ij} = \frac{1}{2}(\mathbf{U^{-q/2}})_{mn}^{ij} T_{ab}^{mn} \equiv (\mathbf{U^{-q/2}T})_{ab}^{ij} \tag{5.27}$$

The LPF Energy functional is given as:

$$E_{\mathrm{LPF}} = \langle \Phi_0 | \hat{H} | \Phi_0 \rangle + 2\langle \Phi_0 | \hat{H}_2 T | \Phi_0 \rangle + \langle \Phi_0 |_1 T^\dagger \hat{H}_1 T | \Phi_0 \rangle_L \tag{5.28}$$

5.3 Implementation within the CI code in MOLPRO

The LPF method was implemented within the CI code in MOLPRO [97] with the aim of utilising as much of the existing code as possible. Thus, only the energy expression and the residual vector needed to be modified to contain the new LPF energy and residual.

In this initial implementation double excitations only were considered and Brueckner Orbitals were used, obtained by performing a BCCD calculation, to reduce the singles contribution. In a BCCD calculation the Hartree-Fock orbitals used to construct the Slater Determinants are optimised so that the contribution from single excitations is zero.

5.3.1 Constructing the Energy Expression

Firstly, the LPF method involves two sets of T amplitudes in the energy expression, ${}_1T$ and ${}_2T$ that are transformed by different powers of the transformation matrix **U**. The existing T amplitudes will hold ${}_1T$ and more memory is assigned of the same size as the original amplitudes to hold the ${}_2T$ transformed amplitudes. Each time that a T amplitude is read from disk, a single subroutine *load_t2_ucc* is called to transform the amplitudes. This routine requires the vectors for the T amplitudes and the value of q from Eq.(5.27) for the power that the transformation matrix **U** is raised by. The original CI amplitudes can be restored by passing the value zero for q. The T amplitudes are stored as three vectors $t\alpha\alpha$, $t\alpha\beta$,and $t\beta\beta$ for the α and β spin pair combinations.

Inside of the *load_t2_ucc* subroutine is again a single call to another subroutine *transform_t*. It is this routine, that handles the transformation of the T amplitudes and the assignment of additional memory. Firstly, the **U** matrix is constructed again in three parts for the different spin combinations. The one- hole density matrices are constructed:

$$\eta\alpha_j^i = \frac{1}{2}\sum_{ab} t\alpha\alpha_{ab}^{ik} * t\alpha\alpha_{ab}^{jk} + \sum_{ab} t\alpha\beta_{ab}^{ik} * t\alpha\beta_{ab}^{jk} \tag{5.29}$$

$$\eta\beta_j^i = \frac{1}{2}\sum_{ab} t\alpha\alpha_{ab}^{ik} * t\alpha\alpha_{ab}^{jk} + \sum_{ab} t\alpha\beta_{ab}^{ik} * t\alpha\beta_{ab}^{jk} \tag{5.30}$$

where the sum over virtual orbitals a and b is restricted to combinations with the appropriate symmetry, and the orbital j must have the same symmetry as orbital i. This is done by addressing the appropriate parts of the $t\alpha\alpha$ vectors and taking the trace. In the same manner the contributions from the second-hole density matrix are generated. The matrix **U** is then constructed from a unit matrix, and adding the contributions from the one- and two- hole density matrices following Eq.(5.24) and Eq.(5.25), thus the elements of the $\mathbf{U}\alpha\alpha$ matrix are built as follows:

$$u\alpha\alpha_{kl}^{ij} = \delta_l^j\eta\alpha_k^i + \delta_k^i\eta\alpha_l^j - \delta_l^i\eta\alpha_k^j - \delta_k^j\eta\alpha_l^i - \sum_{ab}\frac{1}{2}t\alpha\alpha_{ab}^{ij}t\alpha\alpha_{ab}^{kl} \tag{5.31}$$

In a similar manner the $\mathbf{U}\alpha\beta$ and $\mathbf{U}\beta\beta$ matrices are built. When constructing the **U** matrix, it is the symmetries of the pairs that it important therefore the pair kl must have the same symmetry as the ij pair.

Each of the **U** matrix is then raised to the power q, by first finding the eigenvalues and

eigenvectors of the matrix **U** and using the relation:

$$\mathbf{A}^x \mathbf{v_i} = \lambda^x \mathbf{v_i} \tag{5.32}$$

where **A** is any square matrix, x is the power that the matrix is to be raised by, $\mathbf{v_i}$ are the eigenvectors of the matrix **A**, and λ the corresponding eigenvalues. The **U** is Hermitian so the eigenvalues will be real and the eigenvectors will be orthogonal. Therefore, the matrix **U** raised to the power q can be obtained from the transpose of the matrix containing the eigenvectors of **U** rather than the inverse:

$$\mathbf{U}^q = \mathbf{v_i}^{\mathrm{T}} \mathbf{v_i} \lambda^q \tag{5.33}$$

The new T amplitudes are then constructed by using the transformation matrix **U** raised the appropriate power q. The $t\alpha\alpha$ amplitudes require only the $\mathbf{U}\alpha\alpha$ part of the transformation matrix, and the same is true for the other spin pair combinations. Thus, the new $t\alpha\alpha$ amplitudes are built according to the following equation:

$${}_q t\alpha\alpha^{kl}_{ab} = \frac{1}{2}(\mathbf{U}\alpha\alpha^{-\mathbf{q/2}})^{ij}_{kl} t\alpha\alpha^{kl}_{ab} \tag{5.34}$$

After the transformation of the T amplitudes the memory that was used to store the **U** is released. At this point all the modifications to calculate the LPF energy have been made.

5.3.2 Constructing the Residual Vector

The next task is to construct the residual vector for the LPF method, and store this vector in the same variable name as the original code, so that the parts of the code that handle the update of the T amplitudes do not need to be changed. The residual is calculated by taking the differential of the energy expression Eq.(5.28) with respect to the T amplitudes:

$$\frac{1}{2} dE = \langle \Phi_0 | d_2 T^\dagger \hat{H} | \Phi_0 \rangle + \langle \Phi_0 | d_1 T^\dagger \hat{H}_1 T | \Phi_0 \rangle \tag{5.35}$$

The differential of the T amplitudes as defined by Eq.(5.27) is given by:

$$d_q T^{ij}_{ab} = -\frac{q}{4} dU^{ij}_{mn} (\mathbf{U}^{-q/2-1}\mathbf{T})^{mn}_{ab} + \frac{1}{2} (\mathbf{U}^{-q/2})^{ij}_{mn} dT^{mn}_{ab} \tag{5.36}$$

The first term in this expression involves the differential of the transformation matrix **U** with respect to the T amplitudes, and a set of transformed T amplitudes. The differential of the transformation matrix defined by Eqs. (5.24) and (5.25), requires the differentials of the one- and two-hole density matrices:

$$d\eta^i_j = \frac{1}{2}dT^{ik}_{ab}T^{jk}_{ab} + \frac{1}{2}dT^{jk}_{ab}T^{ik}_{ab} \tag{5.37}$$

$$d\eta^{ij}_{kl} = \frac{1}{2}dT^{ij}_{ab}T^{kl}_{ab} + \frac{1}{2}dT^{kl}_{ab}T^{ij}_{ab} \tag{5.38}$$

The differential of the **U** matrix is then given by:

$$dU^{ij}_{kl} = d\eta^i_k\delta^j_l + d\eta^j_l\delta^i_k - d\eta^i_l\delta^j_k - d\eta^j_k\delta^i_l - d\eta^{ij}_{kl} \tag{5.39}$$

The second term in Eq. (5.36) is more straightforward, as it just involves matrix multiplication of the differential of the untransformed T amplitudes with the transformation matrix. Thus, Eq.(5.36) maybe re-expressed in terms that only involve the differentiation by the un-transformed T amplitudes as follows:

$$\begin{aligned} d\,{}_qT^{ij}_{ab} = & -\frac{q}{4}\Big[(\frac{1}{2}dT^{ik}_{cd}T^{mk}_{cd} + \frac{1}{2}dT^{mk}_{cd}T^{ik}_{cd})\delta^j_n + (\frac{1}{2}dT^{jk}_{cd}T^{nk}_{cd} + \frac{1}{2}dT^{nk}_{cd}T^{jk}_{cd})\delta^i_m \\ & - (\frac{1}{2}dT^{ik}_{cd}T^{nk}_{cd} + \frac{1}{2}dT^{nk}_{cd}T^{ik}_{cd})\delta^j_m - (\frac{1}{2}dT^{jk}_{cd}T^{mk}_{cd} + \frac{1}{2}dT^{mk}_{cd}T^{jk}_{cd})\delta^i_n \\ & - \frac{1}{2}dT^{ij}_{cd}T^{mn}_{cd} + \frac{1}{2}dT^{mn}_{cd}T^{ij}_{cd}\Big](\mathbf{U}^{-q/2-1}\mathbf{T})^{mn}_{ab} + \frac{1}{2}(\mathbf{U}^{-q/2})^{ij}_{mn}dT^{mn}_{ab} \end{aligned} \tag{5.40}$$

The above equation can be simplified because if the dummy indices m and n are swapped the sign changes, for example:

$$+(\frac{1}{2}dT^{jk}_{cd}T^{nk}_{cd} + \frac{1}{2}dT^{nk}_{cd}T^{jk}_{cd})\delta^i_m = -(\frac{1}{2}dT^{jk}_{cd}T^{mk}_{cd} + \frac{1}{2}dT^{mk}_{cd}T^{jk}_{cd})\delta^i_n \tag{5.41}$$

Therefore Eq. (5.40) becomes:

$$\begin{aligned} d\,{}_qT^{ij}_{ab} = & -\frac{q}{4}\Big[(dT^{ik}_{cd}T^{mk}_{cd} + dT^{mk}_{cd}T^{ik}_{cd})\delta^j_n + (dT^{jk}_{cd}T^{nk}_{cd} + dT^{nk}_{cd}T^{jk}_{cd})\delta^i_m \\ & - \frac{1}{2}dT^{ij}_{cd}T^{mn}_{cd} + \frac{1}{2}dT^{mn}_{cd}T^{ij}_{cd}\Big](\mathbf{U}^{-q/2-1}\mathbf{T})^{mn}_{ab} + \frac{1}{2}(\mathbf{U}^{-q/2})^{ij}_{mn}dT^{mn}_{ab} \end{aligned} \tag{5.42}$$

To find the differential of the energy expression the matrices ${}_qV$ are introduced:

$$\langle\Phi_0|abj^\dagger i^\dagger\hat{H}|\Phi_0\rangle = ({}_2V)^{ij}_{ab} \tag{5.43}$$

$$\langle\Phi_0|abj^\dagger i^\dagger\hat{H}\,{}_1T|\Phi_0\rangle = ({}_1V)^{ij}_{ab} \tag{5.44}$$

${}_qV$ are structures that are already available in the CI program in MOLPRO. By substituting these into Eq.(5.35), the differential of the energy can be expressed as a sum over q:

$$\frac{1}{2}dE = \sum_{q=1}^{2} \frac{1}{4} d\, {}_qT_{ab}^{ij} \, ({}_qV)_{ab}^{ij} = \frac{1}{4} G_{cd}^{kl} dT_{cd}^{kl} \tag{5.45}$$

The transformed T amplitudes for the differential of the energy are given the symbol ${}_\mathbf{q}\mathbf{W}$ defined by:

$${}_q\mathbf{W} = (\mathbf{U}^{-q/2-1}\mathbf{T}) \tag{5.46}$$

As the matrices ${}_q\mathbf{V}$ are antisymmetric, this leads to a further simplification of the derivative of the energy expression:

$$\begin{aligned} \frac{1}{2}dE &= \sum_{q=1}^{2} -\frac{q}{8}(dT_{cd}^{ik}T_{cd}^{mk} + dT_{cd}^{mk}T_{cd}^{ik})\, {}_qW_{ab}^{mj}\, {}_qV_{ab}^{ij} + \frac{q}{32}(dT_{cd}^{ij}T_{cd}^{mn} + dT_{cd}^{mn}T_{cd}^{ij})\, {}_qW_{ab}^{mn}\, {}_qV_{ab}^{ij} \\ &+ \frac{1}{8}(U^{-q/2})_{ij}^{kl}\, {}_qV_{ab}^{ij} \end{aligned} \tag{5.47}$$

The following intermediates are defined below:

$${}_qZ_{mn}^{kl} = \frac{1}{2}\, {}_qW_{ab}^{kl} V_{ab}^{mn} \tag{5.48}$$

$${}_q\mathbf{Y} = {}_\mathbf{q}\mathbf{Z} + {}_\mathbf{q}\mathbf{Z}^{\mathrm{T}} \tag{5.49}$$

$${}_qX_l^k = {}_q\, Y_{mn}^{kn} \tag{5.50}$$

If the differential is re-expressed in terms of dT_{ab}^{ij}, the following expression is obtained for the definition of G_{ab}^{ij}:

$$G_{ab}^{ij} = \sum_{q=1}^{2} -q T_{ab}^{ij} {}_qX_i^k + \frac{q}{4} T_{ab}^{kl}\, {}_qY_{ij}^{kl} + \frac{1}{2}\, {}_qU_{kl}^{ij}\, {}_qV_{ab}^{kl} \tag{5.51}$$

Thus the new structures needed for constructing the residual vector can be constructed in much the same way as the changes that were required to construct the energy. Many of the routines created to construct the energy can be utilised for the residual, for example the ${}_q\mathbf{W}$ amplitudes just require the $\mathbf{U}$ matrix raised to a different power. The intermediates Eq.(5.48) allows the construction of the residual to easily be broken up into subroutines.

5.4 Results and Discussion

All of the results collected to test the LPF functional have been carried out on closed shell systems where the reference wavefunction was RHF. The LPF functional was initial tested on H_2 system for which the method is the same as CID and therefore exact. For this system the **U** transformation matrix is a scalar of value 1. Therefore it is not a good test molecule whilst coding because any errors in addressing the right parts of the transformation matrix, or in creating the matrix will not be seen. To test the code at various points through the construction of the new method the four electron He_2 system and the eight electron systems of the Neon atom and four He atoms in square planar arrangement were used, as these systems are small enough to able to print out **U**. For the both systems of He atoms, when the distance between each of the atoms is large enough, the LPF method should give the same as the FCI and the value should be twice or four times the value for a single Helium atom.

5.4.1 Bond Breaking in HF, CH_4 and H_2O

The molecules HF, CH_4 and H_2O were chosen to allow comparison with the parametric variational 2-RDM methods of Kollmar [165] and Mazziotti [167].

Fig 5.1 illustrates the potential energy curve for the dissociation of the hydrogen fluoride molecule, an example of simple single bond breaking to closed shell products for the LPF energy functional, and CCSD and CCSD(T) for comparison, as well as the FCI benchmark. Calculations were performed with the 6-31G** basis set. The LPF method performs well in the equilibrium region, with errors increasing as the bond is stretched. The LPF method is slightly better than the CCSD method at 2.6 and 2.8Å, as at these distances the LPF curve is closer to the FCI curve than CCSD. The CCSD(T) method has much smaller errors at equilibrium bond lengths, but drops below the FCI curve at stretched bond lengths, likely to be because of a break down in perturbation theory.

Table 5.1 gives the FCI energies in Hartrees for the potential energy curve of Hydrogen Fluoride and the errors in comparison to the FCI values in mHartrees for each of the

Table 5.1: Potential energy curves for HF with 6-31G** basis set. FCI values given in Hartrees and other methods as energy errors in mHartrees in comparison to the FCI values

R	FCI	RHF	CCSD	CCSD(T)	BCCD	LPFD	CEPA(1)	K	M
0.9	-100.2011	189.4	2.5	0.4	2.8	5.0	2.9	3.4	2.0
1.4	-100.1073	216.7	4.7	0.9	5.2	7.6	3.8	4.9	2.6
1.8	-100.0389	251.0	9.0	0.5	9.5	10.6	4.5	6.8	2.8
2.2	-100.0095	296.1	14.8	-4.4	14.8	13.4	5.8	9.4	2.6
2.6	-100.0005	339.2	19.0	-14.8	18.7	15.0	7.2	11.5	2.3
2.8	-99.9990	357.2	20.3	-20.7	19.8	15.5	7.8	16.3	2.3

Table 5.2: Potential energy curves for abstracting a hydrogen from CH_4 with 6-31G* basis set, with the remaining bond lengths fixed at 1.86Å. FCI values given in Hartrees and other methods as energy errors in mHartrees in comparison to the FCI values

R	FCI	RHF	CCSD	CCSD(T)	BCCD	LPFD	CEPA(1)	K	M
1.1	-40.3562	161.2	3.3	0.4	3.5	4.5	2.6	3.0	1.1
1.6	-40.2891	173.2	4.7	0.6	5.2	6.2	3.3	4.0	1.6
2.2	-40.2146	206.0	9.1	0.4	9.8	10.0	4.5	6.2	2.5
2.8	-40.1869	254.6	14.7	-4.2	14.9	13.8	5.2	8.1	1.9
3.2	-40.1817	286.0	17.1	-9.9	16.9	15.1	5.3	8.7	0.8
3.4	-40.1806	299.8	17.8	-12.7	17.5	15.5	5.2	8.7	0.2

other methods. The table also shows the results obtained from Kollmar parameterised variational RDM method (K) from Mazziotti's functional (M) both taken from published results [167] as well as CEPA(1) results. These results show that the error in the LPF energy functional is 7.6mHartrees at the equilibrium distance, of the same order of magnitude as the CCSD error that has an error of 4.7mHartrees at the same bond length. The error in the LPF roughly doubles as the bond is stretch to 15.5mHartrees. These results also show that the method gives results reasonably similar to Kollmar's energy functional. However both the CEPA(1) and Mazziotti's functional give results with smaller errors in comparison with LPF.

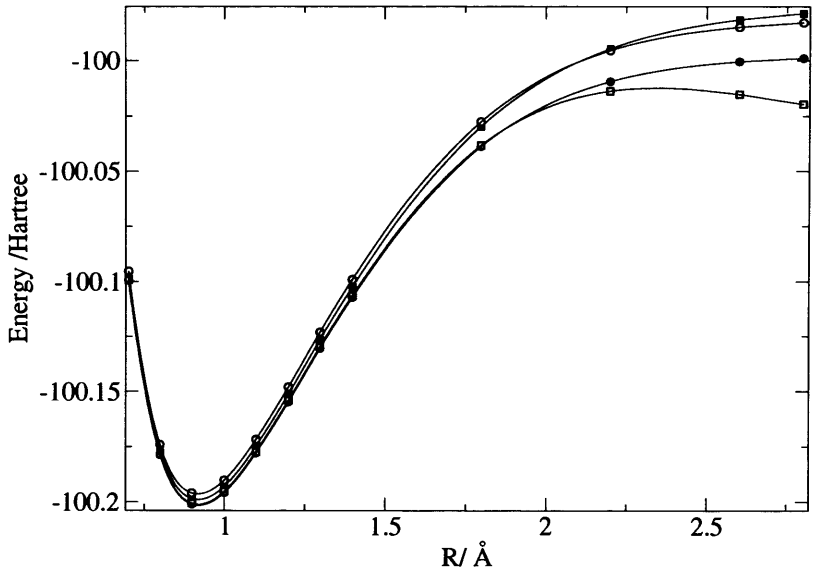

Figure 5.1: Potential energy curve of HF with 6-31G** basis set. ● FCI, ○ LPFD, ■ CCSD, ❑ CCSD(T)

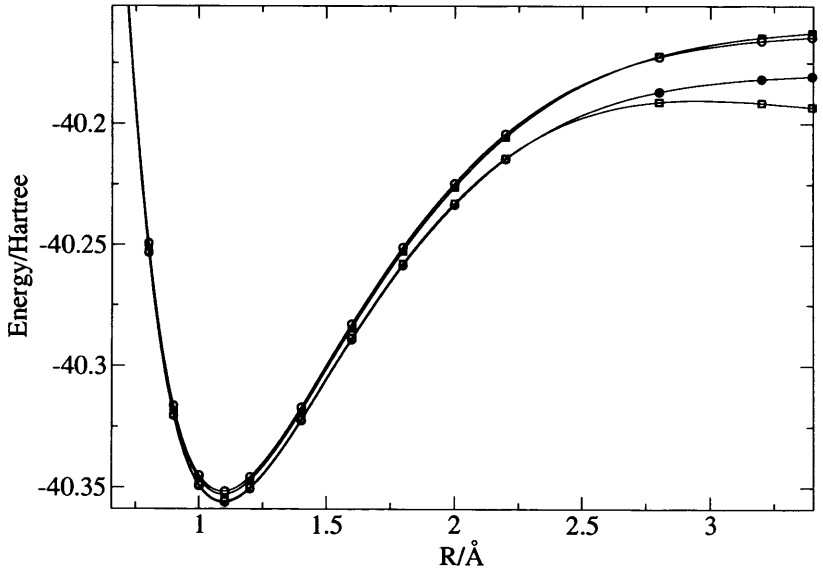

Figure 5.2: Potential energy curve of CH_4 with 6-31G* basis set. Key as Fig. 5.1

The potential energy curves obtained when a single Hydrogen atom is abstracted from CH_4 is shown in Fig. 5.2 and Table 5.2. Calculations were performed using the 6-31G* basis set. The remaining bond lengths were fixed at 1.86Åand with angles fixed as those for a tetrahedral. These results show similar trends to the results obtained for the single bond breaking in hydrogen fluoride. Again, at the equilibrium bond length the error in the LPF method is just a few mHartrees and is comparable to CCSD error. At longer bond lengths the results with the LPFD functional have errors that have increased to 15.5 mHartree at the most stretch geometry of a C-H bond length of 3.4Å, however it does perform slightly better than CCSD which has an error of 17.8mHartrees at the same geometry. The CCSD(T) method again outperforms the LPF and CCSD methods at equilibrium, but drops below the FCI values at long bond lengths.

Table 5.2 gives the errors in mHartrees in comparison with FCI values for LPF method, CCSD and CCSD(T), and additionally, CEPA(1) and the parametric variational 2-RDM methods K and M obtained from ref. [167]. These results again show that the LPFD results are in reasonable agreement with Kollmar's method (K), whereas both the CEPA(1) and Mazziotti's parametric variational 2-RDM method have much lower errors cross the range of geometries for this molecule.

Fig. 5.3 illustrates the potential energy curve along the symmetric stretch of H_2O in cc-pVTZ basis set. The angle between the O-H bonds was fixed at 109.5°. This is a slightly distorted geometry to the normal angle in H_2O, which is 107.6° but was chosen to reproduce the RHF results in ref. [167]. This is a more demanding system to test the new LPF code with in comparison to the single bond breaks in HF and CH_4, as it involves the simultaneous breaking of both the O-H bonds.

The LPFD functional again at distances near the equilibrium bond length performs comparably with CCSD. However, at stretched bond lengths LPFD performs significantly better than CCSD as the LPFD curve is smooth, whereas the CCSD shows unphysical behaviour as there is a maxima at 2.3Å, followed by a dip around 2.6Å. As with the previous results, the CCSD(T) results are better in the equilibrium region, but as the bond is stretched the CCSD(T) curve has a maxima at 2.0Å, and afterwards the energy decreases dramatically as the perturbation correction for the triple excitations breaks down. CEPA(1) results fail to converge for this system after 1.8 Å.

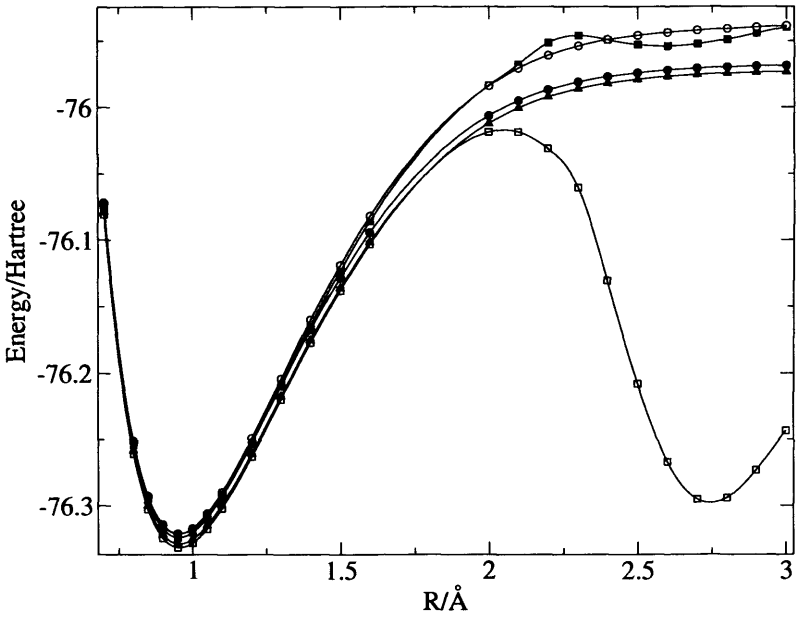

Figure 5.3: Potential energy curve of H_2O with cc-pvtz basis set. ● MRCI, ▲ MRCI+Q, ❍ LPFD, ■ CCSD, ❑ CCCSD(T)

5.4.2 Equilibrium Properties

The equilibrium energies, bond lengths, R_e and frequencies, ω_e for the diatomic molecules HF, F_2 and CO are presented in Table 5.3. For each of the diatomic molecules, energies were calculated at five points around the equilibrium bond length, and the spectroscopic quantities were obtained by fitting a forth order polynomial through the points. The derivative of the fit at the minimum gives the force constant, k, and from this the vibrational frequencies, ω_e can be calculated using the following expression:

$$\omega_e = \frac{1}{2\pi}\sqrt{\frac{k}{\mu}} \tag{5.52}$$

where μ is the reduced mass. The basis set used for these calculations was cc-pVQZ.

The results show that the LPFD functional over-binds in comparison to CCSD for HF and CO, as is indicated by a shorter equilibrium bond length, R_e and higher frequency, ω_e. However, for F_2 the LPFD functional under binds in comparison to CCSD. Further calculations on the potential energy curve of F_2 presented in the next section, show that this system is difficult for the LPFD functional to reproduce CCSD results. The

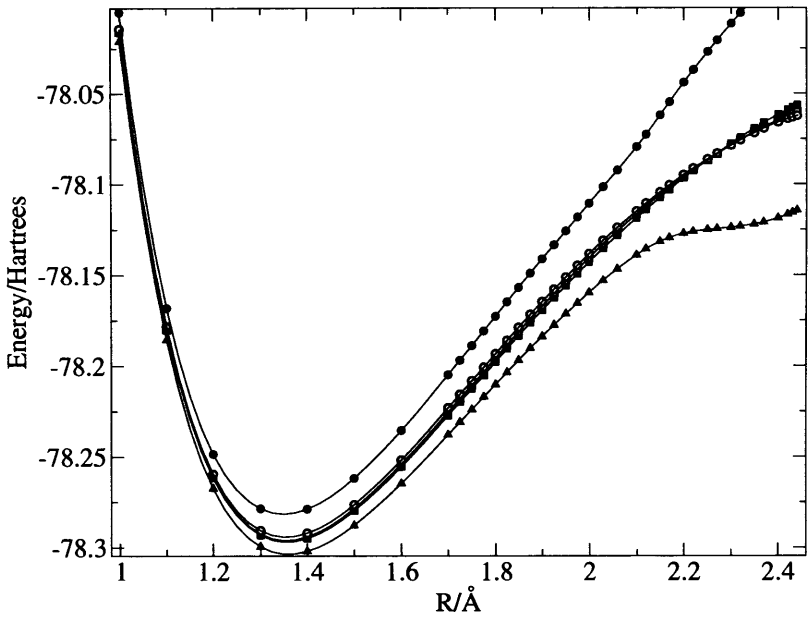

Figure 5.4: Potential energy curve of C_2H_4 with cc-pCDZ basis set. ● MRCI, ▲ MRCI+Q , ○ LPFD, ■ CCSD, ❑ BCCD

parametric variational 2-RDM methods of Kollmar and Mazziotti are both give lower energies, longer bond lengths and lower frequencies in comparison with CCSD results for each of the diatomic molecules. Kollmar's method lies close to the CEPA(1) method, whereas the LPFD method appears to lie between CISD and CCSD results for equilibrium properties.

5.4.3 Potential Energy curves for F_2, N_2, C_2 and C_2H_4

The potential energy curve of ethene is a much more stringent test of the new LPFD method as it involves the breaking of the double bond. In the calculations presented here, the distance between the carbon atoms is varied whilst the remaining parameters of angle 120 degrees and C-H bond lengths 1.08Å are kept fixed. These calculations were perform using the cc-pVDZ basis set over the geometry range of 1Å to 2.45Å.

The results of these calculations are shown in Fig. 5.4. The LPFD method is able to reproduce the CCSD curve reasonably well in the equilibrium region. At stretched geometries, over 2.3Å, it looks like the LPF curve starts to plateau, and starts to give

Table 5.3: Equilibria energies, bond lengths and frequencies are presented for HF, F_2 and CO in cc-pvqz basis set.

Molecule	Method	Energy/E_h	R_e/Å	ω_e/cm^{-1}
HF	CISD	-100.3554	0.9105	4259
	CCSD	-100.3654	0.9137	4205
	BCCD	-100.3650	0.9134	4211
	K	-100.3657	0.9140	4195
	M	-100.3691	0.9153	4174
	LPFD	-100.3625	0.9126	4223
	CEPA(1)	-100.3660	0.9142	4190
F_2	CISD	-199.2986	1.3660	1116
	CCSD	-199.3383	1.3906	1016
	BCCD	-199.3373	1.3892	1021
	K	-199.3417	1.3984	974
	M	-199.3520	1.4082	934
	LPFD	-199.3349	1.3941	989
	CEPA(1)	-199.3449	1.4066	941
CO	CISD	-113.1447	1.1182	2288
	CCSD	-113.1694	1.1243	2234
	BCCD	-113.1682	1.1231	2249
	K	-113.1725	1.1256	2217
	M	-113.1807	1.1288	2183
	LPFD	-113.1652	1.1219	2262
	CEPA(1)	-113.1740	1.1268	2202

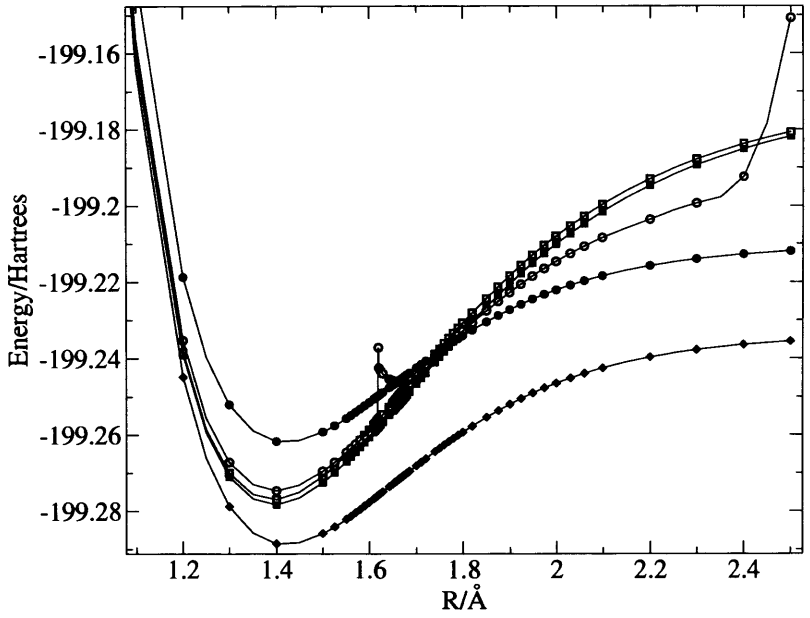

Figure 5.5: Potential energy curve of F_2 with cc-pVTZ basis set. ● MRCI, ▲ MRCI+Q, ❍ LPFD, ■ CCSD, ❑ BCCD

energies lower than the CCSD results. Unfortunately, no data points were possible for the LPFD beyond 2.45Åbecause the LPFD fails to converge.

The F_2 potential energy curve is shown in Fig. 5.5. The basis set used for these calculations was cc-pVTZ. The plot again shows that LPFD reproduces the CCSD curves reasonably in the bonded region, around 1.4Å, with energies just a little higher than CCSD energies. At the point 1.6Å on the potential energy curve for the LPFD method there is a discontinuity, with the energy rising sharply by 0.0461Hartrees, or 29.0kcal/mol. After this point the potential energy curve with LPFD shows a second unphysical minima around 1.7Å. The LPFD curve starts to plateau to an energy that is 7kcal/mol lower than the CCSD curve.

This discontinuity was investigated further, by seeing if the same curve could be generated for the LPFD by scanning from long F-F bond length to a short bond length, whereas the original curve was obtained by stretching the bond. The results obtained were exactly the same as for Fig. 5.5 if the starting point was chosen to be 2.5Å. At a longer starting distance, very different results were obtained for the LPFD as is shown if Fig. 5.6. This graph shows a minima for the LPF around 1.85Å, far removed from the true minima

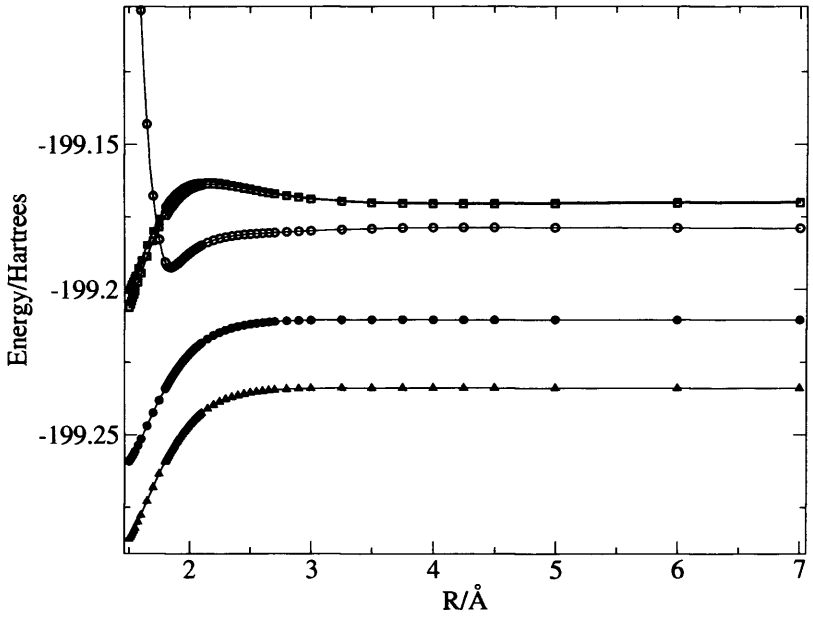

Figure 5.6: Potential energy curve of F_2 with cc-pVTZ basis set. ● MRCI, ▲ MRCI+Q, ❍ LPFD, ■ CCSD, ❑ BCCD

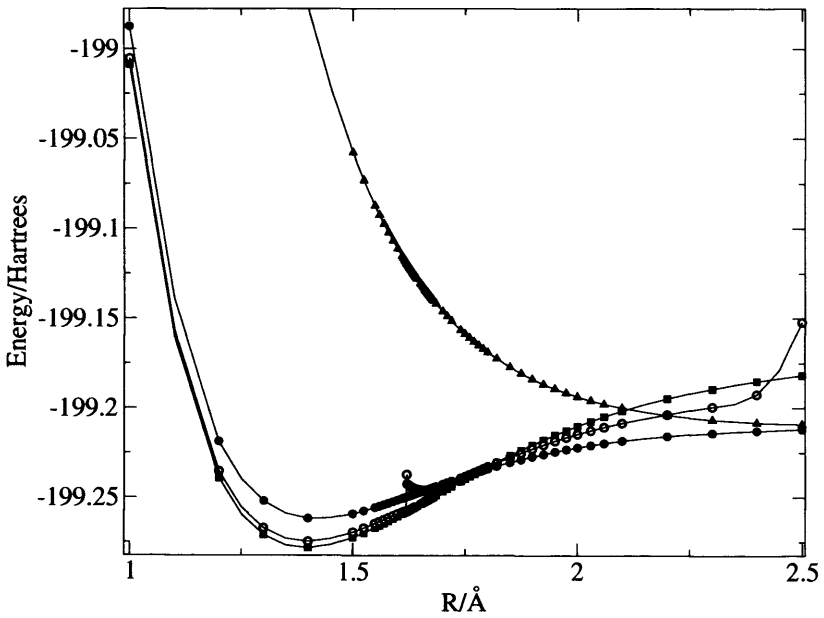

Figure 5.7: Potential energy curve of F_2 with cc-pVTZ basis set. ● MRCI - state 1, ▲ MRCI - state 2, ❍ LPFD, ■ CCSD

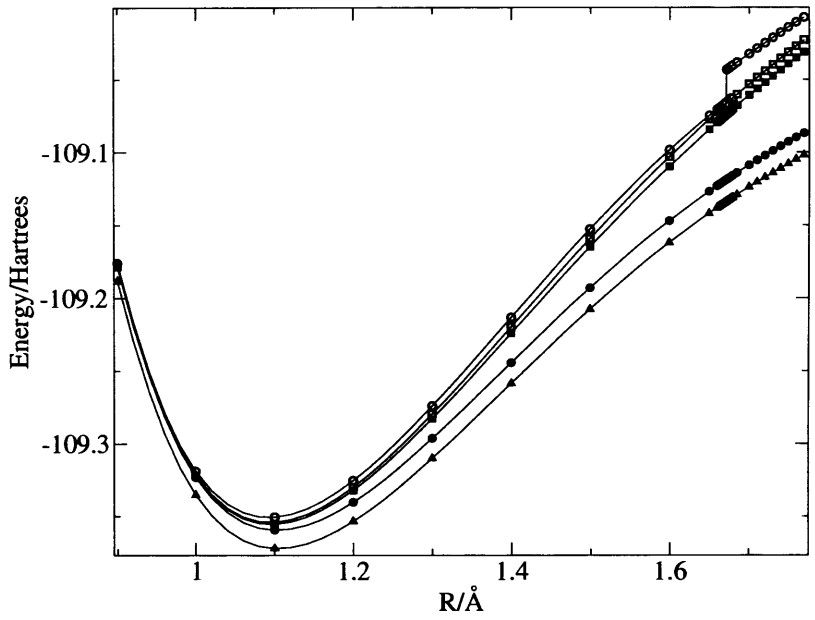

Figure 5.8: Potential energy curve of N_2 with cc-pVTZ basis set. ● MRCI, ▲ MRCI+Q, ❍ LPFD, ■ CCSD, ❑ BCCD

around 1.4Å. Again, the LPFD potential energy curve is markedly different from the CCSD energy curve.

Using the MRCI code, it was possible to look at the different electronic states of F_2 by specifying different wavefunction parameters used in the preceding CASSCF method. Fig 5.7 shows the MRCI results for the lowest two states of F_2, as well as the LPFD and CCSD curves. From this it can be seen that this discontinuity in the LPFD is unlikely to be caused by an intruder state.

The potential energy curve for N_2 provides an extremely hard test for the new LPFD method as it involves the breaking of a triple bond, and as such is a system with strong static correlation at stretched bond lengths. Calculations were performed with the cc-pVTZ basis set.

The results of these calculations are shown in Fig. 5.8 where it can be seen that LPFD again shows good agreement with the CCSD method in the bonded region with energies just a little higher than the CCSD energies. Just like the F_2 curve, there is a discontinuity in the LPFD energy when the bond length is stretched to 1.65Å, with subsequent energies

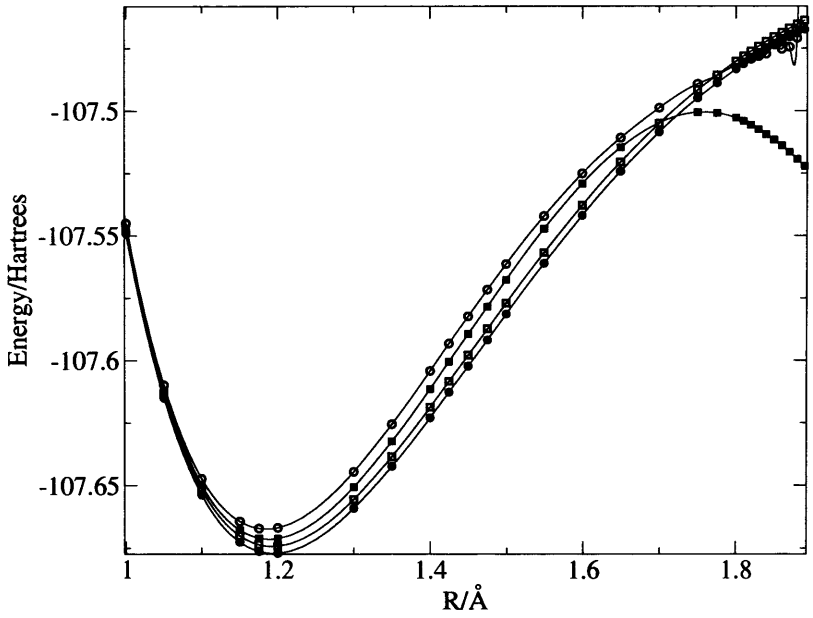

Figure 5.9: Potential energy curve of N_2 with STO-3G basis set. ● FCI, ○ LPFD, ■ CCSD, ❑ VCCSD

approximately 10mHartrees too high in comparison with CCSD results.

The potential energy for N_2 was also calculated in a smaller STO-3G basis set with the results of this shown in Fig. 5.9. This was done so that FCI benchmarks can also be included. Firstly, the discontinuity in the LPFD energy has disappeared when a smaller basis set is used. However, the LPFD energies do go below the FCI values as the stretched distance of 1.8Åshowing that the method is not an upper bound to the exact energy, but the failure seen is not as severe as with the CCSD method, as the LPFD goes below FCI results at a longer bond length, and by a lower energy difference in comparison with CCSD.

A final test case for the new LPFD code was the C_2 potential energy which is again a difficult system for approximate methods to generate an accurate energy curve. The calculations were again performed with the cc-pVTZ basis set and the results of these calculations is shown in Fig. 5.10. The graph shows that the LPFD method is not quite as good as CCSD in the bonding region as the energies are higher. The LPFD curve also shows an unphysical maxima at 1.9Å. Unlike the F_2 and N_2 energy curves, this does not appear to be a discontinuity as the curve is smooth at this point.

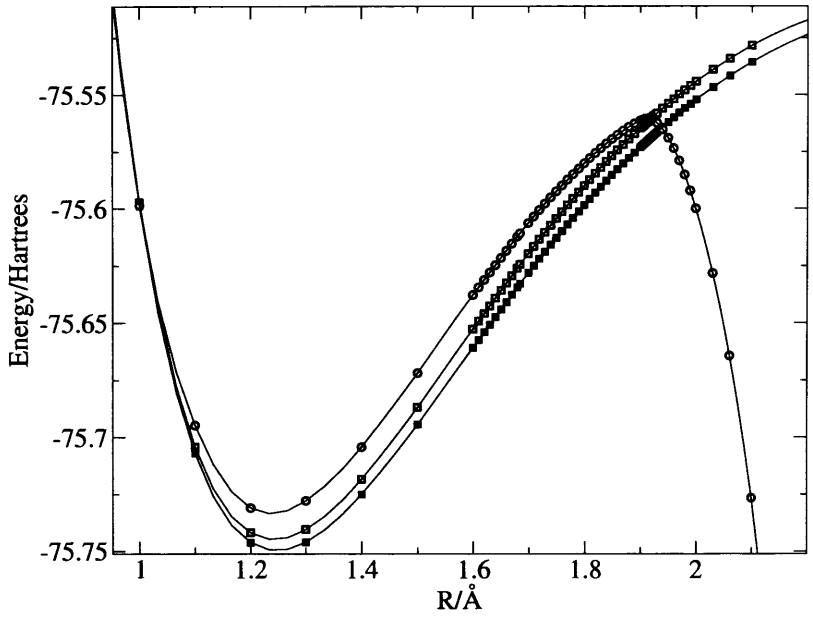

Figure 5.10: Potential energy curve of C_2 with cc-pVTZ basis set. ○ LPFD, ■ CCSD, ❑ BCCD

5.5 Conclusions

In this chapter the new LPFD method has been extensively tested on many small chemical systems. It has been shown that the method is capable of describing the simple bond breaking in hydrogen fluoride, abstracting a single hydrogen atom from a methane molecule, and the double dissociation of water. The method has been shown to have similar errors to CCSD near the equilibrium, with errors increasing as the static correlation increases as bonds are stretched. The LPFD also performs slightly better than CCSD at stretched bond lengths for these systems. LPFD has been shown to have similar errors to Kollmar's parametric variational 2-RDM method. The LPFD method also performs well for the double bond breaking in ethene, although convergence problems start to creep in at longer bond lengths.

Equilibrium properties are also well replicated by the LPFD method in comparison with CCSD results, with the LPFD over-binding in comparison to CCSD results. However, the opposite trend is seen in comparison to the parametric variational 2-RDM which are under-binding in comparison to CCSD results.

The LPFD method developed here has been shown to perform poorly for the potential energy curves of F_2, N_2 and C_2. In these LPFD curves there is unphysical behaviours such as discontinuities in the energies, and minima and maxima that are present in curves generated with other approximate correlation methods.

Chapter 6

Summary

The purpose of this thesis is to provide benchmark calculations for projection and variational coupled cluster methods, and to develop and test a new method for treating the correlation in molecular energies in the Linked Electron Pair method.

Benchmark calculations have been performed on various closed shell systems for each of the Coupled Cluster methods. Calculations on the polarisability of Neon and the potential energy curve of the beryllium dimer showed little difference in the different coupled cluster methods with only single and double excitations included in the cluster operator. The inclusion of triple excitation led to improvements in errors in comparison with FCI results, most notably in that TCCSDT and TCCSD(T) methods were able to give a qualitatively correct potential energy curve for Be_2 as these methods were able to capture the stronger shorter bond.

When multiple bonds are broken, the differences between each of the Coupled Cluster methods becomes more apparent. Calculations on water and nitrogen molecules showed that all the Coupled Cluster methods work well at equilibrium bond lengths, but that errors increase significantly when multiple bonds are stretched or broken. When breaking the triple bond in Nitrogen, TCCSD, fails to produce an accurate qualitative description of the potential energy curve, whereas the VCCSD method is superior as it follows the potential curve of FCI. Quadratic Coupled Cluster, the next step between TCC and full ECC, is significantly better at describing the potential energy curve of N_2.

Benchmark calculations were also performed on open-shell systems by using a UHF reference wavefunction. Large errors are seen at the onset of the UHF solution for each of the Coupled Cluster methods for N_2, however, the asymptotic region is well described with the correct neutral species for the products. TCCSD performs considerably poorer than VCCSD or ECCSD in the region of the onset of the UHF solution.

The errors in the Coupled Cluster results using a UHF wavefunction have been shown to be linked to the remaining spin contamination in the wavefunction. Both the analysis of the discontinuity in the energy derivative, and the evaluation of S^2 for N_2 showed more spin contamination remaining in the TCCSD method, than the other Coupled Cluster methods. Similar trends were observed for the $CN^{\cdot}$ a system know to have large spin contamination in the equilibrium region.

The final set of benchmark calculations was performed on systems with quasi degenerate states, which are known to be problematic for single reference correlation methods, as usually two or more configurations become important in the quasi degenerate region. Again, significant improvements were seen with VCCSD compared with TCCSD for the insertion of Be into H_2 and the H_4 systems.

In the last section of this thesis the new LPFD method was extensively tested on many small chemical systems. The method is capable of describing the simple bond breaking in hydrogen fluoride, abstracting a single hydrogen atom from a methane molecule, and the double dissociation of water. LPFD has been shown to have similar errors to Kollmar's parametric variational 2-RDM method for these systems. The LPFD method also performs well for the double bond breaking in ethene. Equilibrium properties are also well replicated by the LPFD method in comparison with CCSD results, with the LPFD over-binding in comparison to CCSD results. However, LPFD results are not similar to the parametric variational 2-RDM methods which are under-binding in comparison to CCSD results.

The LPFD method developed here has been shown to perform poorly for the potential energy curves of F_2, N_2 and C_2. In these LPFD curves there is unphysical behaviours such as discontinuities in the energies, and minima and maxima that are present in curves generated with other approximate correlation methods.

Bibliography

(1) C. C. J. Roothaan, *Revs. Mod. Phys*, 1951, **23**, 69–89.

(2) W. J. Hehre, R. F. Stewart and J. A. Pople, *J. Chem. Phys.*, 1969, **51**, 2657.

(3) W. J. Hehre, R. Ditchfield and J. A. Pople, *J. Chem. Phys.*, 1972, **56**, 2257.

(4) T. H. Dunning Jr, *J. Chem. Phys.*, 1989, **90**, 1007.

(5) H. F. Schaefer, *Methods of electronic structure theory*, Plenum Press New York, 1977.

(6) J. Hinze, *J. Chem. Phys.*, 1973, **59**, 6424.

(7) P. J. Knowles and H. J. Werner, *Chem. Phys. Lett.*, 1985, **115**, 259–267.

(8) H. J. Werner and P. J. Knowles, *J. Chem. Phys.*, 1985, **82**, 5053.

(9) E. Dalgaard and P. Jørgensen, *J. Chem. Phys.*, 1978, **69**, 3833.

(10) H. J. Werner and W. Meyer, *J. Chem. Phys.*, 1980, **73**, 2342.

(11) H. J. Werner and W. Meyer, *J. Chem. Phys.*, 1981, **74**, 5794.

(12) B. O. Roos, P. R. Taylor and S. P. E. M., *Chem. Phys.*, 1980, **48**, 157–173.

(13) P. E. M. Siegbahn, J. Almlöf, A. Heiberg and B. O. Roos, *J. Chem. Phys.*, 1981, **74**, 2384.

(14) P. Å. Malmqvist and B. O. Roos, *Chem. Phys. Lett.*, 1989, **155**, 189–194.

(15) B. O. Roos, *Chem. Phys. Lett.*, 1972, **15**, 153.

(16) W. Meyer, *J. Chem. Phys.*, 1976, **64**, 2901.

(17) P. Siegbahn, *Chemical Physics*, 1977, **25**, 197–205.

(18) P. J. Knowles and H. J. Werner, *Chem. Phys. Lett.*, 1988, **145**, 514–522.

(19) H. J. Werner and P. J. Knowles, *J. Chem. Phys.*, 1988, **89**, 5803.

(20) O. Sinanoğlu, *Adv. Chem. Phys.*, 1964, **6**, 315–412.

(21) W. Meyer, *J. Chem. Phys.*, 73, **58**, 1017.

(22) R. K. Nesbet, T. L. Barr and E. R. Davidson, *Chem. Phys. Lett.*, 1969, **4**, 203–204.

(23) F. Wennmohs and F. Neese, *Chem. Phys.*, 2008, **343**, 217–230.

(24) F. Neese, A. Hansen, F. Wennmohs and S. Grimme, *Acc. Chem. Res*, 2009, **42**, 641–648.

(25) J. Čížek, *J. Chem. Phys.*, 1966, **45**, 4256–4266.

(26) R. A. Chiles and C. E. Dykstra, *J. Chem. Phys*, 1981, **74**, 4544.

(27) C. Hampel, K. A. Peterson and H. J. Werner, *Chem. Phys. Lett.*, 1992, **190**, 1–12.

(28) J. F. Stanton, J. Gauss and R. J. Bartlett, *J. Chem. Phys.*, 1992, **97**, 5554.

(29) N. C. Handy, J. A. Pople, M. Head-Gordon, K. Raghavachari and G. W. Trucks, *Chem. Phys. Lett.*, 1989, **164**, 185–192.

(30) K. Raghavachari, J. A. Pople, E. S. Replogle, M. Head-Gordon and N. C. Handy, *Chem. Phys. Lett.*, 1990, **167**, 115–121.

(31) G. E. Scuseria, *Chem. Phys. Lett.*, 1994, **226**, 251–256.

(32) J. Pople, M. Head-Gordon and K. Raghavachari, *The Journal of Chemical Physics*, 1987, **87**, 5968.

(33) C. Møller and M. S. Plesset, *Physical Review*, 1934, **46**, 618–622.

(34) F. Jensen, *Introduction to Computational Chemistry*, John Wiley and Sons, 1999.

(35) P. G. Szalay, M. Nooijen and R. J. Bartlett, *J. Chem. Phys.*, 1995, **103**, 281.

(36) W. Kutzelnigg, *Theor. Chim. Acta*, 1991, **80**, 349–386.

(37) J. L. Stuber and J. Paldus, *J. Mol. Struct.-Theochem*, 2002, **591**, 219–230.

(38) K. Kowalski and P. Piecuch, *J. Chem. Phys.*, 2000, **113**, 18.

(39) P. Piecuch, K. Kowalski, I. S. O. Pimienta, P. D. Fan, M. Lodriguito, M. J. McGuire, S. A. Kucharski, T. Kuś and M. Musiał, *Theor. Chim. Acta.*, 2004, **112**, 349–393.

(40) P. Piecuch, K. Kowalski, I. S. O. Pimienta and M. J. McGuire, *Int. Rev. Phys. Chem.*, 2002, **21**, 527–655.

(41) K. Kowalski and P. Piecuch, *J. Chem. Phys.*, 2000, **113**, 5644.

(42) P. Piecuch, M. Włoch and A. J. C. Varandas, *Theor. Chim. Acta.*, 2008, **120**, 59–78.

(43) K. Kowalski and P. Piecuch, *J. Chem. Phys.*, 2001, **115**, 2966.

(44) J. Noga and R. J. Bartlett, *J. Chem. Phys.*, 1987, **86**, 7041.

(45) S. A. Kucharski and R. J. Bartlett, *J. Chem. Phys.*, 1992, **97**, 4282.

(46) Y. J. Bomble, J. F. Stanton, M. Kállay and J. Gauss, *J. Chem. Phys.*, 2005, **123**, 054101.

(47) Y. S. Lee and R. J. Bartlett, *J. Chem. Phys.*, 1984, **80**, 4371.

(48) Y. S. Lee, S. A. Kucharski and R. J. Bartlett, *J. Chem. Phys.*, 1984, **81**, 5906.

(49) M. Kállay and P. R. Surján, *J. Chem. Phys.*, 2000, **113**, 1359.

(50) S. Hirata and R. J. Bartlett, *Chem. Phys. Lett.*, 2000, **321**, 216–224.

(51) R. J. Bartlett and J. Noga, *Chem. Phys. Lett.*, 1988, **150**, 29.

(52) S. Pal, M. Durga Prasad and D. Mukherjee, *Theor. Chim. Acta.*, 1983, **62**, 523–536.

(53) W. Kutzelnigg, *J. Chem. Phys.*, 1982, **77**, 3081.

(54) W. Kutzelnigg and S. Koch, *J. Chem. Phys.*, 1983, **79**, 4315.

(55) W. Kutzelnigg, *J. Chem. Phys.*, 1984, **82**, 4166.

(56) R. J. Bartlett and J. Noga, *Chem. Phys. Lett.*, 1988, **150**, 29–36.

(57) R. J. Bartlett, S. A. Kucharski and J. Noga, *Chem. Phys. Lett.*, 1989, **155**, 133–140.

(58) J. D. Watts, G. W. Trucks and R. J. Bartlett, *Chem. Phys. Lett.*, 1989, **157**, 359–366.

(59) M. R. Hoffmann and J. Simons, *J. Chem. Phys.*, 1988, **88**, 993.

(60) M. R. Hoffmann and J. Simons, *Chem. Phys. Lett*, 1987, **142**, 451–454.

(61) S. Pal, *Theor. Chim. Acta.*, 1984, **66**, 207–215.

(62) J. Arponen, *Ann. Phys.*, 1983, **151**, 311–382.

(63) S. Pal, *Phys. Rev. A*, 1986, **34**, 2682–2686.

(64) A. B. Kumar, N. Vaval and S. Pal, *Chem. Phys. Lett.*, 1998, **295**, 189–194.

(65) N. Vaval, A. B. Kumar and S. Pal, *Int. J. Mol. Sci*, 2001, **2**, 89–102.

(66) S. Pal, *Phys. Rev. A*, 1989, **39**, 2712–2714.

(67) S. Pal, *Phys. Rev. A*, 1986, **33**, 2240–2244.

(68) P. U. Manohar, N. Vaval and S. Pal, *Chem. Phys. Lett.*, 2004, **387**, 442–447.

(69) P. D. Fan, K. Kowalski and P. Piecuch, *Mol. Phys.*, 2005, **103**, 2191–2213.

(70) T. Van Voorhis and M. Head-Gordon, *Chem. Phys. Lett.*, 2000, **330**, 585–594.

(71) S. R. Gwaltney, E. F. C. Byrd, T. Van Voorhis and M. Head-Gordon, *Chem. Phys. Lett.*, 2002, **353**, 359–367.

(72) N. C. Handy, *Chem. Phys. Lett.*, 1980, **74**, 280–283.

(73) P. J. Knowles and N. C. Handy, *Chem. Phys. Lett.*, 1984, **111**, 315–321.

(74) G. L. Bendazzoli and S. Evangelisti, *J. Chem. Phys.*, 1993, **98**, 3141.

(75) C. W. Bauschlicher Jr and S. R. Langhoff, *J. Chem. Phys.*, 1987, **86**, 5595.

(76) C. W. Bauschlicher Jr and P. R. Taylor, *J. Chem. Phys.*, 1987, **86**, 5600.

(77) C. W. Bauschlicher Jr, S. R. Langhoff, P. R. Taylor, N. C. Handy and P. J. Knowles, *J. Chem. Phys.*, 1986, **85**, 1469.

(78) C. W. Bauschlicher Jr and P. R. Taylor, *J. Chem. Phys.*, 1986, **85**, 2779–2783.

(79) C. W. Bauschlicher Jr and P. R. Taylor, *J. Chem. Phys.*, 1987, **86**, 1420–1424.

(80) C. W. Bauschlicher Jr and P. R. Taylor, *J. Chem. Phys.*, 1986, **85**, 6510.

(81) C. W. Bauschlicher Jr and S. R. Langhoff, *J. Chem. Phys.*, 1987, **87**, 2919.

(82) C. W. Bauschlicher Jr and S. R. Langhoff, *J. Chem. Phys.*, 1988, **89**, 4246.

(83) R. J. Harrison and N. C. Handy, *Chem. Phys. Lett.*, 1983, **98**, 97–101.

(84) C. W. Bauschlicher Jr and P. R. Taylor, *J. Chem. Phys.*, 1987, **86**, 2844.

(85) P. J. Knowles, K. Stark and H. J. Werner, *Chem. Phys. Lett.*, 1991, **185**, 555–561.

(86) S. Evangelisti, G. L. Bendazzoli and L. Gagliardi, *Chem. Phys.*, 1994, **185**, 47–56.

(87) K. A. Peterson and R. C. Woods, *J. Chem. Phys.*, 1987, **87**, 4409.

(88) A. Halkier, H. Larsen, J. Olsen, P. Jørgensen and J. Gauss, *J. Chem. Phys.*, 1999, **110**, 734.

(89) H. Larsen, C. Hättig, J. Olsen and P. Jørgensen, *Chem. Phys. Lett.*, 1998, **291**, 536–546.

(90) H. Koch, O. Christiansen, P. Jørgensen and J. Olsen, *Chem. Phys. Lett.*, 1995, **244**, 75–82.

(91) M. L. Abrams and C. D. Sherrill, *J. Chem. Phys.*, 2004, **121**, 9211–9219.

(92) M. Musiał and R. J. Bartlett, *J. Chem. Phys.*, 2005, **122**, 224102.

(93) J. Olsen, P. Jørgensen, H. Koch, A. Balkova and R. J. Bartlett, *J. Chem. Phys.*, 1996, **104**, 8007.

(94) H. Larsen, J. Olsen, P. Jørgensen and O. Christiansen, *J. Chem. Phys.*, 2000, **113**, 6677.

(95) T. Van Voorhis and M. Head-Gordon, *J. Chem. Phys.*, 2000, **113**, 8873.

(96) N. Vaval and S. Pal, *Phys. Rev. A*, 1996, **54**, 250–258.

(97) H.-J. Werner, P. J. Knowles, R. Lindh, F. R. Manby, M. Schütz, P. Celani, T. Korona, A. Mitrushenkov, G. Rauhut, T. B. Adler, R. D. Amos, A. Bernhardsson, A. Berning, D. L. Cooper, M. J. O. Deegan, A. J. Dobbyn, F. Eckert, E. Goll, C. Hampel, G. Hetzer, T. Hrenar, G. Knizia, C. Köppl, Y. Liu, A. W. Lloyd, R. A. Mata, A. J. May, S. J. McNicholas, W. Meyer, M. E. Mura, A. Nicklass, P. Palmieri, K. Pflüger, R. Pitzer, M. Reiher, U. Schumann, H. Stoll, A. J. Stone, R. Tarroni, T. Thorsteinsson, M. Wang and A. Wolf, *MOLPRO, version 2009.1, a package of ab initio programs*, 2009, see http://www.molpro.net.

(98) E. R. Davidson, *J. Comp. Phys.*, 1975, **17**, 87 - 94.

(99) T. H. Dunning Jr, *J. Chem. Phys.*, 1970, **53**, 2823.

(100) V. E. Bondybey, *Chem. Phys. Lett.*, 1984, **109**, 436–441.

(101) I. Cernusak, J. Noga, G. H. F. Diercksen and A. J. Sadlej, *Chem. Phys.*, 1988, **125**, 255–260.

(102) J. M. L. Martin, *Chem. Phys. Lett.*, 1999, **303**, 399–407.

(103) M. Kállay and P. R. Surján, *J. Chem. Phys.*, 2001, **115**, 2945.

(104) M. Kállay, P. G. Szalay and P. R. Surján, *J. Chem. Phys*, 2002, **117**, 980.

(105) M. Kállay, J. Gauss and P. G. Szalay, *J. Chem. Phys.*, 2003, **119**, 2991.

(106) M. Kállay and J. Gauss, *J. Chem. Phys.*, 2005, **123**, 214105.

(107) J. Olsen, P. Jørgensen, T. Helgaker and O. Christiansen, *J. Chem. Phys.*, 2000, **112**, 9736.

(108) P. Piecuch, S. A. Kucharski, V. Špirko and K. Kowalski, *J. Chem. Phys.*, 2001, **115**, 5796.

(109) S. Hirata, P. D. Fan, A. A. Auer, M. Nooijen and P. Piecuch, *J. Chem. Phys.*, 2004, **121**, 12197.

(110) J. W. Krogh and J. Olsen, *Chem. Phys. Lett.*, 2001, **344**, 578–586.

(111) K. Kowalski and P. Piecuch, *J. Chem. Phys.*, 2000, **113**, 5644.

(112) L. Meissner, S. Hirata and R. J. Bartlett, *Theor. Chim. Acta*, 2006, **116**, 440–449.

(113) H. J. Werner and P. J. Knowles, *J. Chem. Phys.*, 1991, **94**, 1264.

(114) J. A. Pople and R. K. Nesbet, *J. Chem. Phys.*, 1954, **22**, 571–572.

(115) P. O. Löwdin, *Phys. Rev.*, 1955, **97**, 1509–1520.

(116) A. Szabo and N. S. Ostlund, *Modern Quantum Chemistry - Introduction to Advanced Electronic Structure Theory*, Dover Publications, Inc., 1996.

(117) H. Fukutome, *Progr. Theor. Phys.*, 1972, **47**, 1156–1180.

(118) H. Fukutome, *Int. J. Quantum Chem.*, 1981, **20**, 955–1065.

(119) I. Mayer and P. O. Löwdin, *Chem. Phys. Lett.*, 1993, **202**, 1–6.

(120) S. Hammes-Schiffer and H. C. Andersen, *J. Chem. Phys.*, 1993, **99**, 1901.

(121) R. H. Nobes, J. A. Pople, L. Radom, N. C. Handy and P. J. Knowles, *Chem. Phys. Lett.*, 1987, **138**, 481–485.

(122) P. M. W. Gill, J. A. Pople, L. Radom and R. H. Nobes, *J. Chem. Phys.*, 1988, **89**, 7307.

(123) H. B. Schlegel, *J. Chem. Phys.*, 1986, **84**, 4530–4534.

(124) H. B. Schlegel, *J. Phys. Chem.*, 1988, **92**, 3075–3078.

(125) W. Chen and H. B. Schlegel, *J. Chem. Phys.*, 1994, **101**, 5957.

(126) P. J. Knowles and N. C. Handy, *J. Chem. Phys.*, 1988, **88**, 6991.

(127) J. Baker, *Chem. Phys Lett.*, 1988, **152**, 227–232.

(128) J. Baker, *J. Chem. Phys.*, 1989, **91**, 1789–1795.

(129) R. D. Amos, J. S. Andrews, N. C. Handy and P. J. Knowles, *Chem. Phys. Lett.*, 1991, **185**, 256–264.

(130) P. J. Knowles, J. S. Andrews, R. D. Amos, N. C. Handy and J. A. Pople, *Chem. Phys. Lett.*, 1991, **186**, 130–136.

(131) N. L. Ma, B. J. Smith and L. Radom, *Chem. Phys. Lett.*, 1992, **193**, 386–394.

(132) D. Jayatilaka and T. J. Lee, *Chem. Phys. Lett.*, 1992, **199**, 211–219.

(133) T. J. Lee and D. Jayatilaka, *Chem. Phys. Lett.*, 1993, **201**, 1–10.

(134) S. E. Wheeler, W. D. Allen and H. F. Schaefer III, *J. Chem. Phys.*, 2008, **128**, 074107.

(135) J. F. Stanton, *J. Chem. Phys.*, 1994, **101**, 371.

(136) M. Rittby and R. J. Bartlett, *J. Phys. Chem.*, 1988, **92**, 3033–3036.

(137) P. G. Szalay and J. Gauss, *J. Chem. Phys.*, 1997, **107**, 9028.

(138) X. Li and J. Paldus, *J. Chem. Phys*, 1995, **102**, 2013.

(139) X. Li and J. Paldus, *J. Chem. Phys.*, 1995, **102**, 8059.

(140) C. L. Janssen and H. F. Schaefer III, *Theor. Chim. Acta)*, 1991, **79**, 1–42.

(141) M. Nooijen and R. J. Bartlett, *J. Chem. Phys.*, 1996, **104**, 2652.

(142) P. J. Knowles, C. Hampel and H. J. Werner, *J. Chem. Phys.*, 1993, **99**, 5219.

(143) P. Neogrády, M. Urban and I. Hubac, *J. Chem. Phys.*, 1994, **100**, 3706.

(144) D. Jayatilaka and T. J. Lee, *J. Chem. Phys.*, 1993, **98**, 9734.

(145) R. H. Nobes, D. Moncrieff, M. W. Wong, L. Radom, P. M. W. Gill and J. A. Pople, *Chem. Phys. Lett.*, 1991, **182**, 216–224.

(146) H. Yuan and D. Cremer, *Chem. Phys. Lett.*, 2000, **324**, 389–402.

(147) F. Jensen, *Chem. Phys. Lett.*, 1990, **169**, 519.

(148) J. M. L. Martin, J. P. Francois and R. Gijbels, *Chem. Phys. Lett.*, 1990, **166**, 295.

(149) G. D. Purvis III, R. Shepard, F. B. Brown and R. J. Bartlett, *Int. J. Quantum Chem.*, 1983, **23**, 835–845.

(150) M. Hanrath, *J. Chem. Phys.*, 2008, **128**, 154118.

(151) N. Oliphant and L. Adamowicz, *J. Chem. Phys.*, 1991, **94**, 1229.

(152) A. Banerjee and J. Simons, *Chem. Phys.*, 1983, **81**, 297–302.

(153) S. Chattopadhyay, U. S. Mahapatra and D. Mukherjee, *J. Chem. Phys.*, 2000, **112**, 7939.

(154) M. Hanrath, *J. Chem. Phys.*, 2005, **123**, 084102.

(155) F. A. Evangelista, W. D. Allen and H. F. Schaefer III, *J. Chem. Phys.*, 2006, **125**, 154113.

(156) K. Jankowski and J. Paldus, *Int. J. Quantum Chem.*, 1980, **18**, 1243–1269.

(157) D. Pahari, S. Chattopadhyay, A. Deb and D. Mukherjee, *Chem. Phys. Lett.*, 2004, **386**, 307–312.

(158) K. Kowalski and K. Jankowski, *Chem. Phys. Lett.*, 1998, **290**, 180–188.

(159) H. Meißner and J. Paldus, *J. Chem. Phys.*, 2000, **113**, 2612.

(160) X. Li and J. Paldus, *J. Chem. Phys.*, 2008, **128**, 144119.

(161) S. R. Langhoff and E. R. Davidson, *Int. J. Quantum Chem.*, 1974, **8**, 61–72.

(162) R. Ahlrichs, P. Scharf and C. Ehrhardt, *J. Chem. Phys.*, 1985, **82**, 890.

(163) R. J. Gdanitz and R. Ahlrichs, *Chem. Phys. Lett.*, 1988, **143**, 413.

(164) R. J. Gdanitz, *Int. J. Quantum Chem.*, 2001, **85**, 281–300.

(165) C. Kollmar, *J. Chem. Phys.*, 2006, **125**, 084108.

(166) A. E. DePrince III and D. A. Mazziotti, *Phys. Rev. A*, 2007, **76**, 42501.

(167) D. A. Mazziotti, *Phys. Rev. Lett.*, 2008, **101**, 253002.

(168) A. E. DePrince III, E. Kamarchik and D. A. Mazziotti, *J. Chem. Phys.*, 2008, **128**, 234103.